

# Dissertation

Submitted to the  
Combined Faculties for The Natural Sciences and for Mathematics of  
the Ruperto-Carola University of Heidelberg, Germany for the degree  
of Doctor of Natural Sciences

Presented by  
Hatim Jawhari, MS.  
Rabat, Morocco

Oral examination:

Steps to Reconstitute *in vitro* a Complete Round of  
COPI vesicle Budding, Uncoating and Fusion

Referees: Prof. Dr. Felix T. Wieland  
Prof. Dr. Michael Brunner

*A Julia,*

*pour son soutien de tous les instants*

## Contents

<b>Abstract</b>	<b>1</b>
<b>Introduction</b>	<b>2</b>
<b>1 Protein sorting within the eukaryotic cell</b>	<b>3</b>
1.1 <i>Protein sorting to mitochondria and chloroplasts</i>	5
1.2 <i>Protein sorting to peroxisomes</i>	5
1.3 <i>The Classical secretory pathway</i>	5
<b>2 Golgi vesicular transport, a focus on COPI coated vesicles</b>	<b>9</b>
2.1 <i>Recruitment of COPI coat components to the membrane</i>	9
2.2 <i>COPI coat formation</i>	11
2.3 <i>In vitro generation of COPI coated vesicles from liposomes</i>	11
2.4 <i>SNAREs in the in vitro budding assay</i>	12
<b>Results</b>	<b>13</b>
<b>1 Cloning, expression and purification of proteins</b>	<b>15</b>
1.1 <i>GST-fusion SNAREs</i>	15
1.2 <i>The p24 family members</i>	18
1.3 <i>Native yeast ARF1p and human ARF1</i>	19
1.3.1 <i>Yeast ARF1p</i>	20
1.3.2 <i>Human ARF1</i>	25
1.4 <i>Expression, purification and refolding of Glo3p, an ARF GTPase activating protein (GAP) in E. coli</i>	27
1.5 <i>TAP-Tagged native yeast coatomer complex</i>	28
1.6 <i>Native coatomer complex from rabbit liver</i>	30
<b>2 Setting up a reconstituted system with chemically defined components</b>	<b>31</b>
2.1 <i>Liposomes stand for Golgi membranes</i>	31
2.1.1 <i>Generating large liposomes</i>	31
2.1.2 <i>Synthesis of lipopeptides with cytoplasmic domains of the p24 family members</i>	34
2.1.3 <i>Quality control and quantification of liposomes</i>	36
2.2 <i>Reconstitution of SNARE proteins into liposomes</i>	38
2.2.1 <i>Reconstitution by dilution below the critical micellar concentration</i>	38

	2.2.2	<i>Reconstitution by chemical coupling to a cysteine residue</i>	40
	2.2.3	<i>Orientation of SNAREs after reconstitution</i>	41
<b>3</b>		<b>Functional aspects</b>	<b>42</b>
	3.1	<i>Nucleotide exchange activity of ARF1 and GAP activity of Glo3p</i>	42
	3.2	<i>Attempts to generate COPI coated vesicles from p23 containing liposomes</i>	47
	3.3	<i>Attempts to generate COPI coated vesicles from liposomes containing p23 and SNAREs</i>	49
		<b>DISCUSSION</b>	<b>52</b>
<b>1</b>		<b>Protein components involved in COPI vesicular transport</b>	<b>54</b>
	1.1	<i>SNARE proteins reconstituted in liposomes</i>	54
	1.2	<i>p24 family proteins</i>	54
	1.3	<i>ARF1 GTPase activating protein (ARF1-GAP)</i>	55
	1.4	<i>ADP-ribosylation factor 1 (ARF1)</i>	56
<b>2</b>		<b><i>In vitro</i> budding assay with liposomes mimicking Golgi membranes</b>	<b>58</b>
	2.1	<i>Behavior of SNAREs in the COPI in vitro budding assay</i>	58
	2.2	<i>Generation of large liposomes</i>	60
		<b>Materials and Methods</b>	<b>62</b>
<b>1</b>		<b>Chemicals</b>	<b>63</b>
	1.1	<i>Detergents</i>	63
	1.2	<i>Protease inhibitors</i>	63
	1.3	<i>Buffers</i>	63
	1.4	<i>Media</i>	64
<b>2</b>		<b>Antibodies</b>	<b>65</b>
	2.1	<i>Primary Antibodies</i>	65
	2.2	<i>Secondary Antibodies</i>	65
<b>3</b>		<b>Plasmids</b>	<b>66</b>
<b>4</b>		<b>Oligonucleotides</b>	<b>66</b>
<b>5</b>		<b>Equipments</b>	<b>68</b>

<b>6</b>	<b>Biochemical Methods</b>	<b>68</b>
6.1	<i>Synthesis of p23 and p24 lipopeptides</i>	68
6.2	<i>Preparation of p23 lipopeptide containing liposomes</i>	70
6.3	<i>Electron microscopy</i>	70
6.4	<i>Selection for large liposomes by size exclusion chromatography</i>	71
6.5	<i>Quantification of lipids</i>	71
6.6	<i>in vitro budding assay using p23 containing liposomes and purified proteins</i>	72
6.7	<i>Tryptophan fluorescence assay</i>	73
6.8	<i>Liposomes size determination by Dynamic Light Scattering (DLS)</i>	74
<b>7</b>	<b>Methods in Molecular Biology</b>	<b>74</b>
7.1	<i>Preparation of yeast genomic DNA</i>	74
7.2	<i>Polymerase chain reaction (PCR)</i>	75
7.3	<i>Ligations and subcloning</i>	76
<b>8</b>	<b>Protein expression and purification</b>	<b>77</b>
8.1	<i>Endogenous rabbit coatmer</i>	77
8.2	<i>Endogenous yeast TAP-tagged coatmer</i>	78
8.3	<i>Recombinant yeast ARF1p</i>	80
8.4	<i>Recombinant human ARF1</i>	80
8.5	<i>Recombinant Glo3p</i>	81
8.6	<i>Recombinant human p23</i>	81
8.7	<i>Recombinant yeast SNAREs</i>	82
8.8	<i>Thrombin cleavage of GST fusion proteins</i>	83
<b>9</b>	<b>SDS-PAGE and Western Blot analysis</b>	<b>83</b>
9.1	<i>SDS-PAGE for separation of proteins</i>	83
9.2	<i>Transfer proteins from SDS-PAGE to a PVDF membrane</i>	83
9.3	<i>Incubation of PVDF membranes with antibodies</i>	84
<b>10</b>	<b>Protein Determination</b>	<b>85</b>
10.1	<i>Protein Determination by BCA</i>	85
10.2	<i>Protein Determination by Lowry</i>	85
<b>11</b>	<b>Protein Precipitation</b>	<b>86</b>
11.1	<i>Chloroform-Methanol Precipitation</i>	86
11.2	<i>TCA precipitation</i>	86

<b>References</b>	<b>87</b>
<b>Acknowledgments</b>	<b>100</b>

## ABREVIATIONS

AC	Acetate
ADP	Adenosine-5'-diphosphat
APS	Ammoniumperoxodisulfat
ARF	ADP-ribosylation factor1
ARNO	ARF nucleotide-binding-site opener
ATP	Adenosin-5'-triphosphat
BCA	Bicinchoninic Acid Solution
BFA	Brefeldin A
bp	Base pair
BSA	Bovine serum Albumin
BMW	broad molecular weight
CFP	Cyan fluorescent protein
cDNA	complementary DNA
CHO	chinese hamster ovary
CMC	Critical micellar concentration
Coatomer	coat protomer
COP	coat Protein
DLS	Dynamic light scattering
DMSO	Dimethylsulfoxid
DNA	Desoxyribonucleic acid
DTT	Dithiothreitol
<i>E. coli</i>	<i>Escherichia coli</i>
ECL	enhanced chemoluminescence
EDTA	ethylenediaminetetraacetic acid
ER	Endoplasmic Reticulum
ERGIC	ER-Golgi-Intermediate Compartment
EtOH	Ethanol
FPLC	fast protein liquid chromatography
g	Gravitation (10 m.s <sup>-2</sup> )



GAP	GTPase activating Protein
GEF	Guanosinnucleotid-exchange factor
GDP	Guanosin-5'-diphosphat
GDP $\beta$ S	Guanosin-5'[\mathbf{\beta}-thio]-diphosphat
GST	Glutathione S-transferase
GTP	Guanosin-5'-triphosphat
GTP $\gamma$ S	Guanosin-5'[\mathbf{\gamma}-thio]-triphosphat
h	hour
Hepes	N-2-Hydroxyethylpiperazine-N'-2-ethanesulfonic acid
His	Histidine
HPLC	high performance liquid chromatography
IC	intermediate compartment
IgG	Immunglobulin G
IPTG	Isopropyl- $\beta$ -D-Thiogalactopyranosid
KD	Kilodalton
M	molar
mARF	N-myristoylated ARF
MeOH	Methanol
min	Minute
NSF	N-Ethylmaleimid-sensitiv Fusion protein
OG	n-Octyl- $\beta$ -D-glucopyranoside
OD	Optical density
PAGE	Poly Acrylamid Gel Electrophoresis
PBS	Phosphate buffered saline
PM	Plasmamembran
PMSF	Phenylmethylsulfonylfluorid
PVDF	Polyvinylidifluorid
RT	Room temperature
rpm	rotations per minute
s	Second
SDS	Sodium dodecyl sulfat

SNAP	soluble N-Ethylmaleimid-sensitiv Fusion protein attachment protein
SNARE	soluble N-Ethylmaleimid-sensitiv Fusion protein attachment protein Receptor
TAP-tag	Tandem Affinity Purification tag
TCA	Trichloroacetic acid
TEMED	N, N, N' N'- Tetramethylethylenediamine
TFA	Trifluoroacetic acid
TGN	Trans-Golgi-Network
Tris	Tris-(hydroxymethyl)-aminomethan
Tween 20	Polyoxyethylene sorbitan monolaureate
t-SNARE	target membrane-SNARE
v-SNARE	vesicle membrane-SNARE
v/v	Volume per volume
w/v	weight per volume
w/w	weight per weight
YFP	Yellow fluorescent protein

## ABSTRACT

Among the three functionally characterized vesicles within the cell (Clathrin, COPII and COPI coated vesicles), COPI vesicles mediate the transport in both anterograde and retrograde transport within the Golgi complex (Orci et al., 1997) as well as recycling of proteins from the Golgi to the ER (Cosson and Letourneur, 1994; Letourneur et al., 1994). An *in vitro* based assay using soluble coatamer and ARF1 together with synthetic liposomes containing p23 tail peptide yielded generation of COPI vesicles, thus establishing the minimal requirements for COPI coat assembly (Bremser et al., 1999). In a program to reconstitute one round of budding, uncoating and fusion of a COPI vesicle from defined components, the next step is to include in a liposomal system the components needed for the fusion reaction. For that purpose, SNAREs (Soluble N-Ethylmaleimid-sensitive fusion protein Attachment protein REceptors) were required since they were shown to be the machinery for fusion (McNew et al., 2000; Nickel et al., 1999; Sollner et al., 1993; Weber et al., 1998)). To study their behavior in the COPI budding process, different ER and Golgi SNAREs (Sec22p, Vti1p, Gos1p, Bos1p, Bet1p, Ykt6p) were produced in bacteria, purified and reconstituted into liposomes in their correct physiological orientation. Sec22p and Vti1p do not seem to be preferentially taken up in COPI coated vesicles under the conditions of the *in vitro* budding assay. Preliminary data allowed reconstitution of SNARE complexes and further experiments should allow the study of the mechanisms involved in their specific uptake in COPI vesicles. Prior to fusion, vesicles need to be uncoated. This process was shown to be dependent on ARF1-GTP hydrolysis (Tanigawa et al., 1993), a reaction catalyzed by ARF-GTPase activating protein (ARF-GAP). Therefore myristoylated yeast ARF1p as well as its ARF-GAP (Glo3p) was produced in bacteria, purified to apparent homogeneity and in an active state with regard to exchange of nucleotide and GTP hydrolysis in presence of liposomes. Moreover, selecting for large size liposomes used in the *in vitro* budding assay was critical to ensure newly formed vesicles are authentic ones and not preexisting small structures. Therefore, gel filtration experiments were successfully used to achieve this goal. Tools were provided to reconstitute one round of vesicular transport *in vitro*. Active proteins (ARF1p, coatamer) involved in coat assembly, ARF-GAP required for uncoating and the fusion machinery proteins SNAREs were provided. A Homogenous population of large liposomes was generated so that the total signal observed after budding is due only to *de novo* generated COPI vesicles and not to preexisting small structures.

# INTRODUCTION

## 1 Protein sorting within the eukaryotic cell

For a cell to function properly, each of its proteins must reach the correct cellular membrane or aqueous compartment (the mitochondrial matrix, chloroplast stroma, lysosomal lumen and cytosol).

Hormone receptor proteins, for example, must be delivered to the plasma membrane, soluble enzymes such as DNA polymerases must be targeted to the nucleus, while proteolytic enzymes must go to lysosomes. Other proteins such as collagen or other components of the extra cellular matrix must reach the cell surface and be expressed there. Thus directing the newly made proteins to their correct localization is critical to the functioning of eukaryotic cells.

The secretory pathway consists of separate membrane-enclosed organelles that lead to the cell surface. Newly synthesized proteins destined for secretion enter this pathway at the ER. When the ribosomes synthesizing the secretory proteins are bound to the rough ER, the proteins cross the ER membrane cotranslationally. Then soluble proteins are sorted to the lumen of other organelles or secreted while the integral membrane proteins are either permanently inserted into the ER membrane or eventually localize to the Golgi apparatus, the endosomes or the lysosomes or the plasma membrane.

Secretory proteins and enzymes on route to the ER, Golgi, lysosomes and plasma membrane proteins are synthesized on ribosomes attached to the ER. All proteins entering the secretory pathway contain a sequence of hydrophobic amino acids at the N-terminus that directs the ribosomes to the surface of the ER. This ER signal sequence is recognized by a signal recognition particle (SRP) that binds to an SRP receptor on the ER membrane. The SRP directs the insertion of the nascent polypeptide chain as well as the binding of ribosomes to the ER membrane. GTP hydrolysis by a subunit of the SRP, P54, and the  $\alpha$ -subunit of the SRP receptor provides the energy necessary for this process. Nascent proteins cross the ER through the translocon, a multiple protein complex composed of Sec61 complex and TRAM protein.

Once membrane proteins are inserted into the ER, they adopt their orientation in the ER membrane that will be kept during the transport to their final destination. This phenomenon involves topogenic sequences that are either an N-terminal cleaved sequence, a signal-anchor sequence, a stop-transfer anchor sequence (transmembrane domains) or a GPI anchor attachment sequence.

Before reaching their final destinations, newly synthesized secretory proteins are modified in the ER. Disulfide bonds are formed, correct folding is accomplished, sugar chains are added and the protein may be assembled as a multimer.

Disulfide bonds are formed and rearranged in the ER lumen. The oxidative local environment in this organelle allows this modification to happen. Cytosolic proteins lack this modification.

The correct folding of proteins within the ER lumen is a crucial step since only properly folded proteins can continue their journey in the secretory pathway. A folding quality control step involves the combined action of several players such as protein disulfide isomerase (PDI) that accelerates the rearrangement of disulfide bonds, or peptidyl prolyl isomerases that catalyse the rotation of peptidyl-prolyl bonds in unfolded parts of the protein.

Chaperones like Bip bind to proteins and prevent them from misfolding or aggregating. Eventually, misfolded proteins accumulating in the ER are transported back to the cytosol through the translocon and degraded in the proteasomes.

Resident ER proteins like Bip and PDI are retained in the lumen of this organelle to carry out their function. When ER resident proteins escape the ER, they are retrieved back. This is accomplished by a C-terminal sequence, KDEL (Lys-Asp-Glu-Leu) that targets them to the ER since this sequence is recognized by a receptor at the Cis-Golgi, Erd2 in yeast or KDEL receptor in mammals.

## 1.1 Protein sorting to mitochondria and chloroplasts

Mitochondria and chloroplasts contain organelle DNA that encodes rRNA and tRNA but only a few organelle proteins. Most of the proteins are encoded by nuclear genes, synthesized on cytosolic ribosomes and then imported to these organelles.

A Specific N-terminal uptake targeting sequence allows the proteins to reach the mitochondrial matrix or the chloroplastic stroma. The process of import of these organelle proteins is regulated by chaperone proteins and proteases that cleave the targeting sequences.

The energy required for translocation into the mitochondrion matrix is given by ATP hydrolysis and by an electrochemical gradient across the inner mitochondrial membrane. This gradient is maintained by the pumping of  $H^+$  from the matrix to the intermembrane space, driven by electron transport processes in the inner membrane.

## 1.2 Protein sorting to peroxisomes

Unlike in mitochondria and in chloroplasts, the total of peroxisomal proteins is synthesized in the cytosol, since no DNA is present in this organelle. All peroxisomal membrane and matrix proteins are post-translationally incorporated into the organelle as folded proteins. Peroxisomal proteins bear a targeting signal at the C-terminus that is a Ser-Lys-Leu sequence. The energy required for the peroxisomal import is provided by the hydrolysis of ATP.

## 1.3 The Classical secretory pathway

To exit the ER, secretory proteins are taken up into COPII vesicles, that fuse together to form the ER-Golgi intermediate compartment (ERGIC). At this point, ER residents are recycled back to the ER in another set of vesicles, COPI, and the cargo proteins to be transported further enter the Golgi where

other enzymatic modifications occur. Finally at the trans-Golgi network, cargo proteins are sorted to different compartments such as the plasma membrane, endosomes or lysosomes.

The Golgi complex is the central organelle of the secretory pathway. It consists of stacks of flattened membrane-bound cisternae interconnected to form a ribbon (Marsh et al., 2001a; Pisam et al., 1990; Rambourg and Clermont, 1990). Each cisterna contains different resident enzymes that process the forward trafficking of cargo proteins by glycosylation, phosphorylation, acylation, sulfation, and enzymes for the synthesis of lipids, sphingolipids and glycolipids.

Transport of cargo molecules in the secretory pathway involves at least three vesicular carriers. COPI vesicles traffic from the Golgi to the ER and between Golgi cisternae in both retrograde and anterograde directions. COPII vesicles traffic between ER and Golgi, while clathrin coated vesicles travel between the plasma membrane and the early endosomes, from the Golgi to the endosomes and from the trans-Golgi network (TGN) to the plasma membrane (Figure 1).

On the other hand, coat independent pathways arose in the last years that show clathrin-independent endocytosis to the TGN (Nichols, 2002) or a transport pathway from plasma-membrane caveolae through an intermediate organelle (called the caveosome) to the ER (Pelkmans et al., 2001). The focus here will be on the three different classes of coated vesicles that have been so far characterized at a molecular level.

COPII vesicles were first identified in the yeast *Saccharomyces cerevisiae* (Barlowe, 2000; Springer et al., 1999). Newly synthesized secretory proteins are sorted into COPII vesicles. Three cytosolic protein complexes are sufficient to drive the COPII transport: Sec23p-Sec24p, the Sec13-Sec31 complexes and the small GTPase Sar1p (Barlowe, 2000; Barlowe et al., 1994).

The cytosolic Sar1p in its GDP inactive form is recruited to the ER membrane upon exchange of GDP to GTP (Barlowe and Schekman, 1993) via the interaction with an ER attached protein Sec12 that is a Guanine exchange



factor (GEF) for Sar1p. Sar1p-GTP now bound to the membrane recruits the Sec23p-Sec24p complex to members of the p24 family proteins, putative cargo receptors, through a cytosolic FF motif, and to v-SNAREs Bet1p and Bos1p (Peng et al., 2000; Springer et al., 2000). Once sar1p and Sec23p-sec24p are in place, the second complex Sec13p-Sec31p is recruited and this growing coat scaffold is thought to deform the membrane leading to budding of vesicles. GTP is hydrolyzed by the action of one coat component, Sec23p that acts as a GTPase activating protein (GAP). The coat is dissociated and all its components are ready for a further cycle.

Clathrin coated vesicles were the first vesicles to be identified (Pearse, 1975; for review see Kirchhausen, 2000). At the trans-Golgi network, ARF1-GTP activates the recruitment of clathrin coat to the membrane whereas in the plasma membrane this activation is not well understood. ARF1-GTP recruits Adaptor Protein-1 complex (AP1) to trans-Golgi membranes where it binds to membrane receptors. ATP, GTP and phosphoinositides are necessary to recruit a second Adaptor protein complex (AP2) to the plasma membrane and endosomes. These two adaptors bind to sorting signals found in the cytoplasmic tails of many transmembrane proteins, e.g dileucine motifs. Coat assembly starts then with the recruitment of cytosolic clathrin to AP1 or AP2 in a nucleotide dependant manner. A coated pit forms with the polymerization of the clathrin heavy and light chains. At the neck of this forming pit, another cytosolic protein, Dynamin, polymerises around the neck and hydrolyses GTP, allowing the clathrin vesicle to pinch off (Takei et al., 1995).

COPI vesicles are involved in transport within the Golgi in both retrograde (from Golgi to ER) and anterograde (within the Golgi) directions. Their composition, biogenesis, and function will be addressed in the next chapter.

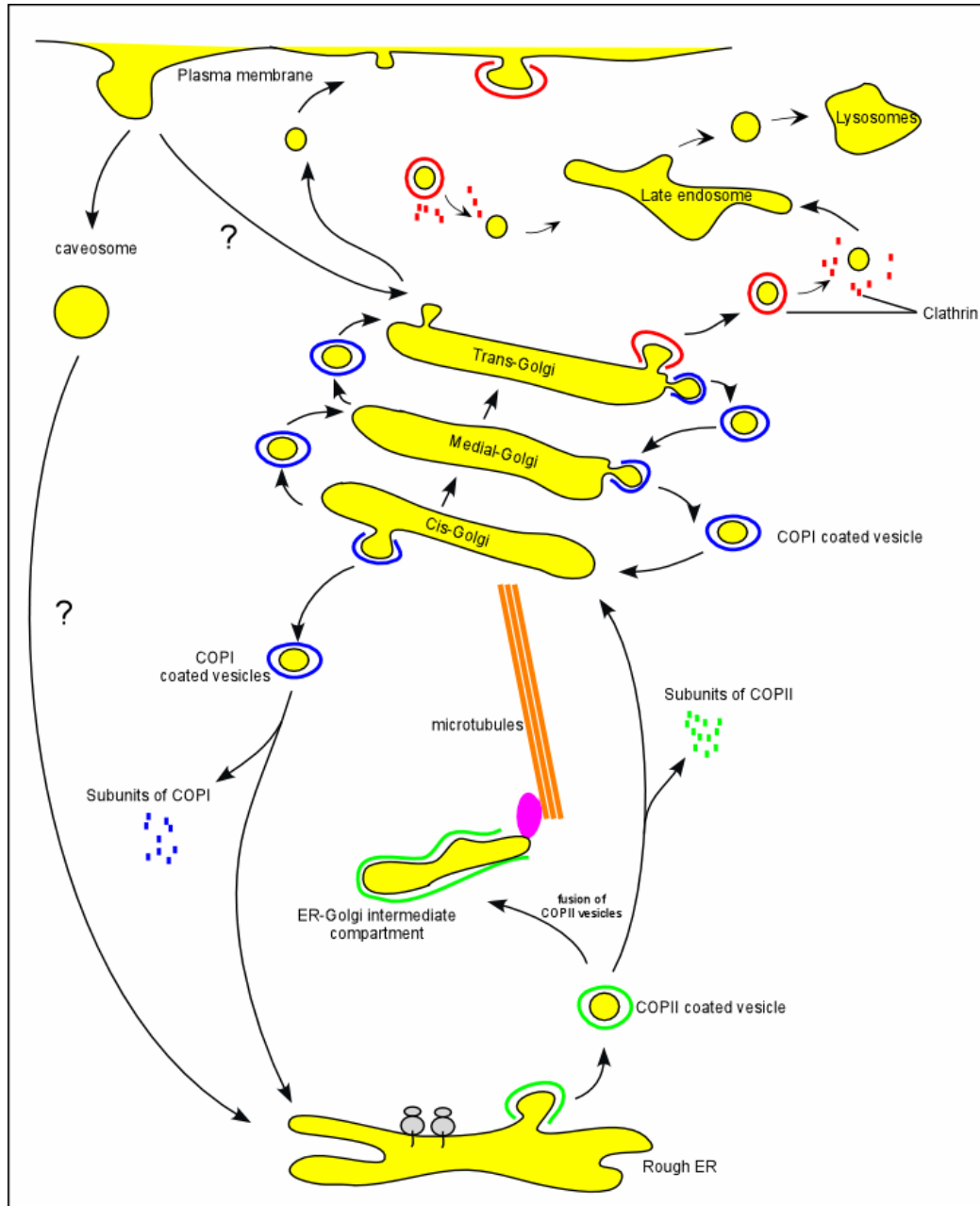


**Figure 1: The three major types of transport vesicles,** COPII vesicles transport proteins from the ER to the ER-Golgi intermediate compartment and to the Cis-Golgi. COPI vesicles are involved in the forward transport within the Golgi and in the retrograde transport from the Cis-Golgi to the ER-Golgi intermediate compartment to the ER as well as from the trans to medial to the Cis-Golgi. The clathrin coated vesicles are responsible for transport from the plasma membrane and the trans-Golgi network. The question marks point to recent research that has shown a possible coat independent trafficking of caveosomes from the plasma membrane to the TGN and to the ER.

## 2 Golgi vesicular transport, a focus on COPI coated vesicles

### 2.1 Recruitment of COPI coat components to the membrane

Whereas COPII trafficking is unidirectional (ER to Golgi), COPI trafficking functions primarily in retrograde transport (Golgi to ER) and is also important in forward transport within the Golgi.

The COPI coat is made of the seven subunits ( $\alpha$ ,  $\beta$ ,  $\beta'$ ,  $\gamma$ ,  $\delta$ ,  $\epsilon$  and  $\zeta$ -cops) of the coatamer and the small GTPase ADP ribosylation factor 1 (ARF1). Recently, novel isoforms of COPI subunits were identified ( $\gamma_2$  and  $\zeta_2$  cop) (Futatsumori et al., 2000) that define three subpopulations of COPI vesicles in higher eukaryotes (Wegmann et al., submitted).

ARF1 exists in the cytosol in its GDP form and its recruitment to the membrane depends on the exchange of GDP to GTP, a nucleotide exchange that is achieved by the action of a guanine-nucleotide exchange factor (GEF). This protein is the target for the fungal metabolite Brefeldin A (BFA) (Donaldson and Klausner, 1994; Helms and Rothman, 1992; Robineau et al., 2000) and its action causes a redistribution of Golgi enzymes to the ER (Lippincott-Schwartz et al., 1998), arrest of COPI vesicles formation and the redistribution of its coat components to the cytosol.

The association of ARF1-GTP upon nucleotide exchange to the membrane (Rothman, 1994) was thought to be the initial step in the coat assembly until it was recently shown that ARF1 in its GDP form interacts with the C-terminal cytosolic tail of p23, a member of the p24 family proteins, before exchange of nucleotide (Gommel et al., 2001). In consistency with this finding, recent *in vivo* data showed an energy transfer between p23 and ARF1 tagged respectively with CFP and YFP under ARF1-GTP hydrolysis conditions (Majoul et al., 2001). However this interaction does not seem to be a basic prerequisite for nucleotide exchange since the GEF mediated nucleotide

exchange on ARF can occur in the presence of liposomes and in the absence of additional proteins (Beraud-Dufour et al., 1999), or even without an exchange factor.

The p24 proteins are highly conserved type I transmembrane proteins that cycle in the early secretory pathway where they are involved in COPI coat assembly (Bremser et al., 1999; Jenne et al., 2002; Sohn et al., 1996). They are assumed to be receptors for COPI since they can bind its components (Dominguez et al., 1998; Sohn et al., 1996). In fact, the cytoplasmic domain of p23 interacts with the  $\gamma$ -COP subunit of coatamer (Harter and Wieland, 1998) and recruits ARF1-GDP (Gommel et al., 1999). Moreover, they are part of the minimal machinery for COPI budding (Bremser et al., 1999). The topology of these proteins consists of a luminal domain of about 180 amino acids with a predicted coiled coil domain and a short cytoplasmic tail of 10 to 15 amino acids that in some cases contain a K(X)KXX motif for Golgi to ER retrieval (Dominguez et al., 1998; Jackson et al., 1990; Jackson et al., 1993; Marsh et al., 2001b; Sohn et al., 1996). Since the identification of the first member of this family (Wada et al., 1991), six members were then identified in higher eukaryotes (Stamnes et al., 1995) and eight members in yeast (Emery et al., 2000). These proteins were shown to be present either as dimers or as monomers (Jenne et al., 2002) in contrast to other data, where they were described in a higher oligomeric state (Dominguez et al., 1998; Marzioch et al., 1999).

The interaction between the p23 tail peptide and ARF1 might play a role in regulating the ARF1 retention at the site of budding. It was shown that upon exchange, ARF1-GTP dissociates from p23 (Gommel et al., 1999) and thus priming the membrane for coatamer recruitment via interactions with ARF1 (Zhao et al., 1997; Zhao et al., 1999) and p23 (Dominguez et al., 1998; Sohn et al., 1996). In addition, coatamer was shown to stimulate ARF1 mediated GTP hydrolysis 1000-fold in an ARF-GAP dependent manner (Goldberg, 1999). Therefore a tripartite complex formed by ARF, ARF-GAP and coatamer was suggested. Moreover, the cytoplasmic domain of p24 inhibits coatamer and ARF-GAP dependent GTP hydrolysis (Goldberg, 2000). This down

regulation of GTP hydrolysis was proposed to enable formation of priming complexes providing a time frame where coatomer remains attached to the membrane long enough to allow polymerization of the COPI coat, leading to vesicle formation.

## **2.2 COPI coat formation**

Coatomer and ARF1-GTP polymerization is likely to provide the mechanical force needed to pinch off a COPI coated vesicle. Polymerization of coatomer and ARF1-GTP deforms the shape of the membrane and eventually results in the formation of a vesicle (Malhotra et al., 1989; Orci et al., 1986). Studies using coatomer and p23 and p24 tail peptides allowed understanding the mechanisms underlying coat polymerization on the membrane. Usage of homodimers of p23 and p24 tail peptides resulted in aggregation of coatomer on one hand and in a conformational change of its  $\gamma$ -cop subunit on the other hand (Reinhard et al., 1999). Knowing that this subunit interacts with p23 tail peptide (Harter and Wieland, 1998), this study has established this interaction to be crucial for COPI coat formation.

However in yeast, knock-out of all known p24 family members in a single strain did not result in any severe effect on vesicular transport (Springer et al., 2000). In contrary, similar p23 knock-out in mouse was lethal at a very early stage of the embryo (Denzel et al., 2000).

## **2.3 *In vitro* generation of COPI coated vesicles from liposomes**

Coatomer, ARF1 and p23 tail peptides were hypothesized to be sufficient to trigger the budding of COPI vesicles. An *in vitro* budding assay was developed that used p23 tail peptide containing liposomes resembling in their lipid composition the Golgi membranes, ARF1, coatomer and nucleotide (Bremser et al., 1999). Under incubation at 37°C, coated vesicles were

formed that resemble in their size, morphology and density the original COPI vesicles derived from Golgi membranes in accordance with previous experiments using Golgi membranes to bud COPI vesicles (Orci et al., 1993). In such a minimal system, the core components needed for budding were provided. Interestingly, COPI vesicles formation could not occur unless p23 tail peptide was used, regardless of the liposomal lipid composition. Although the lipid composition might be important for the efficiency of budding (De Camilli et al., 1996; Roth and Sternweis, 1997), it does not seem to be one of the minimal requirements for budding to take place.

## 2.4 SNAREs in the *in vitro* budding assay

Coatomer, ARF1 and p24 family proteins are the minimal machinery needed to generate COPI coated vesicles as shown previously by usage of liposomes and purified proteins.

It was shown that SNARE proteins are required for targeting and fusion. In fact, they form the minimal machinery for fusion and allow, in a very specific manner, the fusion of v-SNAREs containing vesicles to t-SNAREs containing target membranes (McNew et al., 2000; Nickel et al., 1999; Sollner et al., 1993; Weber et al., 1998).

To further investigate the mechanisms that lead to a complete cycle of COPI transport, including the disassembly of the coat and the fusion of COPI vesicles to a target membrane, tools need to be provided to link the machinery for budding to the machinery for fusion. That was the purpose of the present work.

Full length yeast SNAREs as well as their cytoplasmic domains were produced as fusion proteins and reconstituted in p23 containing liposomes. It was suggested that coat assembly can direct v-SNARE incorporation into COPII vesicles (Matsuoka et al., 1998). Because SNAREs might have a role in segregation of distinct COPI vesicle populations, their incorporation into COPI vesicles was addressed using the *in vitro* budding assay.

Endogenous yeast coatmer was produced as well as recombinant ARF1. An active recombinant ARF-GTPase activating protein (ARF-GAP) was produced and attempts to restore its biological activity were successful.

A large part of the present work was dedicated to generate large liposomes since the presence of small liposomes turned out to be a limiting step in the *in vitro* budding assay. As coated small liposomes float at the same density as bona fide COPI vesicles, they were indistinguishable from newly generated COPI coated vesicles. Attempts to select for large size liposomes were successful.

## **RESULTS**



# 1 Cloning, expression and purification of proteins

## 1.1 GST-fusion SNAREs

SNARE proteins are key players in the fusion of vesicles in the cell. They are class II transmembrane proteins that consist of a coiled coil domain at the N-terminus in addition to one membrane span at the C-terminus. However Ykt6p does not share this topology and is anchored to the membrane via an isoprenyl residue (McNew et al., 1997). In addition, they are highly conserved among species.

Although *in vitro* experiments have shown that COPI, COPII and clathrin coated vesicles can form from liposomes without addition of cargo proteins and transport factors (Bremser et al., 1999; Matsuoka et al., 1998; Spang and Schekman, 1998), these factors need to be packaged *in vivo* into COPI vesicles thus allowing efficient transport. SNARE proteins represent a prominent class of transport factors that are essential in consumption of vesicles.

To address the question how SNAREs are packaged into COPI vesicles during budding, they were produced to be reconstituted into synthetic liposomes. As they are exposed to the cytosolic face of a membrane compartment, they are likely to interact with cytosolic factors ARF1 and coatamer (Rein et al., 2002; Spang and Schekman, 1998) or with the cytoplasmic tail of the transmembrane p24 family members, all involved in budding of COPI vesicles. Six yeast SNARE proteins were chosen, namely Bos1p, an ER protein that recycles between Golgi and ER in a COPI dependant manner (Ossipov et al., 1999), Gos1p (McNew et al., 1998) a SNARE involved in intra Golgi transport, Sec22p which is associated with the pre Golgi intermediate compartment (Zhang et al., 1999); (Ballensiefen et al., 1998), Bet1p an early Golgi SNARE (Ossipov et al., 1999), Vti1p implicated in Golgi retrograde traffic (Lupashin et al., 1997) and Ykt6p . They are all present

in the ER and Golgi and participate in the process of fusion of COPII and COPI vesicles, respectively.

Two cloning strategies were developed; the first was to clone the full length proteins while the second consists of cloning their cytoplasmic domain to which a cysteine was added (Fig.1). In this case the cysteine will allow a chemical anchoring of the protein to a lipid moiety leading to its reconstitution into liposomes. This reaction allowed originally to synthesize lipopeptides by anchoring peptides to a lipid moiety (Bremser et al., 1999). In both cases the SNARE genes were fused to GST at the N-terminus and for this purpose cloned into PGEX-2T vector (Amersham biosciences).

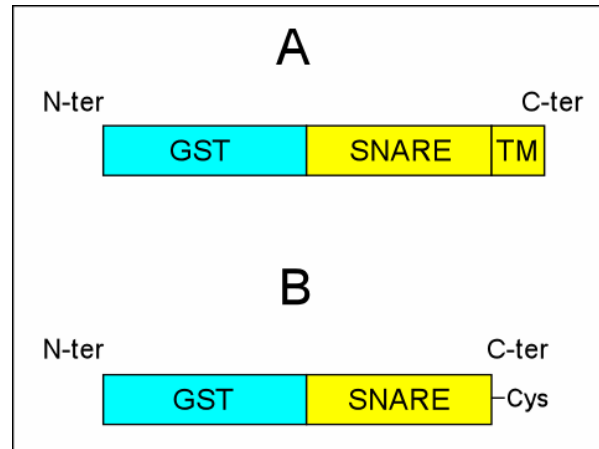


**Figure 1: Cloning strategies of the yeast SNAREs.** The first strategy shown in panel A consists in cloning Bos1p, Gos1p, Sec22p, Bet1p, Vti1p as full length proteins fused to GST. The second strategy (panel B) consists in cloning only the cytoplasmic domains of these fusion proteins to which a cysteine was added. GST was fused to the N-terminus. For Ykt6p, only the second version was possible since no transmembrane domain is present in this protein.

SNARE proteins were produced in BL21 (DE3)-pLys *E. coli*. The cultures were grown until an  $OD_{600} = 0.5$  and their expression were induced with 0.1 mM IPTG. As the proteins were fused to GST, they were purified by affinity chromatography on Glutathion-Sepharose beads (Amersham biosciences). Fig. 2 shows the purification of various SNAREs. Panels A, B, C, D show the purification of full length Gos1p, Bet1p, Vti1p and sec22p as well as their cytoplasmic domains. Panel D shows the purification of Ykt6 to which a cysteine was added at the C-terminus and the cytoplasmic domain of Bos1p.

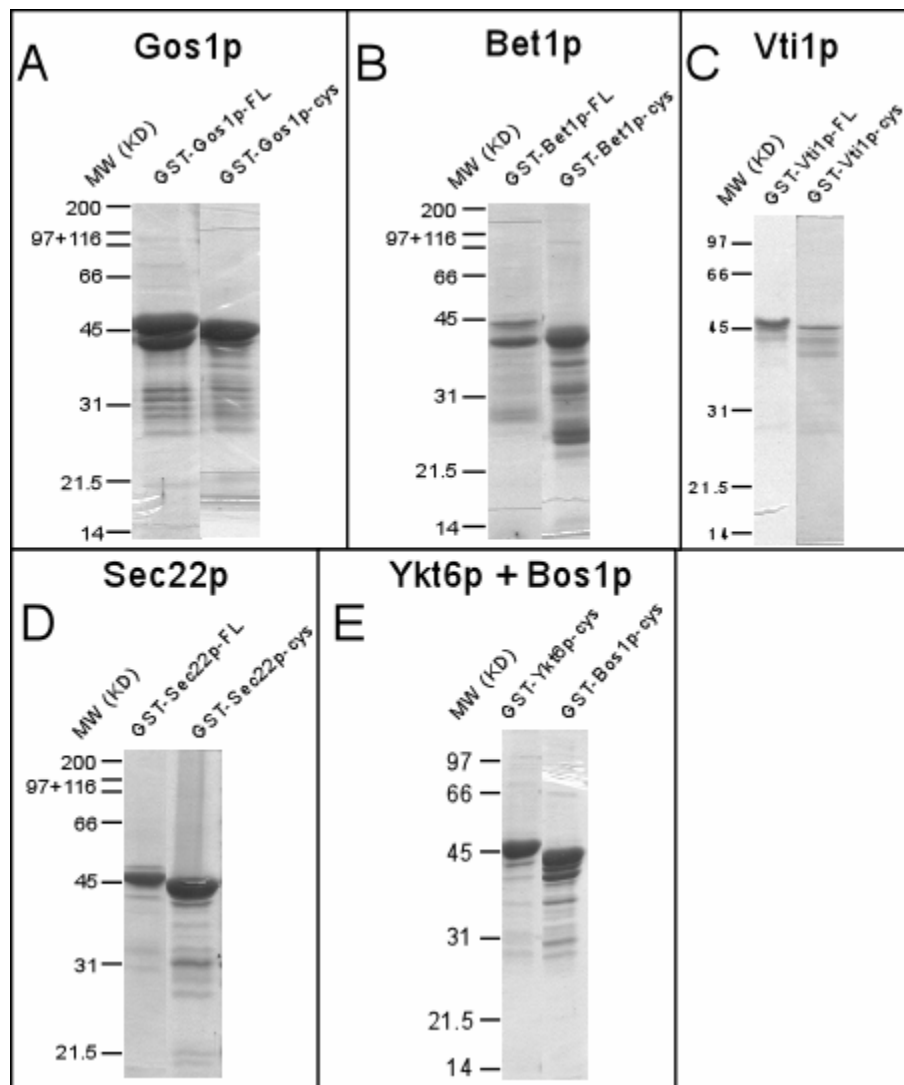


**Figure 2: SDS-PAGE analysis of affinity purified of GST-SNAREs (Gos1p, Bet1p, Vti1p, Sec22p, Ykt6p and Bos1p) on Glutathione-sepharose beads.** BL21(DE3) p-Lys *E. coli* bacteria were transformed with pGEX-2T plasmids carrying Ampiciline resistance in which different SNARE genes were cloned under the control of T7 promoter. Cells were grown in LB medium (typically 1 liter) at 37°C until OD=0.5-0.6 and expression was induced with IPTG at a concentration of 0.1 mM for 3 hours at 37°C. Cells were pelleted and resuspended in PBS buffer, pH=7.3 containing protease inhibitor tablets (Roche) and broken using a cell disrupter (Avestin EmulsiFlex-C5) at a pressure of 10000 to 15000 psi. The homogenates are ultra centrifuged at 100,000g for 60 minutes. The resulting supernatant is incubated with Glutathione-Sepharose beads (previously washed with PBS in the case of SNARE cytoplasmic domains or with PBS supplemented with 1% (w/v) n-Octyl- $\beta$ -D-glucopyranoside (OG) in the case of full length proteins) for 1 hour at 4°C to allow binding of GST to the Glutathione-Sepharose beads. This mixture is loaded onto disposable columns (Bio-Rad) with a frit so that the beads to which GST-SNAREs have bound are retained. After extensive washing with PBS (in the case of cytoplasmic domains) and PBS+OG (in the case of full length proteins), the bound protein is eluted with 20 mM Glutathion in Tris-HCl at pH = 8. Proteins were loaded on 15 % SDS-PAGE and stained with Coomassie blue.

## 1.2 The p24 family members

The p24 family members are class I conserved transmembrane proteins that cycle in the secretory pathway. They are regarded as putative cargo receptors (Schimmoller et al., 1995; Sohn et al., 1996; Stamnes et al., 1995) that are necessary for vesicular transport (Schimmoller et al., 1995). In fact, p24 family members were shown to interact with coatamer (Dominguez et al., 1998; Sohn et al., 1996) and with ARF1 (Gommel et al., 2001) via their cytoplasmic tail. Past attempts to produce these proteins in a native form resulted in total insolubility even in presence of detergent. Therefore to increase their solubility, the signal peptide was removed and the proteins were tagged with thioredoxin and purified in presence of 1% (w/v) OG. Pure proteins are then obtained (Fig. 3). The p23 human cDNA was cloned with a thioredoxin-tag, a 6XHis-tag and an S-tag placed under the control of T7 promoter in pET-32 Xa/LIC plasmid. Origami (DE3) *E. coli* were transformed with the constructed plasmid, grown in LB medium until  $OD_{600} = 0.6$  and expression was induced by addition of 0.1 mM IPTG. The protein was purified over a Nickel-Agarose column (Fig. 3), analyzed by SDS-PAGE and stained with Coomassie.

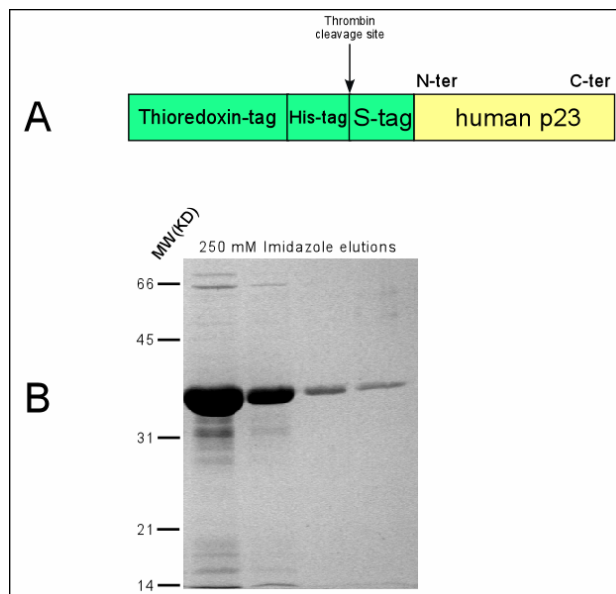


**Figure 3: SDS-PAGE analysis of affinity purified human p23.** Panel **A** shows the construct that serves to express human p23 in bacteria. It was tagged with Thioredoxin, a 6XHis tag and an S-tag. Purification was achieved by affinity chromatography (panel **B**); After binding to the Nickel-Agarose column, and extensive washing, the full length p23 protein tagged to thioredoxin and 6Histidine was eluted in 250 mM Imidazole containing 1% (w/v) OG at pH 8. Proteins were loaded on an SDS-PAGE and stained with Coomassie blue.

### 1.3 Native yeast ARF1p and human ARF1

ADP-ribosylation factor1 (ARF1) is a member of the Ras GTPase superfamily. These proteins are critical in different vesicular transport pathways in eukaryotic cells. As with other members of the Ras superfamily, ARF1 is present in the cell in two different nucleotide states, a cytosolic inactive form (ARF1-GDP) and a membrane bound active form (ARF1-GTP). It is recruited to the membrane in its GDP form by p23 tail peptide (Gommel et al., 2001) and is anchored to the membrane upon exchange of GDP to GTP. This very slow reaction (Franco et al., 1998; Frank et al., 1998; Goldberg, 1998; Mossessova et al., 1998; Peyroche et al., 1996; Togawa et al., 1999) is markedly accelerated by the action of nucleotide exchange factors (GEFs). To be released from the membranes and thus be available for other rounds of action, ARF-GTP has to be converted back to ARF-GDP, a reaction that is accelerated by GTPase activating proteins (GAPs) (Cukierman et al., 1995; Goldberg, 1998; Makler et al., 1995).

In the context of budding vesicles from membranes, ARF1 is a key protein since it has been shown to be one of the minimal requirements for this process to occur (Bremser et al., 1999).

### 1.3.1 Yeast ARF1p

ARF1p is subject to a major co-translational modification that insures its membrane targeting, the addition of myristic acid (C<sub>14</sub>:0) at its N-terminus. Myristoylation is catalyzed by NMT1 (N-myristoyl-transferase1) (Towler et al., 1987), an enzyme that links specifically the C<sub>14</sub> saturated fatty acid to the first glycine residue at the N-terminus of ARF1p via an amide bound (Olson et al., 1985). This reaction occurs cotranslationally to the production of ARF1p (Olson and Spizz, 1986; Wilcox et al., 1987) and is preceded by the action of another enzyme, Methionine amino peptidase that removes the starting methionine at the N-terminus of ARF1p leaving the glycine residue accessible to NMT1.

The ARF1 and NMT1 genes were amplified from yeast genomic DNA by PCR. To obtain myristoylated ARF1p, a co-expression of both ARF1p gene and the *N*-myristoyl transferase 1 (NMT1) was necessary. The ARF1p gene was then cloned in pET24a vector (Novagen) while NMT1 was cloned in pACYC DUET1 (Novagen) vector. The two vectors carry two different antibiotic resistances (Kanamycine and Chloramphenicol, respectively) and have different origins of replication, so that they do not compete for the machinery of replication. BL21 (DE3) STAR *E. coli* cells (Invitrogen) were co-transformed with the two plasmids. These cells contain a chromosomal copy of the gene encoding the RNA polymerase from the T7 phage which is placed under the control of the *lac* repressor. Addition of IPTG allows the expression of the T7 polymerase (by derepressing the *lac* repressor) that acts on the T7 promoter to express the cloned gene. Practically, cells were grown in 1 liter LB medium until an OD<sub>600</sub>= 0.2 to 0.4 before addition of myristic acid. When an OD<sub>600</sub> of 0.6 was reached, cells were induced with 1mM IPTG at 27°C for 3 hours. At this temperature, the

myristoylation is increased due to the fact that methionine aminopeptidase becomes rate limiting (Franco et al., 1995).

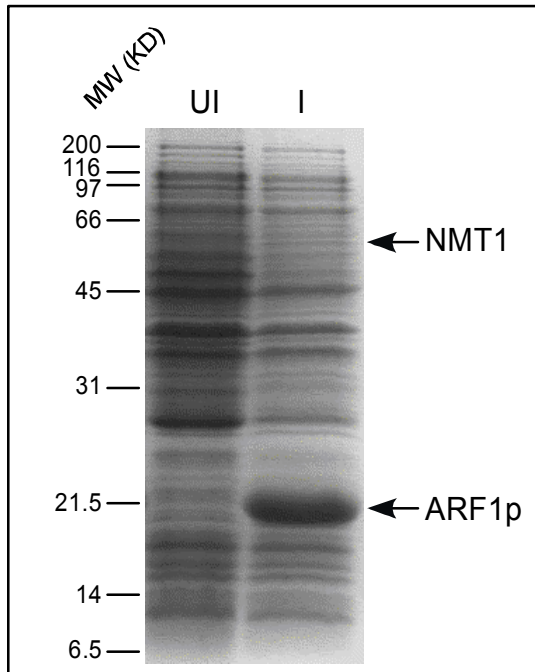


**Figure 4: Co-expression of ARF1p-Pet24 and NMT1-pACYC-DUET1 in BL21 (DE3) STAR bacteria.** The two plasmids carry respectively Kanamycine and Chloramphenicol resistances. After induction with 1mM IPTG at 27°C for 3 Hours (I), only small amounts of NMT1 are produced whereas ARF1p is highly over expressed and represents around 50% of total protein. The promoter is tight since no expression is observed in the uninduced bacteria (UI).

The bacterial pellet was resuspended in MES buffer (25 mM MES, 1mM DTT, 5 $\mu$ M GDP, 1mM MgCl<sub>2</sub>, pH=5.7). The post lysate supernatant was precipitated with ammonium sulfate at 35% saturation. Myristoylated ARF1p precipitates while its non-myristoylated counterpart remains soluble. Ammonium sulfate was removed by gel filtration and ARF1p was purified by cation exchange chromatography over a Source-S column.

Typically myristoylated ARF1p elutes between 17% and 25% buffer B corresponding to 85 mM to 125 mM NaCl. Apparent homogeneity after one column step is observed in fractions 19 and 20 yielding 3.5 to 4 mg pure myristoylated ARF1p (Fig.5)

A high degree of myristoylation is necessary for the biological activity of ARF1p on membranes. For comparison, non-myristoylated ARF1p was also produced as a negative control.

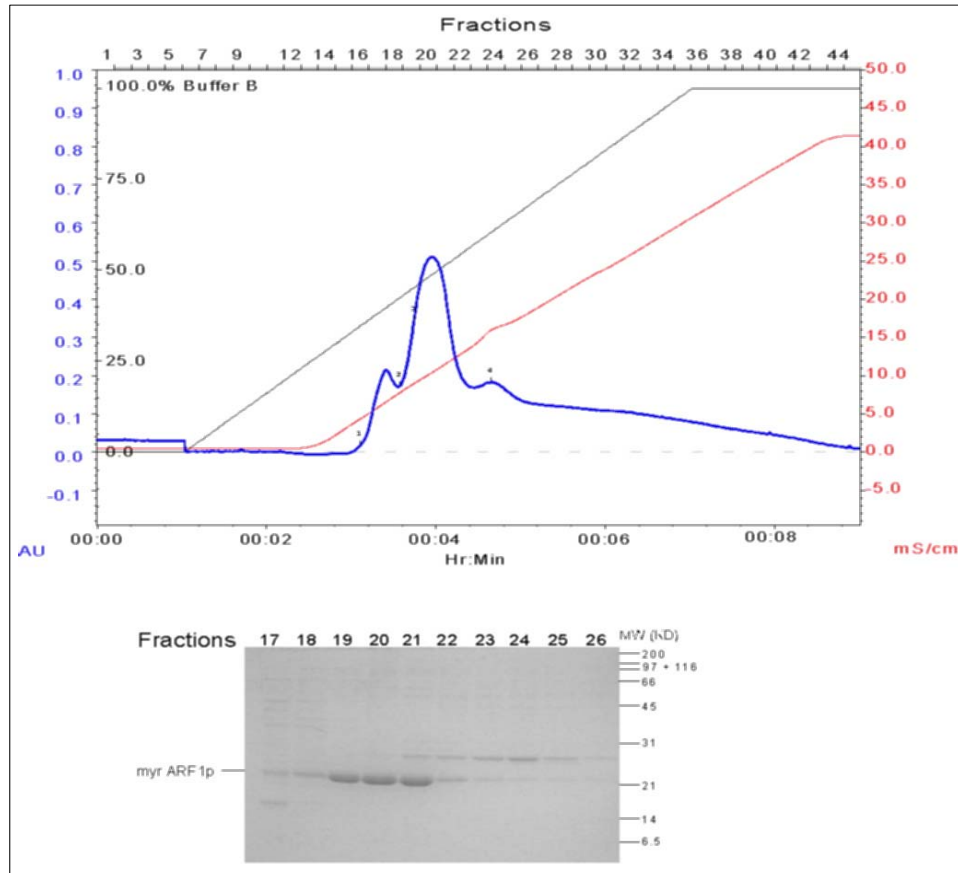


**Figure 5: Purification of myristoylated ARF1p by cation exchange chromatography.** The column was equilibrated with buffer A followed with buffer B to provide the exchange group with the counter ion  $\text{Na}^+$ , then with additional 2 column volumes of buffer A. After Ammonium sulfate precipitation (35% saturation), the sample was desalted using PD10 column to remove any trace of salts and loaded onto the Source-S column. Most of the proteins flow through at this pH. Submitted to a NaCl gradient after binding to the SOURCE-S material, myristoylated ARF1p eluted between 17% and 25% buffer B corresponding to 85 mM to 125 mM NaCl. 5 $\mu$ l of each fraction (from 17 to 26) were loaded on a 15% SDS-PAGE that was stained with Coomassie blue.

To produce non-myristoylated ARF1p, neither myristic acid nor NMT were present during its expression. After lysing the cells, the soluble fraction was precipitated with 50% Ammonium Sulfate saturation to make sure ARF1p will not remain soluble, since at 35% saturation, non-myristoylated ARF1 remains soluble. The purification was carried out as described for myristoylated ARF1p and after Source-S column, 3 mg of pure ARF1p were obtained in fractions 24, 25 and 26 (Fig. 7).



On the other hand, the question whether providing appreciable amounts of NMT would increase the degree of myristoylation of ARF1p and therefore its biological activity was addressed by co-expressing the two proteins after cloning their respective genes into a bicistronic vector (Fig. 6). As compared to the system described above (Fig.4), this allowed the production of significant amounts of NMT1 (Fig. 6).

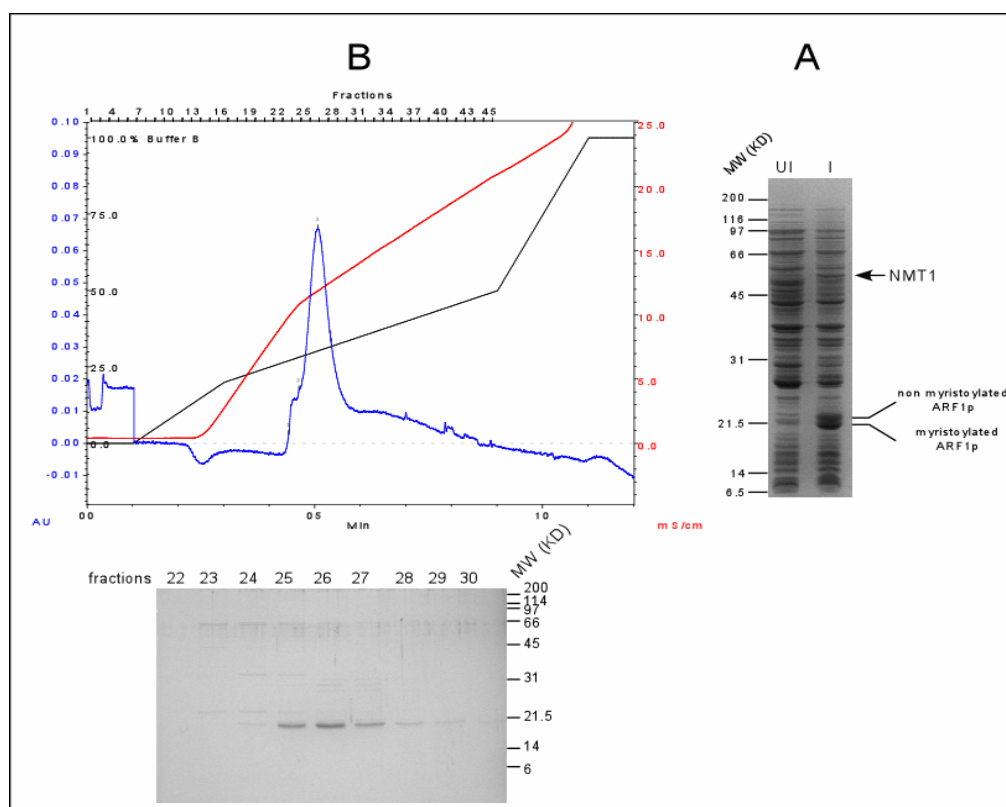


**Figure 6: Co-expression of NMT1 and ARF1p in *E. coli* using a bicistronic vector and purification of myristoylated ARF1p by cation exchange chromatography.** In order to overcome the low level of expression of NMT1 when co transformed with vector carrying the ARF1p gene (See Fig. 4), these two genes were cloned in a bicistronic vector pACYC-DUET1 that carries chloramphenicol resistance. NMT1 gene was cloned in the first multiple cloning site (MCS) while ARF1 was cloned in the second. Both MCS are under the control of a T7 promoter. (A) High expression levels were obtained for NMT1 and ARF1p after 3 hours induction with 1mM IPTG (I) as compared to the uninduced sample (UI). (B) Elution profile of ARF1p from Source-S column. A NaCl gradient (from 0% to 20% buffer B, then from 20% to 50% and finally from 50% to 100% buffer B) was applied under a flow rate of 5 ml/min. ARF1p eluted between 24% and 28% buffer B corresponding to 120 mM to 140 mM NaCl. A volume of 5 $\mu$ l of each fraction (from 22 to 30) was loaded on a 15% SDS-PAGE and stained with Coomassie blue.

Usage of the bicistronic vector yielded a recombinant ARF1p that has the same characteristics as the one produced by double transformation. They have a similar behavior on SDS-PAGE (Fig. 8) and they exchange nucleotide with similar efficiencies. However, as the bicistronic vector is a very low copy vector, the total amount produced in 1 liter is smaller. These data suggest the double expression system is better.

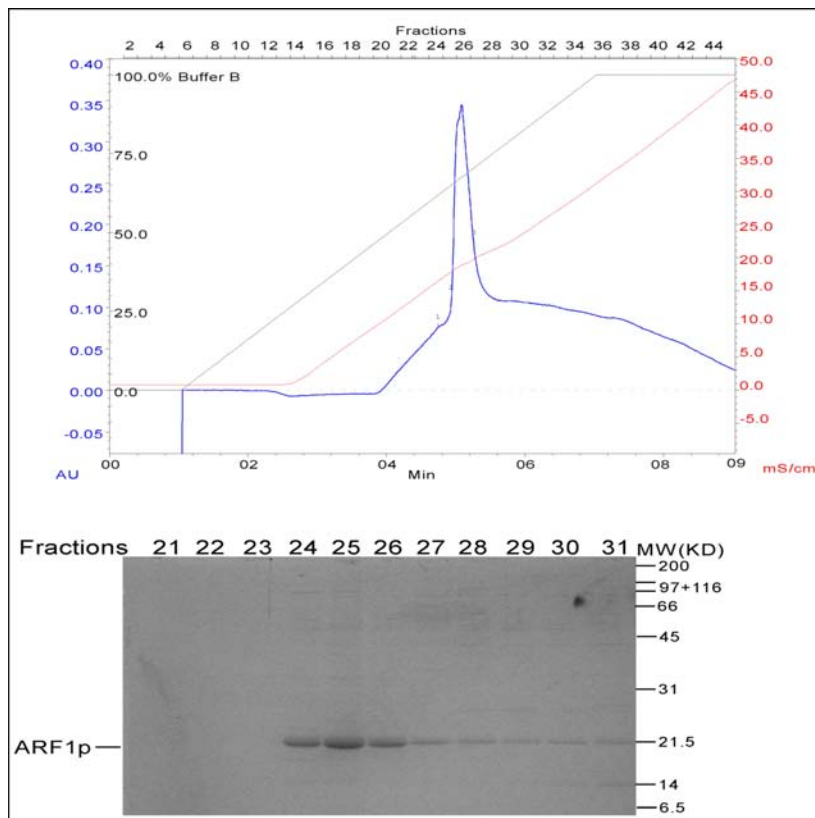


**Figure 7: Elution Profile from a SOURCE-S cation exchange column of non-myristoylated ARF1p over expressed in bacteria.** The column was equilibrated with buffer A then with buffer B to provide the exchange group with the counter ion  $\text{Na}^+$ , in addition the column was equilibrated back with buffer A before loading the sample. After Ammonium sulfate precipitation (50% saturation), the sample was desalted using PD10 column to remove any trace of salts and loaded onto the column. Most of the proteins flew through at this pH. Submitted to a NaCl gradient after binding to the SOURCE-S material, non-myristoylated ARF1p eluted between 35% and 42.5% buffer B corresponding to 175 mM to 212.5 mM NaCl. A volume of 5 $\mu$ l of each fraction (from 21 to 31) was loaded on a 15% SDS-PAGE and stained with Coomassie blue.

To determine that ARF1p is myristoylated, and taking advantage of its property to run slightly faster than its non myristoylated counterpart on SDS-PAGE as shown by Franco and colleagues for the recombinant bovine ARF1 (Franco et al., 1996), migration of the two proteins was compared on SDS-PAGE (Fig. 8). Indeed, two forms appear that migrate differently.

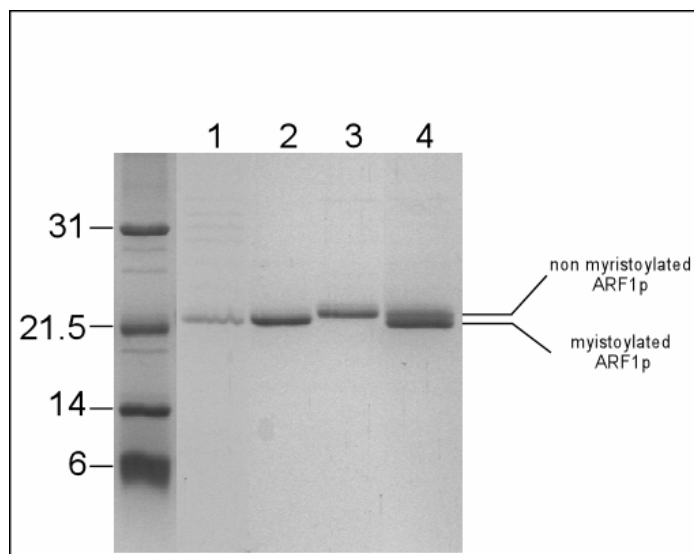


**Figure 8: myristoylated ARF1p runs faster on an SDS-PAGE compared to the non-myristoylated one.** Lane1: myristoylated ARF1p produced in a bicistronic vector together with NMT (fraction 26, Fig. 6). Lane 2: myristoylated ARF1p from fraction 20 (Fig. 5). Lane3: non-myristoylated ARF1p from fraction 25 (Fig. 7). Lane 4: myristoylated and non-myristoylated ARF1p (loaded in lanes 2 and 3). Proteins were loaded on a 15% SDS-PAGE. The myristoylated ARF1p runs slightly faster compared to its non-myristoylated counterpart on an SDS-PAGE.

### 1.3.2 Human ARF1

A protocol by Franco and colleagues (Franco et al., 1996) allows purification of myristoylated human ARF1. It consists of an Ammonium Sulfate precipitation followed by a DEAE column (weak anion exchanger) and a Mono-S column (strong cation exchanger). Herein, a method was established so that only a cation exchange step was used after Ammonium Sulfate precipitation. The same procedure as for yeast ARF1p allows purification to apparent homogeneity of human ARF1p (Fig. 8). Despite the identity between Human and yeast ARF1 (77%), the level of myristoylation of human ARF1 is far lower compared to its yeast homologue. This could be explained by the fact that ARF1p is a natural substrate for NMT1 (both yeast proteins), while the human ARF is not, and therefore the

reaction is less efficient. Ideally human ARF1 is myristoylated up to 20% as indicated in Fig. 9

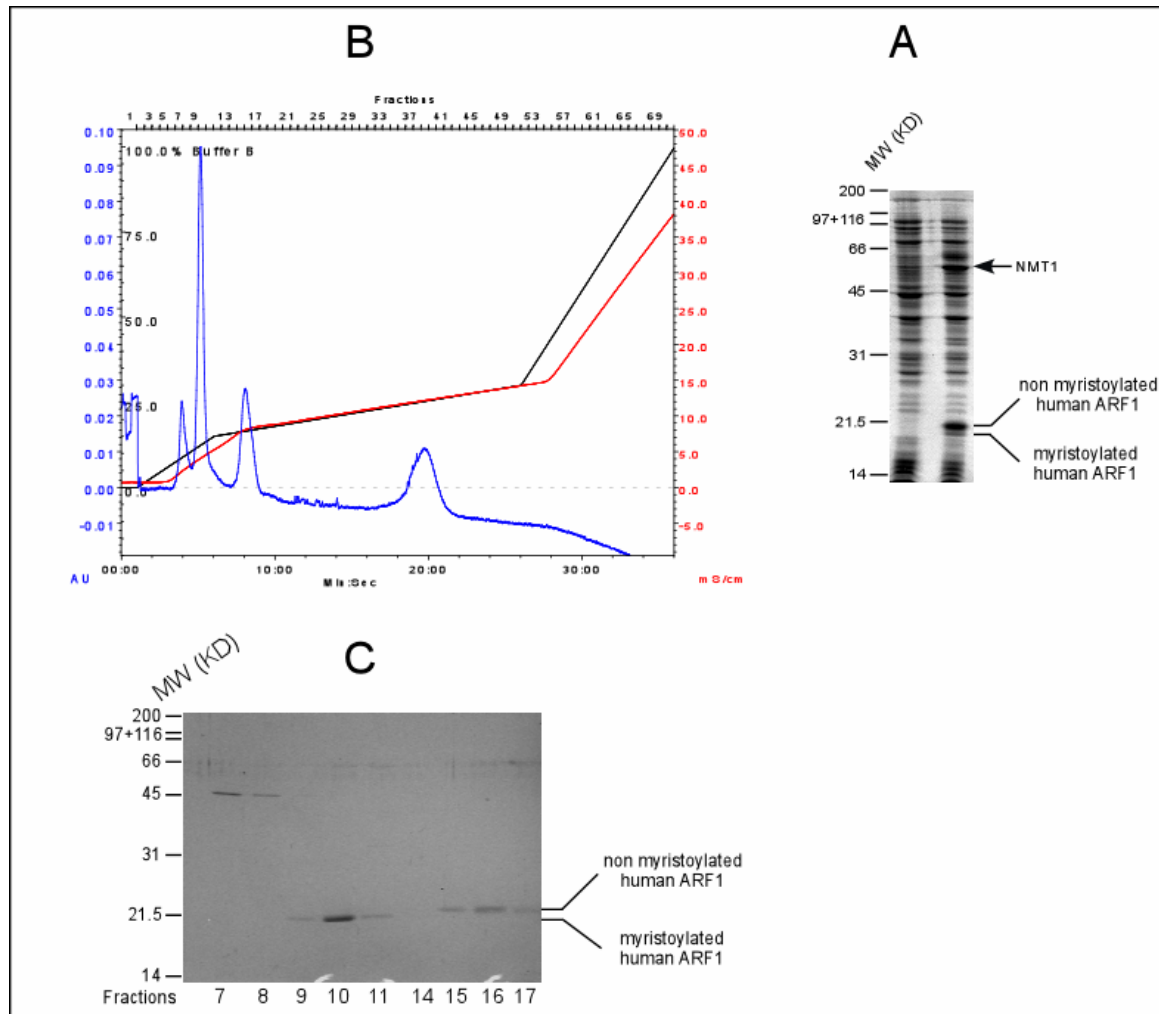


**Figure 9: Over expression and purification of human ARF1 expressed in *E. coli* by cation exchange chromatography.** (A) Expression of human ARF1 cloned into pet11-d (Novagen) and NMT cloned into pBB131 (Duronio et al., 1990) in *E. coli* BL21(DE3). The two vectors have Ampiciline and Kanamycine resistances respectively and the cloned genes are placed under the control of T7 and *tac* promoters respectively. Human ARF1 and yeast NMT1 are expressed after induction with 1 mM IPTG (I) as compared with the uninduced bacteria (UI). Typically about 20% human ARF1 migrates faster on SDS-PAGE, representing the myristoylated form. (B) After precipitation at 35 % Ammonium Sulfate saturation, the precipitate was resuspended in buffer A and desalted. Purification was achieved using a Source-S column as described for the yeast ARF1p. Myristoylated human ARF1 eluted between 17 and 20% buffer B corresponding to 85 to 100 mM NaCl. A volume of 5 $\mu$ l per fraction were loaded on a 15% SDS-PAGE and stained with Coomassie blue.

#### 1.4 Expression, purification and refolding of Glo3p, an ARF GTPase activating protein (GAP) in *E. coli*

ARF-GTPase activating proteins (GAPs) are key regulators of ARFs. One of their major characteristics is the Zinc finger domain which is responsible for GTPase activation. Glo3p seems to be specific for retrograde transport from Golgi to ER in yeast. However its function can be complemented by another yeast GAP, Gcs1p *in vivo*. In addition to their GTPase activation role on ARF1, ARF GAPs were proposed to sort cargo into COPI vesicles since they might interact with the KDEL receptor ERD2 and p24 family proteins (Aoe et al., 1999); (Lanoix et al., 2001). Glo3p is therefore an interesting regulatory element for ARF1p in the context of budding of COPI vesicles using purified proteins and liposomes.

Glo3p was cloned into pET 15-a with a 6XHistidine Tag and was purified according to Poon and colleagues (Poon et al., 1996). BI21(DE3) STAR *E. coli* were transformed with pET15a-GLO3 plasmid and grown at 37°C in LB medium supplemented with 100µM ZnCl<sub>2</sub> until OD<sub>600</sub> = 0.5-0.6 and expression was induced with 1 mM IPTG for 3 hours. After harvesting the cells and breaking them, the post-lysate supernatant does not contain any Glo3p-His since the protein is completely insoluble. Decreasing the temperature with induction down to 16°C did not increase solubility. The post-lysate pellet was resuspended in 8 M urea and pelleted again and Glo3p-His was purified from the soluble fraction by affinity chromatography over Nickel-Agarose beads (Novagen) and eluted with 250 mM Imidazole in presence of 8 M urea (Fig. 10, panel A). The protein concentration is adjusted to 0.1mg/ml and the buffer is exchanged to Hepes buffer (25 mM Hepes, 150 mM KOAc, 1mMDTT, 100 µM ZnCl<sub>2</sub>, 20% glycerol, pH 7.2) by the usage of PD10 column (Amersham biosciences). Each passage through this column removed 95% of urea, therefore after two passages the urea concentration dropped from 8M to 20 mM, a concentration in which the protein is no longer

denatured (Fig. 9, panel B). Renatured Glo3p-His recovers its GTPase activating function on ARF1p as described later in chapter 3.

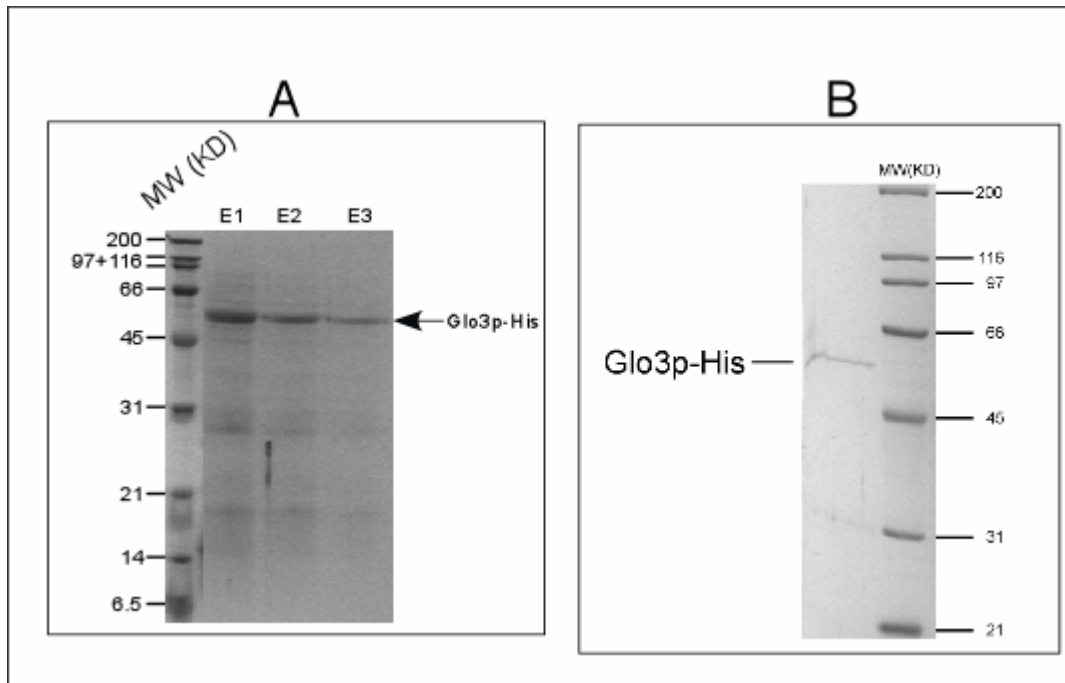


**Figure 10: Purification under denaturing conditions and refolding of Glo3p-His.** (A) Three consecutive elutions of denatured Glo3p-His from Nickel-Agarose beads with 250 mM Imidazole in presence of 8M Urea; (B) Glo3p-6HIS was refolded by rapid buffer exchange in PD10 columns and after adjusting the concentration to 0.1 mg/ml. Gels were stained with Coomassie blue.

## 1.5 TAP-Tagged native yeast coatmer complex

Endogenous coatmer from yeast can be purified to homogeneity using the tandem affinity purification (TAP-Tag) technique (Rigaut et al., 1999). The protein of interest, in this case  $\delta$ -cop, is tagged with a Calmodulin binding domain followed by a TEV protease cleavage site followed by protein A (Cellzome). A first affinity column consisting of IgG beads allowed the binding of protein-A tag. The protein is released from the IgG beads by TEV protease cleavage. A second affinity column consisting of Calmodulin coupled beads allowed the binding of the protein via the Calmodulin binding domain in presence of  $\text{Ca}^{2+}$ . Elution of native endogenous protein with its interacting partners (the other coatmer subunits in this case) is then achieved by addition of EGTA.

The last step in purifying yeast coatmer complex TAP-tagged at the  $\delta$ -cop (Ret2p) subunit is a gel filtration step using Superose-6 (Amersham biosciences). Aggregates were present in the exclusion volume (typically 30% of the bed volume corresponding to 0.8 ml) and coatmer elutes between 1.1 ml and 1.5 ml. Based on the calibration of the column, coatmer complex has an apparent molecular weigh of 750 KD while the predicted size assuming a one to one stoichiometry between the seven subunits is 560 KD.

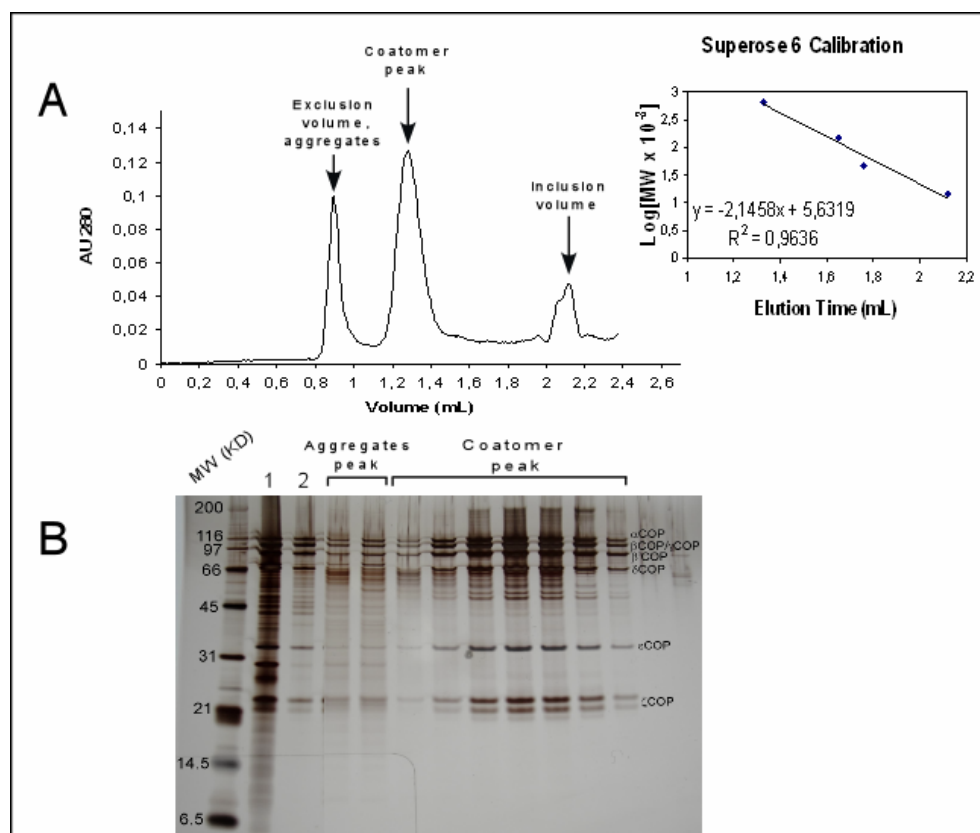


**Figure 11: TAP-tag purification of yeast  $\delta$ -cop-TAP coatmer.** Lanes 1 and 2 in panel B show the eluates from the IgG and the Calmodulin affinity columns respectively. Coatmer was further purified using a Gel filtration column (Superose 6: PC 3.2/30, 2.4 ml bed Volume). Rest of the panel B shows the elution profile of caotmer. The column was previously calibrated (A right) with 4 standard proteins (Thyroglobulin, 660 KD; Alcohol dehydrogenase 150 KD; Ovalbumin, 45 KD; Lysosyme, 14.5 KD). The running buffer contains 25 mM Hepes at pH= 7.4, 200 mM NaCl, 1 mM DTT, 5% Glycerol, 0.02% Sodium Azide. A volume of 10  $\mu$ l of each fraction was loaded on 10% SDS-PAGE and silver stained (Silver Quest, Invitrogen).

## 1.6 Native coatomer complex from rabbit liver

Mammalian coatomer, a seven subunit complex, was first purified in its native state from rabbit liver cytosol (Pavel et al., 1998; Serafini et al., 1991). After Ammonium sulfate precipitation, a DEAE-Sepharose and two consecutive Resource Q columns were used. Typically, from 15 to 20 g of cytosolic protein, 20 to 30 mg coatomer can be obtained to an apparent purity of 50 to 60 %, as shown in Fig. 12

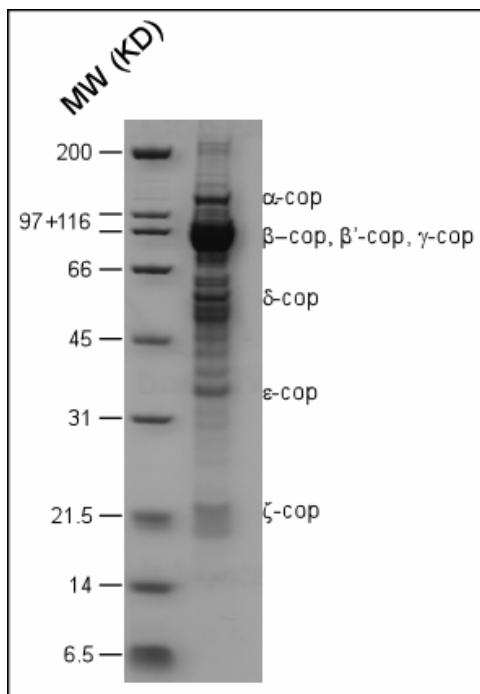


**Figure 12: Purified rabbit liver coatomer.** Coatomer was purified from 15 to 20 g cytosolic proteins in three steps. After Ammonium sulfate precipitation, three columns were used, A DEAE Sepharose and two Resource Q columns. 50% to 60% pure coatomer elutes was obtained. Here is shown a Coomassie stained 10% precast gel (Invitrogen). Details are provided in the methods section.



## 2 Setting up a reconstituted system with chemically defined components

### 2.1 Liposomes stand for Golgi membranes

#### 2.1.1 Generating large liposomes

Reconstitution of COPI vesicular transport *in vitro* requires purified components. In addition to the proteins described in chapter 1, here we address the membrane environment that mimics Golgi membranes and from which COPI vesicles emerge. Analysis of Golgi membranes in mammalian cells (van Meer, 1998) (Brugger et al., 1997) allowed determining their lipid composition as summarized in table 1. As generating large liposomes has been achieved mainly with a modified method from Kinuta and colleagues (Kinuta and Takei, 2002; Kinuta et al., 2002), this method was applied.

To generate Golgi like liposomes, a lipid mixture (referred to as Golgi mix) was dried under Argon to remove solvent. The lipid film obtained was hydrated with a water saturated Argon stream before being finally resuspended in an aqueous buffer (Hepes 25 mM pH = 7.4, KCl 150 mM, Sucrose 2.5% (w/v)). The mixture was submitted to 10 cycles freeze (liquid nitrogen) and thawing (50°C) and kept in a water bath at 37°C for 2 hours. Liposomes that form at this step were finally selected for size by extrusion through 800 nm pore size filters (Avestin).

Lipid	MW [Da]	Amount [mol%]
PC	786,12	42
PE	768,06	19
PS	810,03	5
PI	909,12	10
SM	703,44	7
CL	386,66	16
Rhodamine-PE	1333,81	1

**Table 1: Mammalian Golgi lipid composition used to prepare liposomes (Golgi mix).** PC, phosphatidylcholine. PE, phosphatidylethanolamine. PS, phosphatidylserine. PI, phosphatidylinositol. SM, sphingomyeline. CL, cholesterol. Rhodamine-PE (Rhodamine coupled to phosphatidylethanolamine is used here to serve as a fluorescent tracer for liposomes.

Liposomes were checked by electron microscopy and their size was found still not to be homogenous, although a large part of the liposomes have a diameter of 200 nm (Fig. 13). Bigger structures coexist with small ones. In the context of budding COPI vesicles (~70 nm diameter) from donor liposomes it is critical to make sure the liposomes size is large and that no small preexisting structures would be present, in order to avoid small coated vesicles to be generated by mere coating rather than by coating and budding.

In order to further purify a fraction of large liposomes, gel filtration was applied.

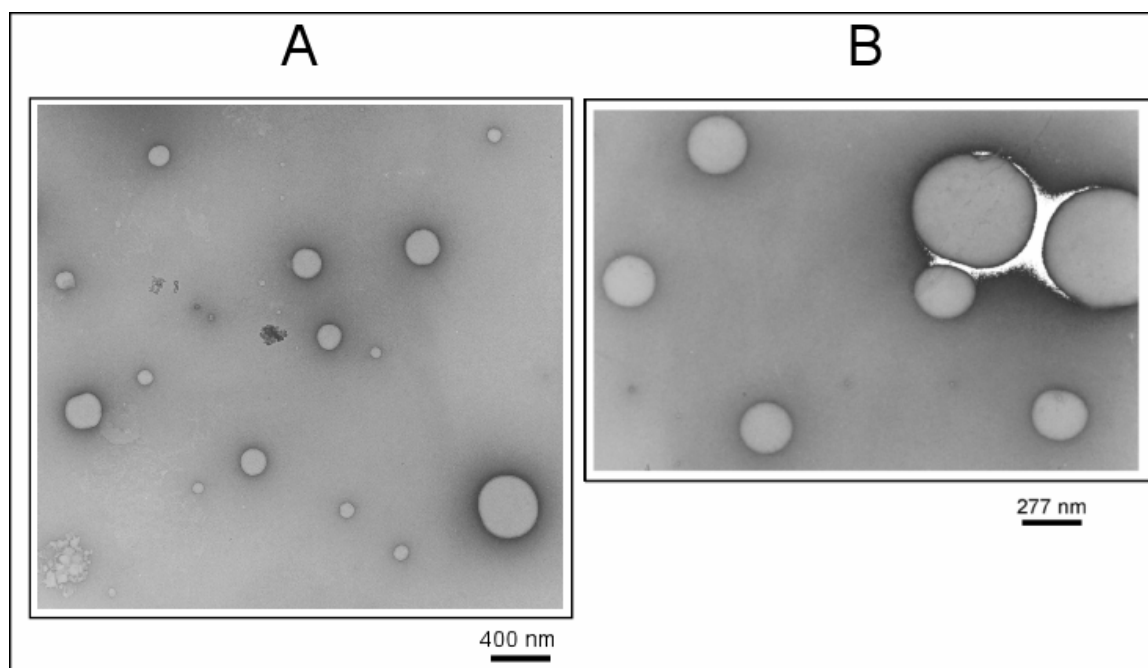
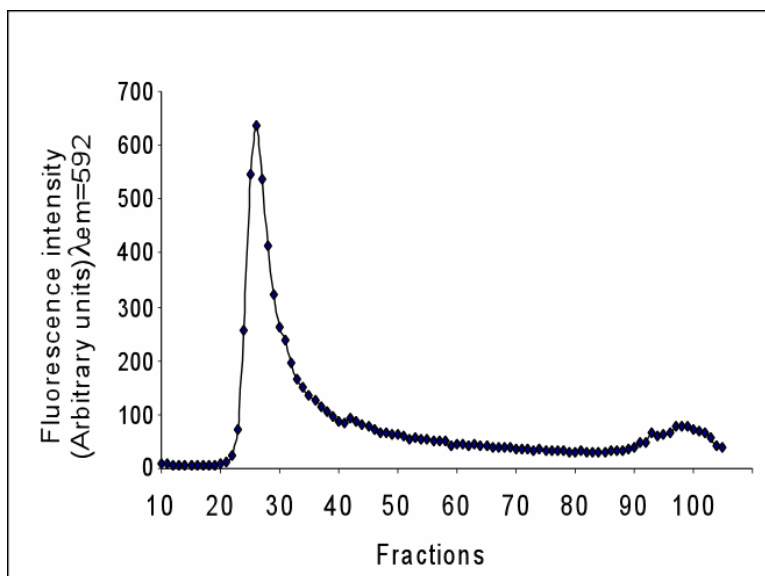


**Figure 13: Analysis of liposomes by electron microscopy.** Two Electron microscopy photographs representing the same preparation of unilamellar liposomes obtained under the conditions described above. Picture **A** shows a broad size distribution of liposomes ranging from less than 100 nm to 400 nm diameter sizes. Picture **B** shows the presence of very large structures (diameter above 500 nm).

A Sephacryl-1000 column (Amersham biosciences) that allows exclusion of particles with a diameter over 400 nm (corresponding to 30% of the bed volume, according to the manufacturer specifications) was equilibrated with 3 bed volumes of a HEPES buffer (HEPES-KOH 25 mM, KCl, 150 mM, pH=7.4) supplemented with 20 mg/ml BSA to prevent liposomes from unspecific interactions with the column.

The liposomes contained 1 mol% of Rhodamine-PE, a fluorophore that is excited at  $\lambda_{\text{ex}}=558$  nm and emits at  $\lambda_{\text{em}}=592$  nm. This way, liposomes are detected by their fluorescence (Fig. 14). The size of liposomes can be directly assessed by Dynamic light scattering (DLS).



150 mM KCl, pH 7.4). Column was previously equilibrated in 3 bed volumes of the same buffer supplemented with 20 mg/ml BSA. Since liposomes contain Rhodamine-PE, a fluorophore that emits at  $\lambda_{\text{em}}=592$  when excited at  $\lambda_{\text{ex}}=558$  nm, they were monitored via the fluorescence intensity of the fluorophore. Liposomes were eluted from the column starting from 22 ml. Fluorescence was measured from fractions 10 to 107.

**Figure 14: Size separation of liposomes by Gel filtration.** Liposomes were loaded onto a 55 ml Sephacryl-1000 column and eluted at a flow rate of 1 ml/min in Hepes buffer (25 mM Hepes,

Directly after gel filtration, the size of liposomes was checked by dynamic light scattering. As expected, the first liposomes to be eluted from the column had the largest size (Fig. 14).

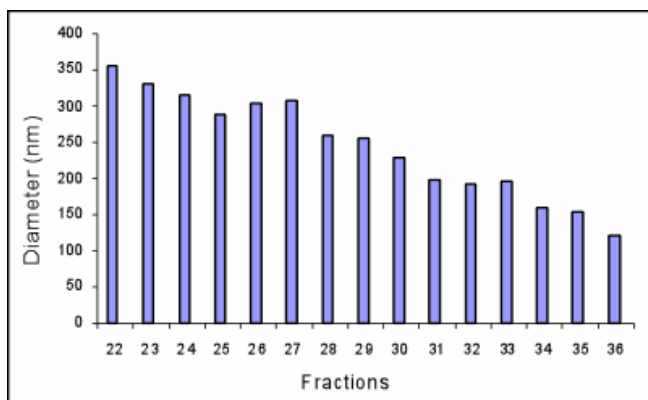


**Figure 15: Size distribution of the liposomes after gel filtration measured by dynamic light scattering (DLS).** Fractions from 22 to 36 were submitted to DLS measurements and their diameter was calculated using an algorithm integrated in the software from the supplier (see details in Materials and methods).

Since the liposomes were made in a buffer containing 2.5% sucrose, a way to concentrate them after separation by size was to pellet the fractions containing the largest liposomes by centrifugation at 900g. They appeared as a red pellet that could be resuspended in a desired volume of buffer. Fractions 22 to 27 were pelleted and their lipid content calculated (see quantification principle in 2.1.3). The lipid content in this case represented 9% of the starting liposomes loaded onto the column. The recovery of large liposomes by gel filtration was usually around 10% of the input.

### **2.1.2 Synthesis of lipopeptides with cytoplasmic domains of the p24 family members**

As a next step to generate the components needed for the formation of budding competent liposomes from chemically defined building blocks, lipopeptides were prepared that contain the cytoplasmic domains of p24 family members proteins. By this way, these coatmer receptor domains can be stably incorporated into liposomes.

The C-terminal cytoplasmic domain of p24 family members can be synthesized and covalently attached to a lipid moiety (Nickel and Wieland, 2001). A commercially available lipid (1,2-dioleoyl-sn-glycero-3-phosphoethanolamine-n-[4-(p-maleimidophenyl) butyramide] (MPB-PE; Avanti Polar lipids) was used. MPB-PE contains a maleimido group which reacts with the thiol group of cysteine added to the peptide to form a stable thioether bond (Fig. 15). Lipopeptide was then purified by reverse phase chromatography on a Sep-Pak C18 cartridge.

Typically the yield of this reaction (based on the input of MPB-PE) was above 60% for p23 and less than 10% for p24 lipopeptides.

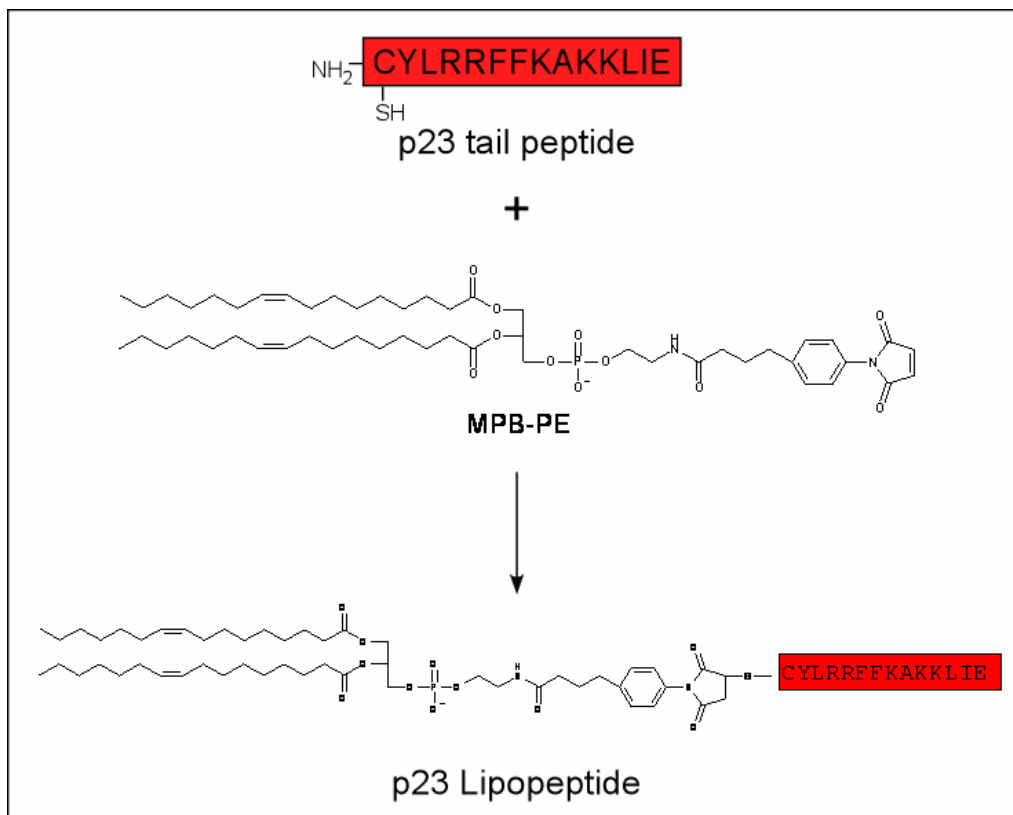


**Figure 16: Synthesis of p23 lipopeptide.** p23 tail peptide carrying an additional cysteine at the N-terminus was chemically anchored to a lipid moiety (MPB-PE) to form a lipopeptide. The maleimido group of MPB-PE reacted with the free thiol group of the cysteine to form a stable thioether bond.

The sample was loaded onto a reverse phase chromatography cartridge (Sep-Pak C18) and subjected to an Acetonitrile step gradient in the presence of 0.1% trifluoroacetic acid (TFA) (Nickel and Wieland, 2001). p23 lipopeptide eluted at 80% and 90% Acetonitrile / 0.1% TFA while p24 lipopeptide elutes at 90% and 100% Acetonitrile (Fig. 17)

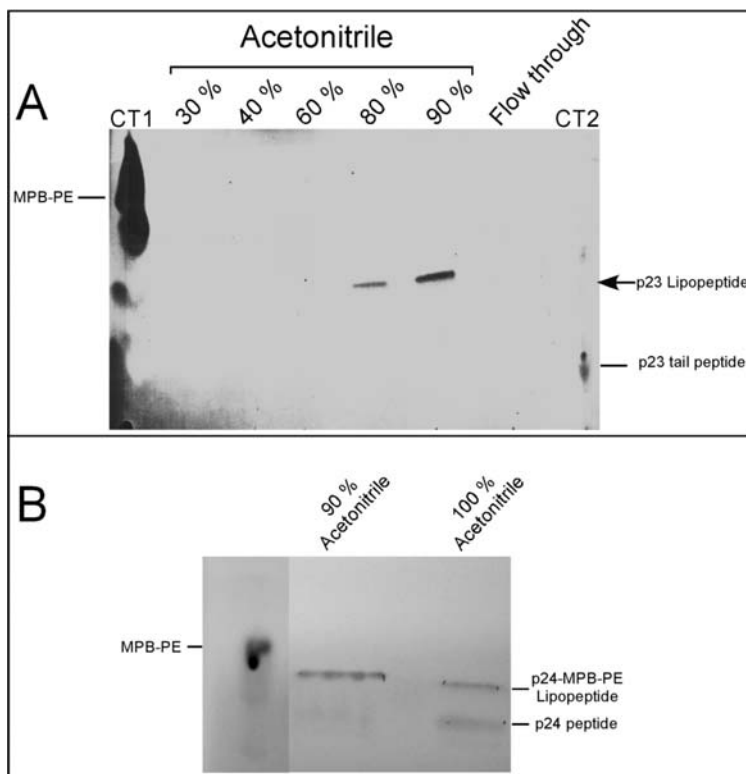


**Figure 17: Analysis of p23 and p24 lipopeptides synthesis by thin layer chromatography (TLC).** Panel A shows p23 lipopeptide eluted from the Sep-Pak C18 column at 80% and 90% Acetonitrile + 0.1% TFA. MPB-PE and p23 tail peptide were also loaded as controls (CT1 and CT2 respectively) on the TLC and showed a different running behavior compared to p23 lipopeptide. Panel B shows that p24 lipopeptide eluted at 90% and 100% Acetonitrile + 0.1% TFA. The running solvent was a mixture of butanol, pyridine, acetic acid (glacial) and water (9.7: 7.5: 1.5: 6; v:v:v). After being developed, silica plates were dried and placed in a chamber containing solid iodine that allowed staining MPB-PE, p23 and p24 peptides and lipopeptides.

### 2.1.3 Quality control and quantification of liposomes

The quality of liposomes is an important criterion for using them as a membrane matrix to study vesicular transport mechanisms *in vitro*. Under the conditions described earlier (paragraph 2.1.1.), liposomes appear to be unilamellar (Fig. 13). Size exclusion chromatography allows selecting for the largest structures. The sizes of liposomes measured by DLS were in accordance with the sizes given by electron microscopy, providing an easy and fast method to check the size of liposomes routinely.

On the other hand, to quantify the lipid content in a sample containing liposomes, a classical method allows determination of their phosphate content (Rouser et al., 1970) that correlates to the lipid content. When Golgi like lipids (Golgi mix) were used, cholesterol (16%) is subtracted since it is not a phospholipid.

Alternatively and in order to increase the sensitivity of the detection of liposomes and to allow a much faster analysis, profit was made of a fluorescent lipid tracer (Rhodamine-PE) to quantify lipids.

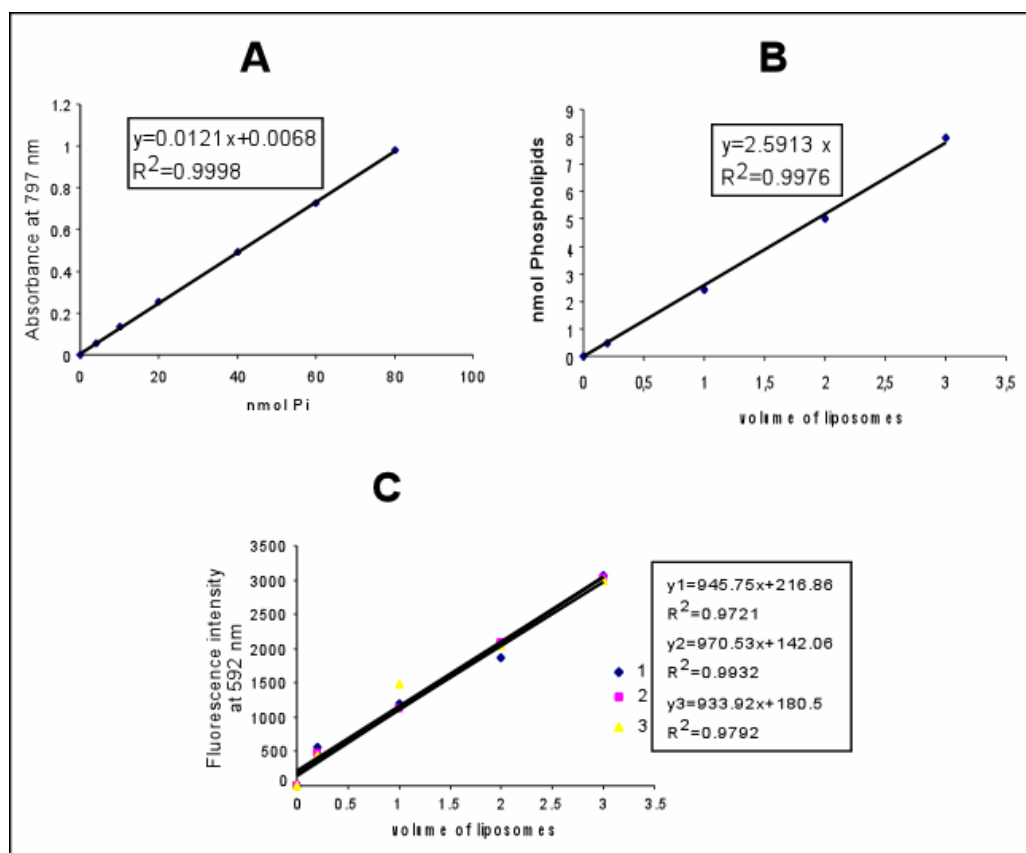


**Figure 18: Quantification of lipids using phosphate determination and Fluorescence.** A shows a standard curve of known amounts of phosphate. B shows the amounts of phospholipids present in various volumes of the liposome preparation as deduced from A. C shows the fluorescence emitted from the same volumes of liposomes analyzed in B. three samples were checked for reproducibility. Liposomes were made under conditions described above so that 1mol% Rhodamine-PE was present. The fluorophore was excited at  $\lambda_{ex}=558$  nm and emission was analyzed at  $\lambda_{em}=592$ .

After standardization (Fig 18, A), the phospholipid amounts present in liposomes were deduced (Fig. 18, B) and correlated to the fluorescence intensities (Fig. 18, C). It was then possible to directly determine the amounts of phospholipids by monitoring the fluorescence of Rhodamine-PE. This was particularly useful to determine the amount of liposomes present after reconstitution.

## **2.2 Reconstitution of SNARE proteins into liposomes**

To study the incorporation of SNAREs into COPI coated vesicles *in vitro*, a major requirement was to include them into liposomes. This was achieved by two different methods. The first consisted of reconstituting the full length SNARE while the second made profit of the strategy described in Fig. 15 to chemically anchor cytoplasmic domains of SNAREs with an additional cysteine to MPB-PE.

### **2.2.1 Reconstitution by dilution below the critical micellar concentration**

This method consisted of mixing the SNARE protein which was purified in presence of detergent (1% (w/v)) OG to a lipid film followed by a rapid dilution of the detergent (OG) below its critical micellar concentration (CMC) promoting liposomes formation (Weber et al., 1998) as shown in Fig. 19.

Liposomes were recovered and concentrated by flotation in a Nycodenz gradient that consisted of 3 steps, 40%, 30% and 0% Nycodenz. The SNARE containing liposomes floated at the interface between 30% and 0% Nycodenz (Fig. 20), while uncoupled protein was found at the bottom of the gradient (40% Nycodenz). Since the liposomes contained 1 mol% Rhodamine-PE, they formed a visible red layer that was easily collected for analysis.



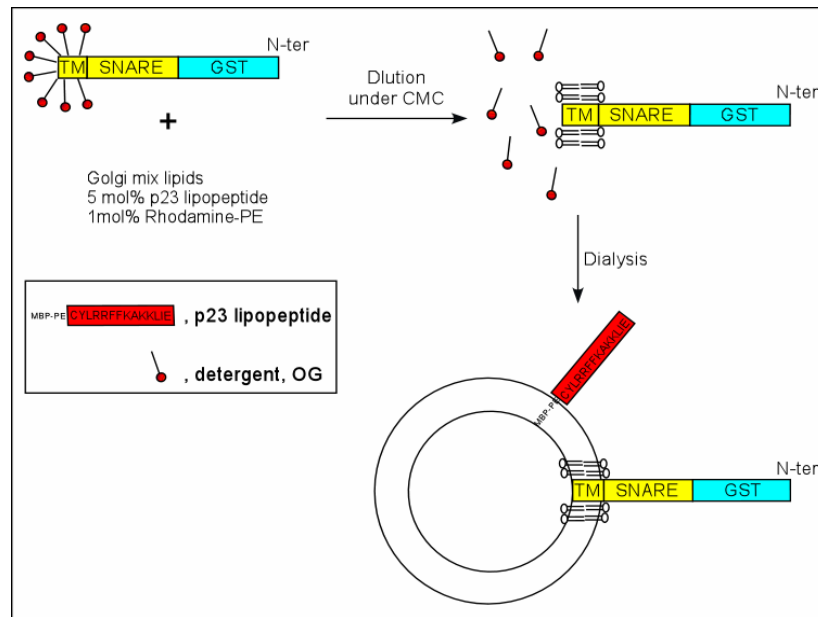


**Figure 19: Preparation of full length SNARE containing donor liposomes.** The micelle surrounding the transmembrane domain of the SNARE is disrupted after dilution, and the protein reconstitutes into liposomes. Detergent is then removed by dialysis.

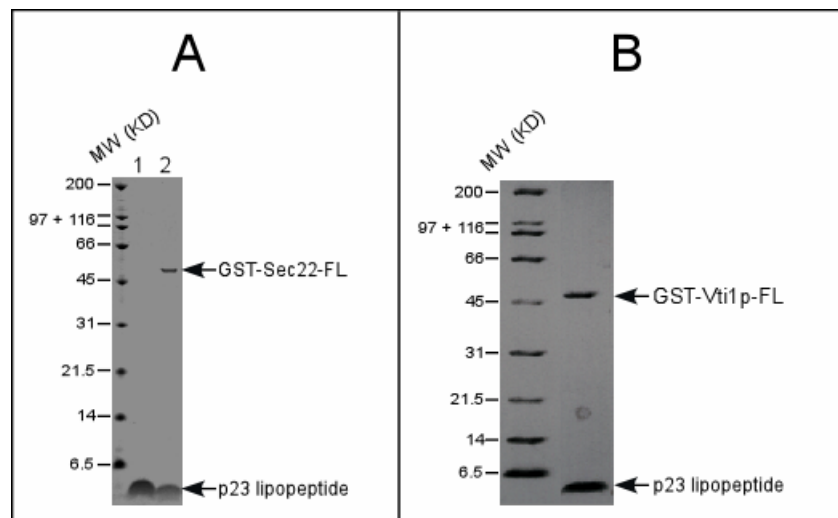


**Figure 20: Reconstitution of GST-Sec22p-FL and GST-Vti1p-FL into p23 containing liposomes by dilution and dialysis.** Panel A, lane 1 shows control p23 containing liposomes formed using the same method without addition of protein and in the presence of 1% OG (w/v) instead, lane 2 shows the reconstitution of GST-Sec22p-FL. Panel B shows the reconstitution of GST-Vti1p-FL. Either p23 containing liposomes or p23 and SNARE containing ones were floated in a Nycodenz gradient and collected in the 30% / 0% Nycodenz interface. 10 $\mu$ l samples were loaded on 10% precast SDS-PAGE (Invitrogen) in A and 15% SDS-PAGE in B and stained with Coomassie blue.

### 2.2.2 Reconstitution by chemical coupling to a cysteine residue

The strategy described in Fig. 15 was used to couple liposomes containing MPB-PE to the cytoplasmic domain of Bos1p fused to GST (GST-Bos1p-cys), and containing a C-terminal additional cysteine to (Fig. 21).

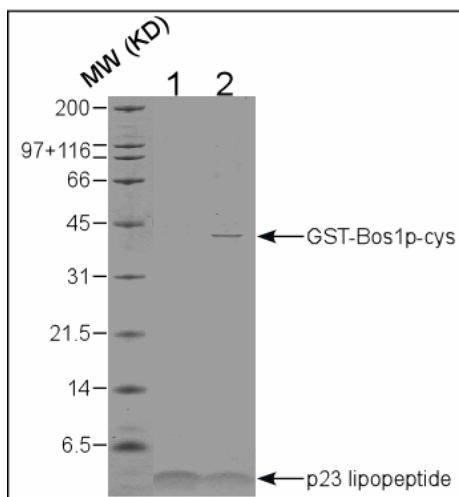


**Figure 21: Chemical coupling of GST-Bos1p-cys to liposomes containing MPB-PE.** Lane 1 shows original liposomes containing p23 lipopeptides. After coupling, liposomes were floated in a Nycodenz step gradient and collected at the interface between 30% and 0%. 10 $\mu$ l samples were loaded on a precast 10% SDS-PAGE (Invitrogen) and stained with Coomassie blue (lane 2).

Recovery of liposomes after floatation was checked by measuring the fluorescence intensity after coupling and comparison to standard amounts (Fig. 17). The protein coupling is estimated from the intensity of the protein band after reconstitution. After flotation, liposomes represent 80% of the input, and 50% of the input protein is present in the liposome fraction, indicating the coupling of 50% of the protein to MPB-PE containing liposomes. Given an average diameter of 200 nm, 65  $\text{\AA}^2$  per phospholipid, and a total amount of 40  $\mu$ g of GST-Bos1-CD that was recovered, each liposome contains 7000 copies of SNAREs for about 2,000,000 phospholipids (1 SNARE for 270 phospholipids).

### 2.2.3 Orientation of SNAREs after reconstitution

The SNAREs reconstituted by dilution and dialysis (Fig. 19) can be oriented either to the lumen of the liposome or to the external part. Since the SNAREs fused to GST contain a thrombin cleavage site, an outside orientation would leave the cleavage site accessible. Interestingly, as shown in Fig. 22, Sec22p is completely digested indicating a total outside orientation, while a majority of Vti1p is digested (up to 80% based on the bands intensities), indicating Vti1p is predominantly oriented to the outside. Reconstitution by dilution and dialysis of SNAREs leads to an orientation that resembles their orientation *in vivo*.

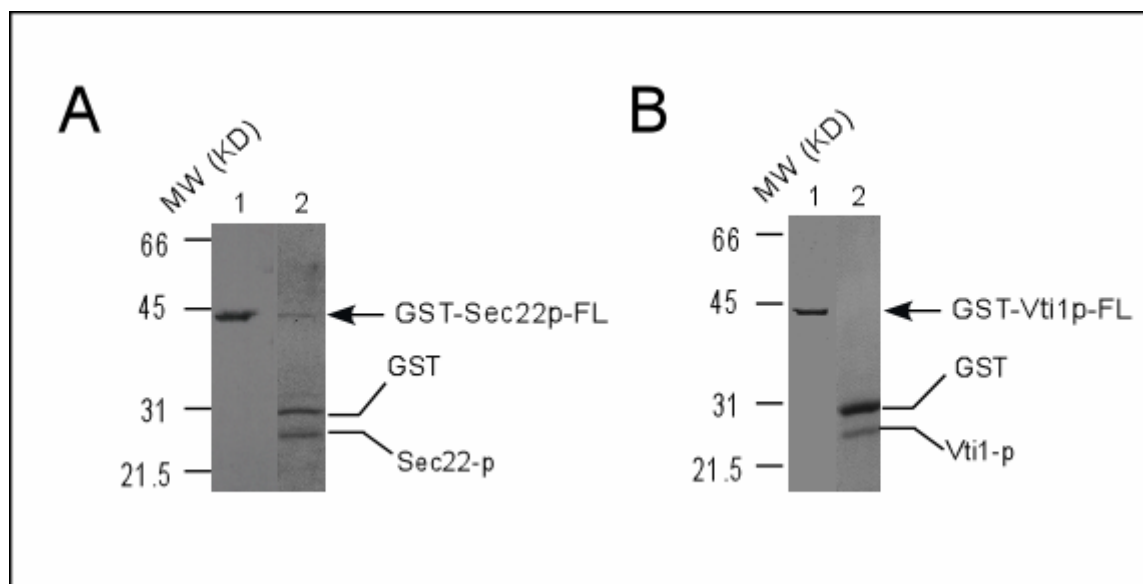


**Figure 22: Orientation of SNAREs reconstituted in liposomes.** After reconstitution, GST-Sec22-FL liposomes (**A**) and GST-Vti1p-FL liposomes (**B**) were submitted to digestion with 1 unit of the thrombin protease (lanes 2 in **A** and **B**) and analyzed by SDS-PAGE and Coomassie blue staining. Digestion was complete in the case of Vti1p (**B**) and complete to about 80% for Sec22p (**A**). Lanes 1 in A and B show the input proteins before digestions.

### 3 Functional aspects

As another prerequisite to reconstitute liposome budding, the small GTPase ARF1 was expressed as a recombinant protein and purified.

#### 3.1 Nucleotide exchange activity of ARF1 and GAP activity of Glo3p

After purification (see materials and methods), the biological activity of ARF1p, that is its conformational change upon exchange of GDP to GTP was measured *In vitro* by monitoring in real time the correlated increase of ARF1p tryptophan fluorescence (Antonny et al., 1997; Kahn and Gilman, 1986). Here, the fluorescence of Trp<sup>78</sup> is monitored. This tryptophan residue is conserved in the switch II domain of G-proteins  $\alpha$  subunits whose fluorescence increases upon GTP binding (Faurobert et al., 1993). Nucleotide exchange activities of myristoylated yeast ARF1p (fraction 19, Fig. 5 and fraction 26, Fig. 6) as well as yeast non myristoylated ARF1p (fraction 25, Fig.7) were measured (Fig. 23, 24, 25). Furthermore, the kinetics of GTPase activation by Glo3p was determined (Fig.23, D). For comparison, nucleotide exchange activity of myristoylated human Arf1 was checked (Fig. 26)

Nucleotide exchange activities were obtained by fitting the curves to a single exponential model ( $Y = IF (X < X_0, \text{Plateau}, \text{Plateau} + (1 - e^{(-K * (X - X_0))})$ ). That takes into account the speed of the fluorescence increase to the plateau, represented by a velocity constant ( $K \text{ (s}^{-1}\text{)}$ ). The span of the curve is a direct function of ARF-GTP concentration. Knowing the amount of ARF-GDP, specific activities can be represented as: **Specific activity = (Span \* K) / [ARF-GDP]**, (proportional to  $\text{mol.L}^{-1}.\text{s}^{-1}.\mu\text{g}^{-1}$ )

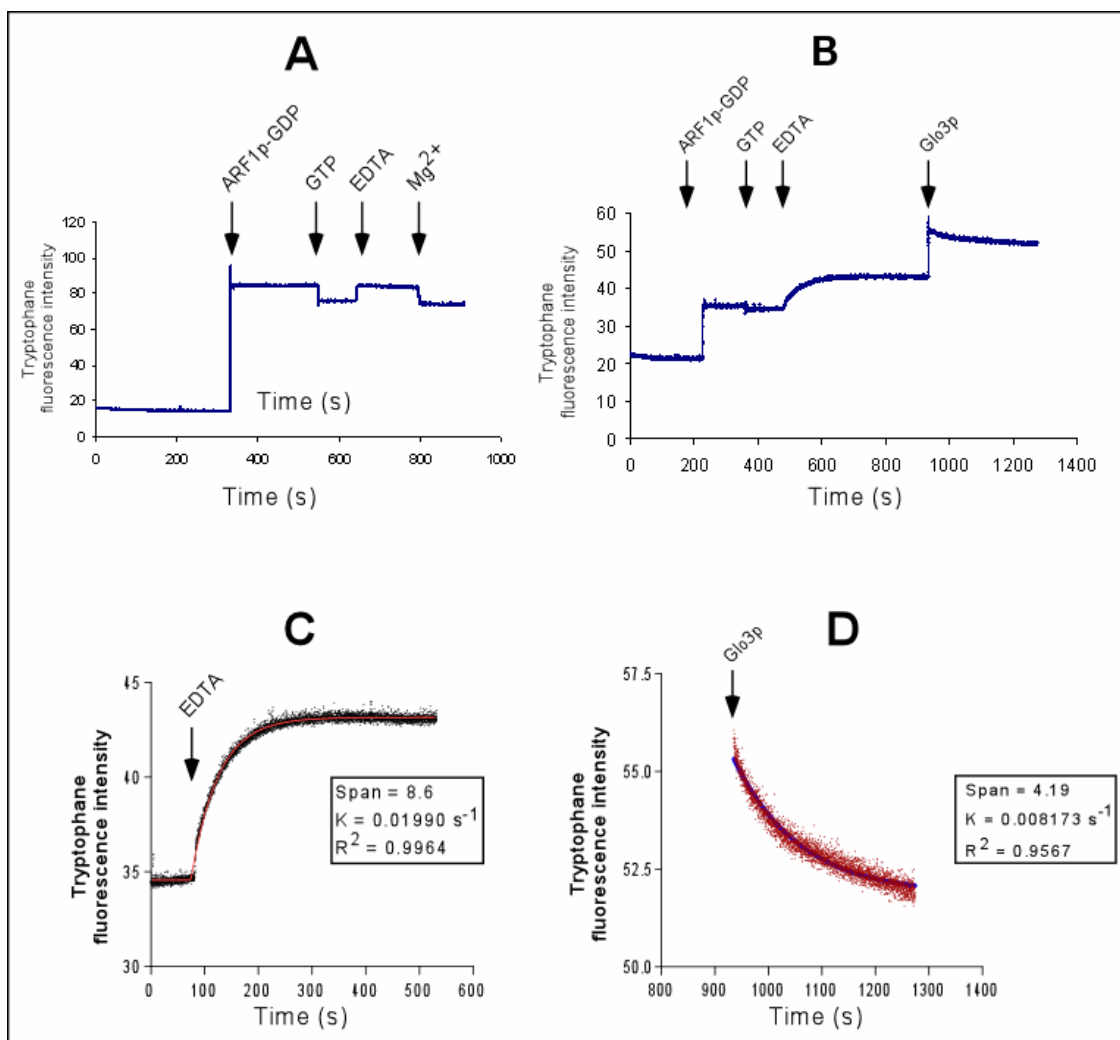


**Figure 23: Nucleotide exchange activity of myristoylated yeast ARF1p and GTPase activation by yeast Glo3p are liposomes dependent.** Conformational change of ARF1p upon nucleotide exchange was monitored by intrinsic tryptophan fluorescence (excitation = 297.5nm, emission = 340 nm) at 37°C. **(A)** Three  $\mu$ l of myristoylated ARF1p-GDP (1.11 $\mu$ g) was injected in a fluorescence cuvette containing 530  $\mu$ l buffer (25 mM Hepes, 150 mM KCl, 2 mM  $MgCl_2$ ) and 60  $\mu$ l of 3mM Golgi like liposomes. At the indicated times, GTP (50 nmol), EDTA (2 mM) and  $MgCl_2$  (2mM) were added. Addition of EDTA did not promote exchange of GDP to GTP since the fluorescence signal stays flat. **(B)** ARF1p-GDP (1.11  $\mu$ g) was added to a fluorescence cuvette containing 180 nmol phosphatidylcholine liposomes in the same buffer as in **(A)**. At the indicated times, GTP (50 nmol), EDTA (2 mM) and the ARF-GAP Glo3p (1 $\mu$ g) were added. Addition of EDTA promoted GDP release and its substitution by GTP (increase of fluorescence). ARF1p GTPase activity was triggered by the addition of Glo3p. **(C)** Increase of fluorescence observed in **(B)** was fitted to an exponential model that determines the velocity constant (K) and the span between the plateau before addition of EDTA and the plateau at saturation. **(D)** After addition of 1 $\mu$ g Glo3p, decrease of fluorescence (hydrolysis of GTP from ARF1p by the action of Glo3p) is plotted according to an exponential regression decay model; the velocity constant (K) and the span were determined.

In order to determine the GTPase activation of Glo3p, the curve was fitted to a single exponential decay model. One  $\mu\text{g}$  of refolded Glo3p (Fig. 10) was added to the fluorescence cuvette after exchange had occurred (Fig. 23, **B**), and resulted in a decrease of fluorescence. Velocity constant ( $K$ ) and span were measured and specific activities calculated (**Specific activity = (Span \* K) / [ARF-GDP]**, (proportional to  $\text{mol.L}^{-1}.\text{s}^{-1}.\mu\text{g}^{-1}$ ).

The activities are summarized in Table 2.

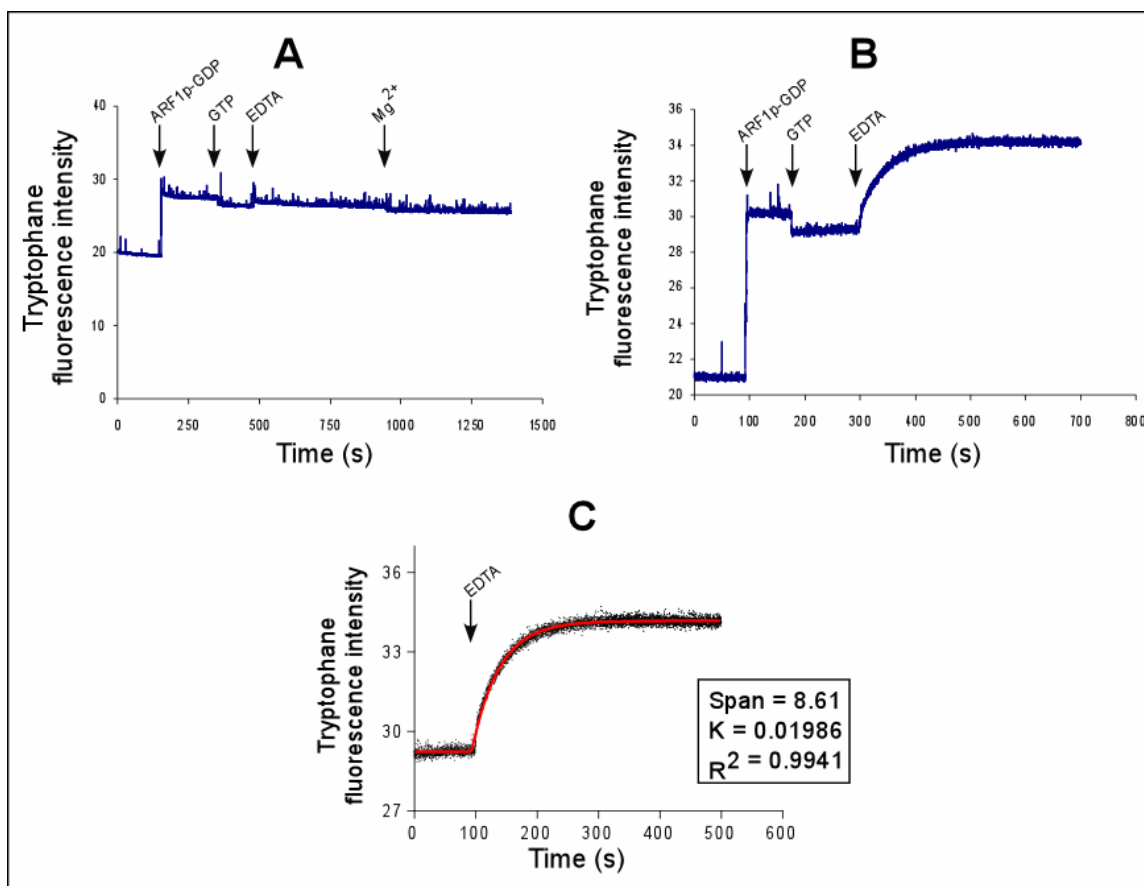


**Figure 24:** myristoylated yeast ARF1p produced using a bicistronic vector encoding AFR1p and NMT1 is comparable to the ARF1p produced by double transformation. Nucleotide exchange activity was measured under the same conditions described in Fig 21 except that 1.4  $\mu\text{g}$  of ARF1p were added. (**A**) No increase of fluorescence was observed in the absence of liposomes. (**B**) In presence of liposomes and upon addition of EDTA, increase of tryptophan fluorescence was observed and fitted to an exponential model. The velocity constant ( $K$ ) and the span were determined.

Non myristoylated ARF1p (fraction 26, Fig. 7) was submitted to the same assay. Non myristoylated ARF1p was able to exchange GDP for GTP both in presence and in absence of liposomes (Fig. 25)

The fact that none of the myristoylated ARF1p described above was able to exhibit a nucleotide exchange in solution (panels **A**) is, in addition to their mobility on SDS-PAGE (Fig. 8), an indication that they are totally myristoylated. Otherwise, one would expect to see a small increase of fluorescence in solution after addition of EDTA, which did not occur (Fig 23 and 24).

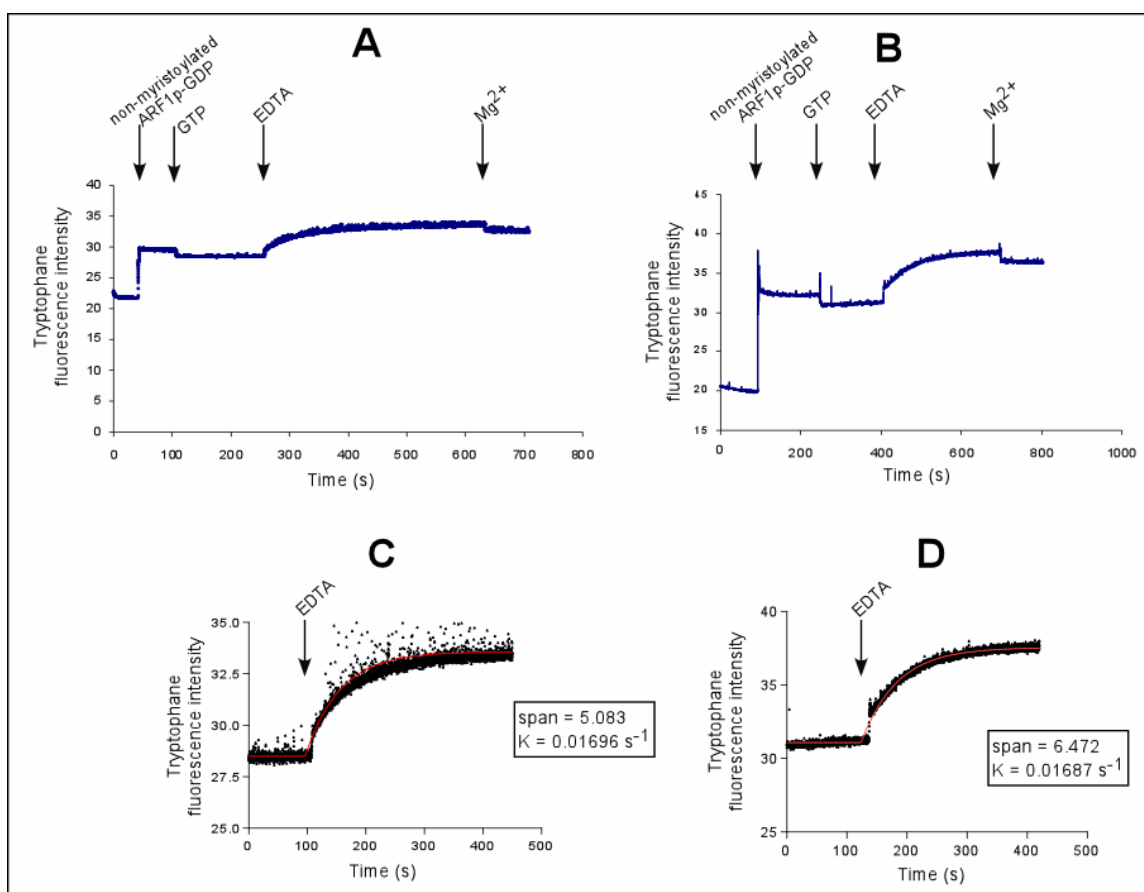


**Figure 25: Non myristoylated ARF1p exhibits a nucleotide exchange activity that is liposome independent.** Nucleotide exchange activity was measured under the same conditions described in Fig. 23 and 24 except that 1.12  $\mu\text{g}$  of ARF1p were added in this case. Upon addition of EDTA, increase of fluorescence was observed both in presence (**A**) and in the absence (**B**) of liposomes. The plateau and the span were fitted to an exponential model and velocity constants (K) were calculated.

The nucleotide exchange activity of human ARF1 was checked (Fig. 26) and compared to yeast ARF1p. Specific activity of the human ARF1 compared to the yeast ARF1p is lower by one order of magnitude. This might be due to the lesser degree of myristoylation of human ARF1 (Van Valkenburgh and Kahn, 2002). However, the non myristoylated yeast ARF1p shows a nucleotide exchange activity comparable to its myristoylated counterpart, indicating that myristoylation is necessary but not sufficient to achieve full nucleotide exchange activity.

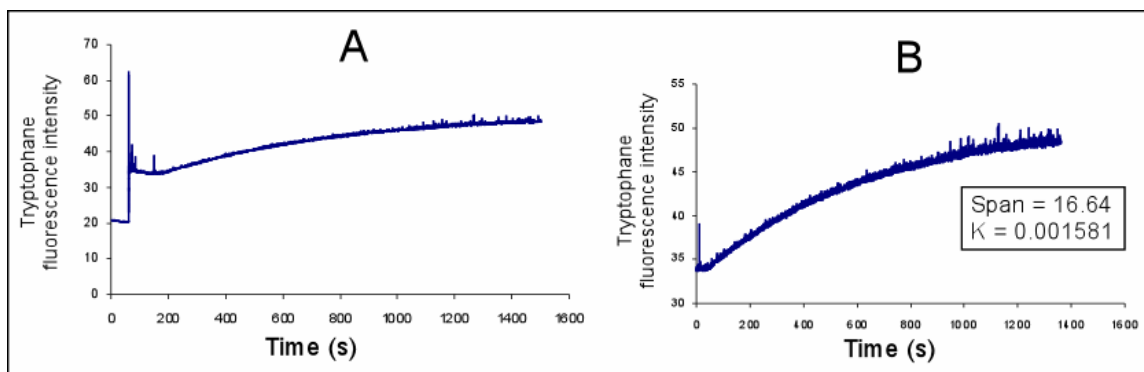


**Figure 26: myristoylated human ARF1 nucleotide exchange activity.** Myristoylated Human ARF1-GDP (1.78 $\mu$ g) was added to a fluorescence cuvette and its nucleotide exchange activity was measured under the conditions described for the yeast ARFs. Instead of GTP, one of its non hydrolysable analogues was used (GMP-PNP). **A** shows the crude measurement. The fluorescence increase was fitted to an exponential model **B**.



Protein	Specific Activity ( $\text{D.mol.L}^{-1} \cdot \text{s}^{-1} / \mu\text{g ARF-GDP}$ )	
	Liposomes	Solution
Myristoylated Yeast Arf1p, fraction 19, Fig. 5	0.15	0
Myristoylated Yeast Arf1p, fraction 26, Fig. 6	0.12	0
Non myristoylated yeast Arf1p, fraction 25, Fig. 7	0.08	0.1
Myristoylated human Arf1*	0.014	0

myristoylated counterpart as well as the myristoylated human ARF1p are compared.

(\*) Since the human ARF1 purified as shown in Fig. 8 failed to exhibit any nucleotide exchange activity, an active human ARF1(\*) contributed by Mölleken J (personal communication) was tested for comparison with the yeast ARF1p.

$\alpha$  is the coefficient of proportionality between the fluorescence intensity and the concentration of ARF1p-GTP.

Data are mean of 2 experiments.

**Table2: Specific activities of myristoylated yeast ARF1p, non myristoylated yeast ARF1p and human ARF1.**  
Activities of the two species of myristoylated ARF1p, the non

With the various components of a reconstitution system at hand, we attempted to generate COPI coated vesicles from liposomes.

### 3.2 Attempts to generate COPI coated vesicles from p23 containing liposomes

COPI coated vesicles can be generated from liposomes containing p23 lipopeptide (Bremser et al., 1999). Purified proteins (ARF1 and coatamer) were incubated at 37°C with p23 containing liposomes. The reaction was stopped at 0°C and submitted to a sucrose floatation gradient that typically yielded separation of donor liposomes (20 to 30 % sucrose (w/w)) and newly generated vesicles (40% sucrose (w/w)). Unreacted proteins (ARF1 and coatamer) were found at the bottom of the gradient (Fig. 27). The experiments shown in Fig. 27 and 28 were performed with non gel filtrated liposomes.

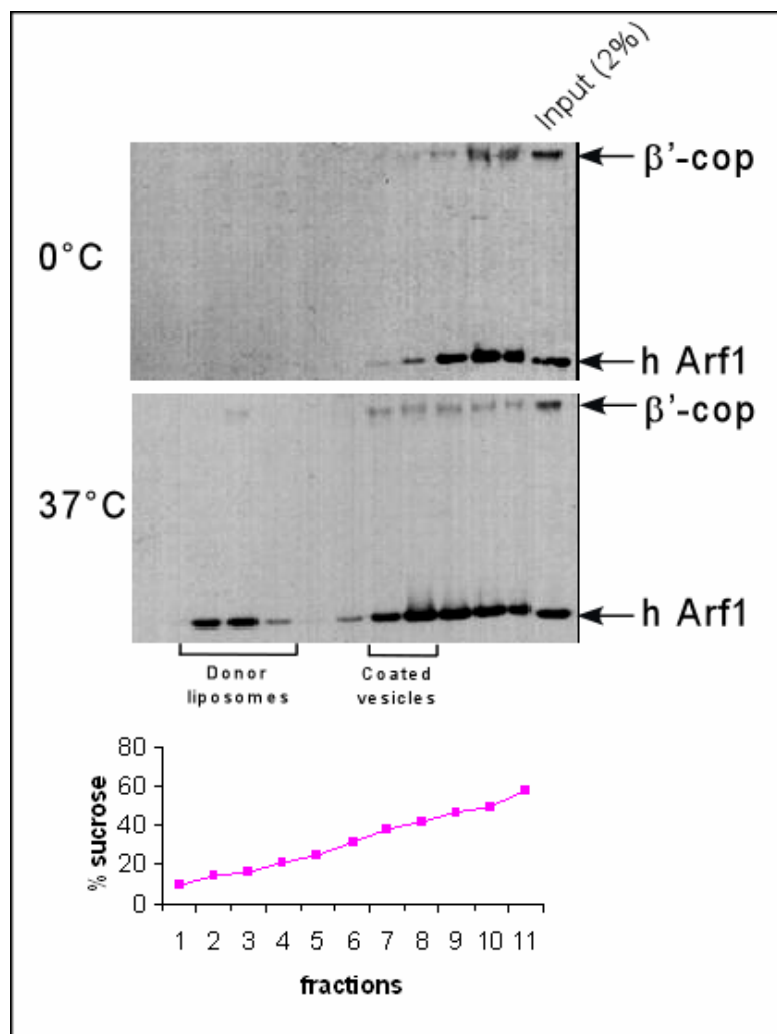


**Figure 27: Biochemical analysis of COPI vesicle formation from p23 containing liposomes.** After separation by centrifugation in a sucrose gradient, fractions were analyzed by western blotting (A) using polyclonal rabbit antibodies directed against ARF1 and  $\beta'$ -cop (Helms et al., 1993; Stenbeck et al., 1993). The percentage of sucrose was determined by refractometry.

When the reaction was conducted at 0°C, coat components (ARF1 and coatamer) were not able to bind liposomes indicating a strict requirement for a physiological temperature (37°C). Furthermore, COPI coated vesicles were not generated at 0°C (no signal at a density of 40% sucrose). However, at 37°C, binding of ARF1 and coatamer occurs (signal in the donor liposome fraction) and coated vesicles were generated at 37°C as indicated by the signal of ARF1 and coatamer in the fractions at around 40% sucrose (Fig.27)

### 3.3 Attempts to generate COPI coated vesicles from liposomes containing p23 and SNAREs

The question whether and how SNAREs are packaged into COPI coated vesicles was addressed using in principle the same methodology, however with liposomes that were reconstituted as described in Fig. 20

GST-Sec22-FL and GST-Vti1p-FL containing liposomes (Fig. 20) were submitted to the budding assay *in vitro* (Fig. 28)

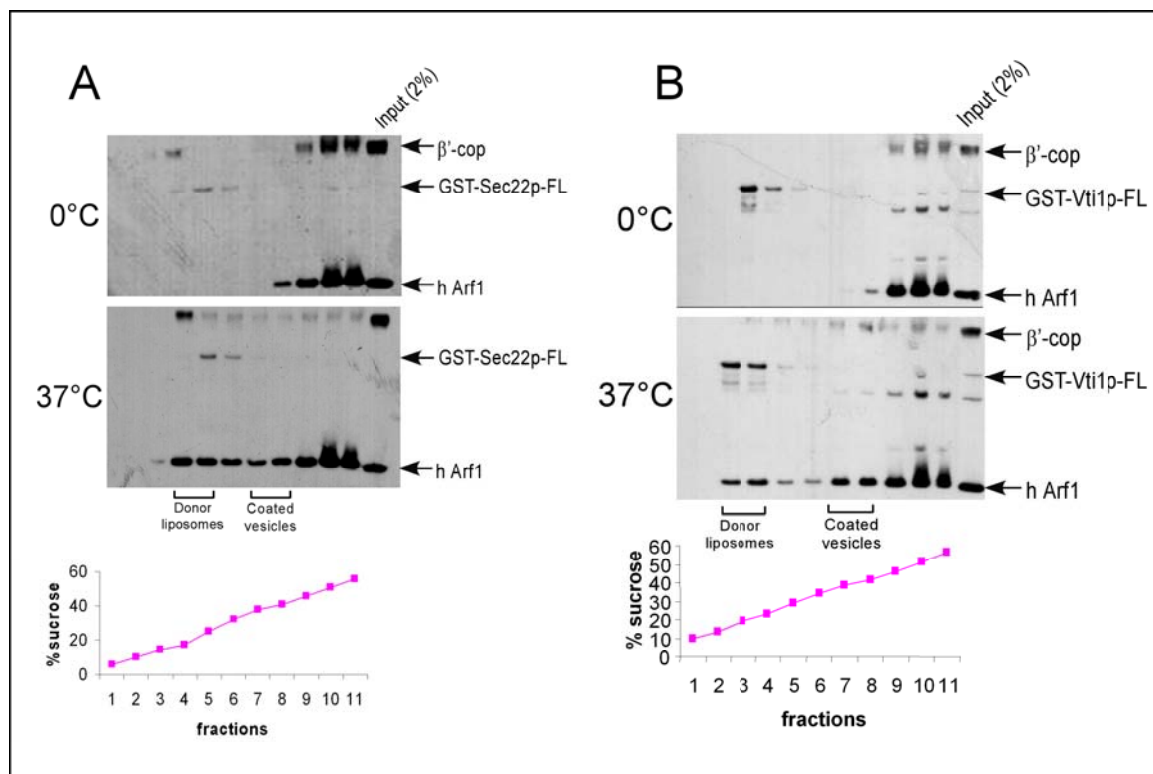


**Figure 28: Biochemical analysis of COPI vesicle formation from liposomes containing either GST-Sec22p-FL (A) or GST-Vti1p-FL (B).** The same conditions as in Fig. 25 were used. Additionally, an antibody against GST (Sigma) allows detection of the GST-SNAREs.

The SNAREs containing liposomes exhibit the same behavior as p23 containing liposomes when submitted to the budding assay. In fact no binding of coat components was observed at 0°C and a signal for ARF1 and coatomer was observed in the 40% sucrose fractions, indicating generation of COPI coated vesicles. In the same fractions, a signal for SNAREs was also observed

indicating their presence in COPI coated vesicles (fractions 7 and 8, Fig. 28). The relative faint signal of the SNAREs may be due to the fact they are not present as coat but as membrane components. It was established that budding efficiency is around 5% of the input of Golgi membranes *in vivo* (Malsam et al., 1999) and around 2% *in vitro* (Bremser et al., 1999). It is then not surprising to see such a weak amount of SNAREs in the coated vesicles.

Moreover, it is not possible to rule out in these experiments that a part of the signals observed for ARF1, coatamer and SNAREs are due to coating of small liposomes rather than budding. Such coated liposomes might float to the same sucrose density.

To address this question, large gel filtrated liposomes were made (Fig. 14) and submitted to the *in vitro* budding assay (Fig. 29) and compared with small liposomes (100 nm after extrusion).

As expected, when small liposomes were used, a signal for ARF1 and coatamer was found in the 40% sucrose region. Assuming these liposomes are too small to generate vesicles, this signal stands for mere binding of coat components. On the other hand, large liposomes show a similar signal at the same density (~ 40% sucrose). In this case, the signal can not be interpreted as mere binding of small liposomes as they do not exist in the starting material indicating *de novo* generation of COPI vesicles.

This confirms the previous observation that the signal present when using non gel filtrated liposomes is due to binding of coat components to small liposomes as well as to newly generated COPI vesicles.

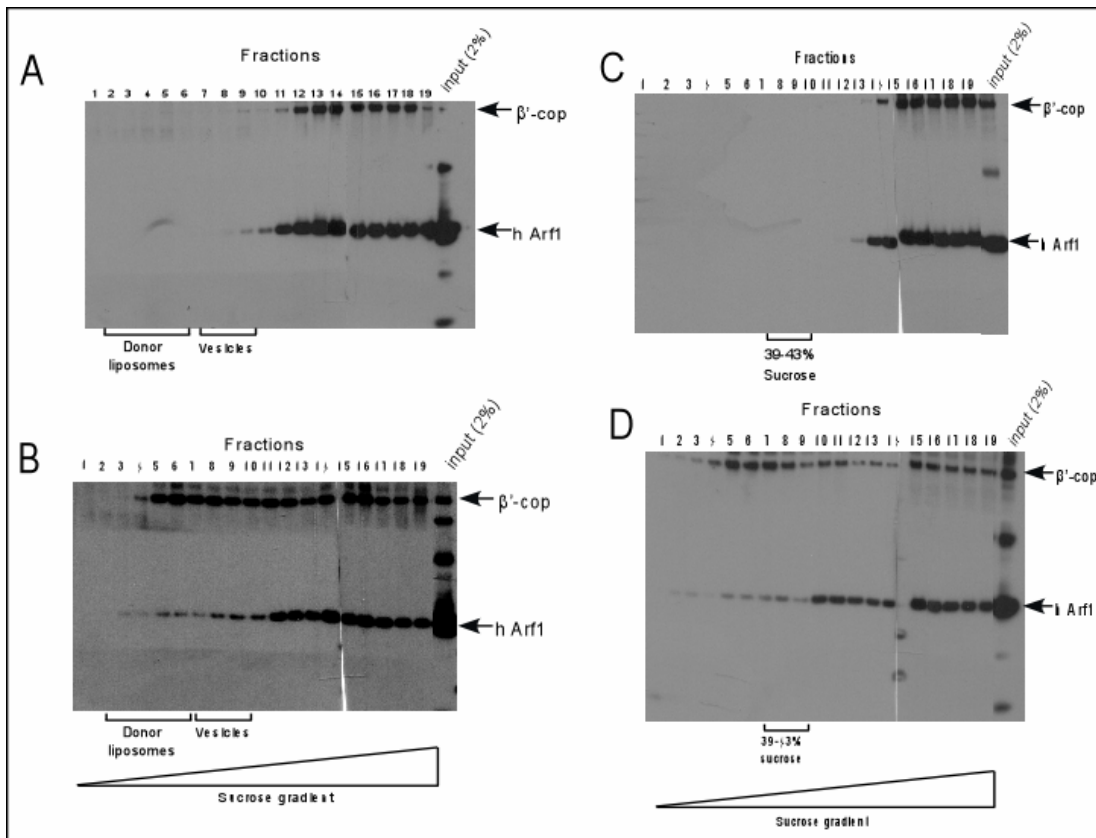


**Figure 29: Biochemical analysis of COPI vesicle formation from large liposomes compared with small ones.** Large liposomes (over 300 nm) containing p23 lipopeptide obtained after gel filtration were incubated with rabbit coatmer, human ARF1 and GTP- $\gamma$ S as a nucleotide. After incubation at 0°C (A) and 37°C (B), the reaction was separated in a sucrose gradient and analyzed by western blotting using polyclonal rabbit antibodies directed against  $\beta'$ -cop and ARF1. Small liposomes (extruded using 100 nm filters) were submitted to the budding assay. At 0°C (C), no signal is observed for donor fractions. At 37°C (D), a signal for coatmer and ARF1 is observed vesicles fractions.

## **DISCUSSION**

COPI vesicle formation from Golgi membranes involves 3 major protein players, the small GTPase ARF1, coatamer and the p24 family proteins. ARF1-GTP interacts with two subunits of coatamer ( $\beta$ -cop and  $\gamma$ -cop) (Zhao et al., 1997; Zhao et al., 1999) and the p23 cytoplasmic domain is able to bind  $\gamma$ -cop (Harter and Wieland, 1998). To identify the minimal machinery that allows formation of COPI coated vesicles, a liposome based assay was established that includes the cytoplasmic tails of p24 family proteins, coatamer and ARF1. After incubation at 37°C in presence of GTP, COPI coated vesicles were generated that resemble in their morphology and size the authentic ones (Bremser et al., 1999).

On the other hand the minimal requirements for fusion of vesicles were also determined in a liposome based manner largely by the work of Rothman and coworkers. SNARE pins were shown to be the minimal machinery for cellular membrane fusion (Weber et al., 1998). Among different v/t-SNARE combinations, only few were able to trigger fusion (McNew et al., 2000a). In fact, bringing the membranes close enough is not sufficient for fusion to occur unless cognate SNAREs (v and t) are present in two populations of liposomes (McNew et al., 2000b).

The work described in this thesis has attempted to provide tools to allow linking the budding of COPI vesicles to the fusion machinery proteins (SNAREs). An *in vitro* system using chemically defined components (liposomes and purified proteins) was used for that purpose.

One part of this work was dedicated to produce the set of proteins involved in coat assembly, namely coatamer and ARF1 (mammalian and yeast). In addition SNARE proteins were purified and included in liposomes. Are SNAREs packaged into newly formed COPI vesicles in a liposomes based system? To what extent does this take place? These questions were addressed in this work.

In the second part, conditions in which homogenous population of large donor liposomes can form were found and a size separation allowed selection for large liposomes.

# 1 Protein components involved in COPI vesicular transport

## 1.1 SNARE proteins reconstituted in liposomes

SNARE proteins were produced in bacteria, purified and reconstituted into liposomes using two methods. The first allowed anchoring the cytoplasmic domain of SNAREs to liposomes and will allow studying the possible interactions either with coat components or with additional cytosolic factors that might be involved. The second method (dilution under the detergent CMC, followed by dialysis) allowed reconstitution of full length SNAREs into liposomes in a way that resembles the situation of these proteins *in vivo*. Indeed, SNAREs seem to keep a natural orientation in liposomes since they are accessible for thrombin protease at the outer side of the liposome.

Following the finding that sphingomyelin and cholesterol were segregated during formation of COPI coated vesicles (Brugger et al., 2000), the authors postulated that preferential interactions of certain membrane phospholipids with parts of the protein machinery mediating COPI vesicles formation might explain this lipid segregation. In this context, and as long as SNAREs interact with COPI components (Ballensiefen et al., 1998; Xu et al., 2002), *in vitro* studies should allow verifying whether they are involved in such a phenomenon.

## 1.2 p24 family proteins

The p24 family of type I transmembrane proteins play a major role in vesicular transport. They were shown to cycle constitutively in the early secretory pathway (Dominguez et al., 1998; Fullekrug et al., 1999; Nickel et al., 1997; Sohn et al., 1996) and interact with ARF1-GDP (Gommel et al., 2001) and coatomer (Harter and Wieland, 1998). Since the interaction with coatomer is mediated by the cytoplasmic tail of p23, usage of p23 lipopeptide was made and has allowed



efficient budding of COPI coated vesicles *in vitro* regardless of the lipid composition (Bremser et al., 1999). However, the luminal part of p24 family members is important as it was shown to be responsible for the dimerization state of these proteins (Emery et al., 2000) and proposed to bind cargo (Schimmoller et al., 1995). It was possible in the current study to express and purify these proteins in their full length native form. This should allow investigation of the role of their transmembrane domain in interactions with lipids on one hand and their luminal domain in cargo uptake on the other hand.

### **1.3 ARF1 GTPase activating protein (ARF1-GAP)**

It is known that ARF1 mediated GTP hydrolysis is required for COPI coat disassembly (Tanigawa et al., 1993) allowing the uncoated COPI vesicle to fuse. Since the GTPase activity of ARF1 is intrinsically low, ARF1-GAP remarkably accelerates this reaction (Cukierman et al., 1995). In addition coatomer increases this reaction 1000-fold through interaction with ARF1 and ARF1-GAP (Goldberg, 1999).

When expressed in bacteria, ARF1-GAP is insoluble. Attempts to obtain a soluble, refolded and active protein seem to be a challenge for many groups. Although refolded (Poon et al., 1996), Glo3p (a yeast ARF1-GAP) is unable to trigger GTPase activity of yeast ARF1 (Anne Spang, personal communication).

In addition the catalytic domain of ARF1-GAP was recently shown to trigger uncoating of COPI vesicles (Reinhard et al., 2003) without affecting coat assembly, ruling out the possibility that ARF1-GAP acts as a coat component as suggested recently (Yang et al., 2002).

In the context of reconstituting one round of COPI vesicular transport (budding, uncoating and fusion) using purified components, usage of a full length active GAP is of importance. The current work has allowed the purification of Glo3p, a yeast ARF1-GAP, from inclusion bodies, and refolding by gel filtration experiments led to a biologically active protein that is able to promote significant

ARF1p dependent GTP hydrolysis as shown by nucleotide exchange assays monitored by tryptophan fluorescence.

#### **1.4 ADP-ribosylation factor 1 (ARF1)**

ARF1 is a member of GTP binding proteins that regulate membrane traffic (Donaldson and Klausner, 1994; Schekman and Orci, 1996). It is present in the cytosol in a GDP bound state. Upon exchange of GDP to GTP on ARF1, a reaction accelerated by nucleotide exchange factors (Chardin et al., 1996; Jackson and Casanova, 2000; Peyroche et al., 1996) ARF1 changes its conformation and stably anchors to the membrane through its myristic acid (Goldberg, 1998). Prior to nucleotide exchange, ARF1 is recruited to the membrane by interacting with the p23 cytoplasmic tail (Gommel et al., 2001) regarded since then as ARF1-GDP receptor. In addition, ARF1 was shown to be necessary and sufficient to promote COPI vesicle formation from chemically defined liposomes (Bremser et al., 1999).

The N-terminus of ARF1 is subject to the covalent attachment of a myristoyl group (C14:0) to its N-terminal glycine residue that is catalyzed by N-myristoyltransferase1 (NMT1) (Towler et al., 1987) after removal of the initiating methionine by a bacterial Methionine amino peptidase. N-myristoylation is a very important modification since it confers to ARF1 the ability to stably anchor to membranes.

Myristoylation of human ARF1, when expressed in a dual plasmid system together with yeast NMT1, typically resulted in 5 to 10% myristoylation (Duronio et al., 1990) that can be increased up to 20% by lowering the temperature during expression. One explanation for the low degree of myristoylation is that human ARF1, although 77% identical to its yeast homolog is not an optimal substrate for yeast NMT1. Interestingly, it was recently demonstrated that human ARF1 is not fully myristoylated when co expressed with human NMT1 and NMT2 (Van Valkenburgh and Kahn, 2002).

Yeast ARF1p was then cloned and expressed with yeast NMT1 in *E. coli* either in a dual plasmid system or in a bicistronic system in presence of myristic acid. In both cases, purity to apparent homogeneity was achieved by ammonium sulfate precipitation and cation exchange chromatography. Expression and purification of yeast ARF1p in absence of NMT1 and myristic acid was conducted to provide a non myristoylated ARF1p as control.

As shown by Franco and coworkers (Franco et al., 1995) for the bovine ARF1 (100% identical in protein sequence to the human one) after expression at 37°C, three bands of ARF1 with increasing mobility in SDS-PAGE are present that correspond to Met1-ARF1 (intact ARF, non myristoylated and uncleaved by Methionine amino peptidase), Gly1-ARF1 (formed by cleavage of the N-terminal Met) and myr-ARF1 (myristoylated ARF1).

When non myristoylated yeast ARF1p was purified, the large majority of the protein was cleaved (Gly1-ARF1) while a small part, appearing as a faint band, was observed that represented Met1-ARF1 (Lane 3, Fig. 8)

When yeast ARF1p was co-expressed with NMT1 in presence of myristic acid, only one band could be observed that runs the fastest on SDS-PAGE (Lanes 1, 2 and 4, Fig. 8) and corresponds to myr-ARF1p. In addition, different salt concentrations were needed to elute the proteins from a cation exchanger (~100 mM NaCl for myr-ARF1p and ~200mM for the non myristoylated protein). Moreover, myristoylated ARF1p was able to exchange GDP to GTP only in presence of liposomes while the non myristoylated ARF1p could exchange nucleotide either in presence or in absence of liposomes with similar efficiency.

Since these two ARF1p behave differently on SDS-PAGE, in cation exchange chromatography and in exchange of nucleotide, the data presented here unambiguously show that full myristoylation of yeast ARF1p was achieved under the described conditions.

Based on the data described here, myristoylation seems necessary but not sufficient to achieve full nucleotide exchange activity on liposomes since the non myristoylated ARF1p is active both in presence and absence of liposomes.

## 2 In vitro budding assay with liposomes mimicking Golgi membranes

A minimal system that contains liposomes and purified components has been used to address fundamental questions in the field of vesicular transport. It was shown that Sar1p, COPII proteins and GTP were the minimal components needed to pinch off COPII coated vesicles from acidic liposomes (Matsuoka et al., 1998b). On the other hand, COPI coated vesicles were generated from synthetic liposomes using ARF1, coatomer and GTP- $\gamma$ -S (a non hydrolysable analogue of GTP) (Spang et al., 1998). However in this study, usage was made of acidic lipids that are more representative of yeast microsomal membranes (Wagner and Paltauf, 1994; Zinser and Daum, 1995) rather than mammalian membranes (Fleischer et al., 1974; Howell and Palade, 1982; van Meer, 1998) suggesting that additional components might be needed for budding.

An *in vitro* budding assay was developed that requires ARF1, coatomer, GTP- $\gamma$ -S and liposomes whose composition resembles Golgi membranes and that contain cytoplasmic tails of p24 family proteins. In this system, *de novo* generation of COPI vesicles was shown and a crucial role was attributed to p24 family tail peptides since no budding occurs in absence of this component (Bremser et al., 1999).

This assay was used to investigate the behavior of SNAREs in COPI vesicles.

### 2.1 Behavior of SNAREs in the COPI *in vitro* budding assay

SNAREs were reconstituted into Golgi like liposomes containing p23 tail peptide. *In vitro* budding assay was conducted with liposomes containing Sec22p (implicated in ER-Golgi transport (Xu et al., 2002)) and Vti1p (implicated in Golgi retrograde traffic (Lupashin et al., 1997)).

By submitting SNARE and p23 containing liposomes to the *in vitro* budding assay, COPI coated vesicles were formed and run at 40% sucrose (w/w) after flotation in a sucrose gradient exactly as the p23 containing liposomes do.

Furthermore, after quantification of the lipid content of the donor liposomes pool and the vesicles pool, and by loading the same amount of each pool on SDS-PAGE and analysis by western blotting, it was possible to address the question whether SNAREs concentrate in COPI vesicles *in vitro*. In fact, no difference was observed between the 0°C and the 37°C reactions indicating GST-Sec22p-FL and GST-Vti1p-FL do not seem to be preferentially taken up in COPI vesicles *in vitro*. By usage of a similar liposome based system, Sec22 was shown to be concentrated in COPII vesicles (Matsuoka et al., 1998a) confirming its implication in fusion of COPII vesicles.

*In vivo*, Sec22 is associated with the pre Golgi intermediate compartment (Zhang et al., 1999) and recycles back from Golgi to the ER in a manner involving COPI components (Ballensiefen et al., 1998). On the other hand, Sec22b is shown to be enriched in COPII coated vesicles that bud from the ER and presumably fuse with nearby vesicular tubular clusters (VTCs)(Hay et al., 1998). Moreover, *In vivo* data have shown that Vti1p exists in a SNARE complex that contains Sed5, GS28, and Ykt6, all implicated in both ER-to-Golgi and intra-Golgi transport (Xu et al., 2002), and *in vitro* can be immunoprecipitated with COPI coat components. *In vivo* these two proteins interact with COPI components and are present in complexes with other SNAREs. In addition the ARF-GAP Glo3p was shown to mediate an interaction of v-SNAREs to COPI components using microsomal membranes (Rein et al., 2002).

Taking this into account, it may well be that concentration (or segregation) effects using the *in vitro* budding assay could be seen more clearly when these SNARE complexes are reconstituted in liposomes and subjected to the budding assay. In that respect, preliminary experiments have allowed reconstitution of a complex of Sec22, Bos1 and Sed5 in liposomes and further experiments should dissect the mode and requirements for specific uptake of SNAREs in pre budding structures. These experiments can now be complemented by the active ARF-GAP Glo3p to test its ability to mediate recruitment of COPI components to SNAREs.

Liposomes as a model for donor membranes characterized by DLS and electron microscopy revealed that the starting liposomes contained a mixed population of large and small structures. When coated, the small liposomes may be indistinguishable from the newly formed vesicles on the flotation gradient. Thus signals observed for coat proteins (ARF1 and coatomer) in the 40% sucrose region could then be due mainly to binding of coatomer and ARF1 to preexisting small liposomes, and not to newly generated COPI vesicles. On the other hand, large liposomes offer a higher surface for budding and are therefore suitable to yield a higher budding efficiency.

Therefore it seemed important to obtain quite homogenous populations of large liposomes as starting material for the *in vitro* budding assay.

## 2.2 Generation of large liposomes

Establishing conditions to obtain large liposomes of a defined size was a challenging task in this work.

Unilamellar liposomes can be formed by reverse-phase evaporation techniques (Szoka and Papahadjopoulos, 1978; Timofeev et al., 1994). This method requires long preparation times, and involves mixing between organic and aqueous phases that is prone to denature proteins. With another method giant unilamellar vesicles (GUVs) are generated by exposing dried lipid films to aqueous solutions for long time hydration (Mueller et al., 1983). A modified method that uses low ac electric fields allows preparation of GUVs and requires special instrumentation. Avoiding these experimental limitations, Takei and coworkers; (Kinuta and Takei, 2002; Kinuta et al., 2002; Takei et al., 2001) have described a procedure to generate large liposomes with a size larger than 1000 nm diameter using a gentle hydration method. In addition, they were able to see small vesicles generated after budding. During this work, the same procedure to obtain liposomes was used, but failed to achieve similar results, although this method

allowed improvement of the standard protocol. However, DLS measurements revealed the presence of additional small liposomes (~100 nm).

The current work describes separation of large liposomes ( $\geq 300$  nm) from small ones by size exclusion chromatography. Typically large liposomes represent 10% of the starting material and can be concentrated by centrifugation since they were formed in a buffer containing 2.5% sucrose (w/w).

Use of such liposomes in the *in vitro* budding assay yielded a signal in the 40% sucrose fractions that is higher than the one generated with small control liposomes. This indicates that small liposomes bind coatamer and ARF1 indeed, and they are present together with newly generated COPI vesicles in the same 40% fractions. This confirms that a part of the signal observed using standard non gel filtrated liposomes is a contamination caused by small preexisting liposomes, and emphasizes a need to use purified large liposomes as a starting material. Taking this into account, quantifying amounts of SNAREs taken up in newly generated COPI vesicles in future experiments will need to be performed with liposomal donor membranes carefully defined by the criteria described here. Usage of gel filtrated liposomes should allow addressing this question.

Taken together, the results shown here have contributed to improve the individual components needed for COPI vesicles biogenesis *in vitro*. Biologically active yeast ARF1p and its ARF-GAP, Glo3p were made available and SNAREs can be included into liposomes in their correct physiological orientation.

In addition, a protocol to prepare a homogenous population of large liposomes (over 300 nm) was established.

With all these components in hand, it should now be possible to study the uptake of SNAREs in COPI vesicles *in vitro* as well as protein and lipid cargo uptake. Eventually this should allow the reconstitution of a full round of COPI vesicular transport from budding to fusion.

## **MATERIALS AND METHODS**



## Materials

### 1 Chemicals

All commonly used chemicals were purchased from either Merck (Darmstadt), Sigma (Deisenhofen), Roth (Karlsruhe), Fluka (Taufkirchen), Roche (Mannheim), Qiagen (Hilden), Amersham-Biotech (Freiburg), BioRad (München) or Boehringer (Mannheim). The reagents were ordered directly at the company or via the chemical centre Heidelberg (Theoretikum der Universität Hiedelberg).

#### 1.1 Detergents

Triton X-100, octyl glucoside (OG) were obtained from Merck and Calbiochem, respectively.

#### 1.2 Protease inhibitors

Mixtures of protease inhibitors were obtained from Roche as tablets. Each tablet was sufficient for a 50 ml solution.

#### 1.3 Buffers

A List of most commonly used buffers during this experimental work is shown below. All buffers were prepared as aqueous solutions.

##### **PBS buffer**

10X PBS: 1.36 M NaCl, 357 mM Na<sub>2</sub>HPO<sub>4</sub>, 143 mM KH<sub>2</sub>PO<sub>4</sub> and 30 mM KCl. PBST was obtained by mixing PBS buffer supplemented with Tween-20 to 0.05% final concentration. PBS was adjusted to pH 7.4.

##### **TAE buffer**

50X TAE contained 242 g Tris base, 57.1 ml of glacial acetic acid and 18.61 g of EDTA, and adjusted to 1 L solution with MiliQ H<sub>2</sub>O.

**Running buffer for electrophoresis**

10X SDS-PAGE running buffer contained 30.2 g Tris base, 188 g of glycine and 10 g of SDS, and adjusted to 1 L solution with MiliQ H<sub>2</sub>O.

**Blotting buffers for semi-dry transfer**

**Anode I:** 300 mM Tris and 20% (v/v) methanol.

**Anode II:** 25 mM Tris and 20% methanol.

**Cathode buffer:** 25 mM Tris, 40 mM aminocaproic acid and 20% methanol.

**Sample cocktail buffers**

**Sample buffer for DNA:** 6X stock solution contained 0.25% bromophenol blue, 40% sucrose, 60 mM Tris-HCl, pH7.4 and 6 mM EDTA.

**Sample cocktail I (SCI):** 50 mM Tris-HCl pH 6.8 and 4% SDS

**Sample cocktail II (SCII):** A 3X stock solution contained 187.5 mM Tris-HCl pH6.8, 15% β-mercaptoethanol, 6% SDS, 30% glycerol and 0.0675% bromophenol blue.

**Staining Solution for SDS-PAGE**

**Staining buffer:** 40% ethanol, 10% glacial acetic acid and 0.25% coomassie blue R-250.

**Destaining buffer:** 20% ethanol and 5% acetic acid.

**Ponseau S solution:** prepared by adding 0.8g of the dye dissolved in 4% (w/v) TCA.

## **1.4 Media**

**Bacteria and yeast culture media**

**Lauria-Bertani broth (LB)** was prepared according to guidelines of Molecular Cloning (3rd Edition). 1 L of medium contained 10 g of sodium chloride, 10 g of Bacto-Trypton and 5 g of yeast extract. pH was adjusted to 7.4. For plates, 15 g/L agar was added to the preparation.

YPD medium was prepared as follows: 10 g of BactoYeast extract, 20 g of BactoPeptone and Dextrose were dissolved in 1 L of MilliQ water and autoclaved.

### **YPD**

20g of peptone, 10g of yeast extract and 20g of D-glucose were dissolved in 1 liter of milliQ water and autoclaved for 15 minutes at 120 °C. For plates, 15 g/L agar was added to the preparation.

### **Xgal plates**

LB-agar plates were prepared as described earlier and X-Gal. 100µl of 100mM IPTG and 20µl of 50mg/ml X-Gal (dissolved in N,N' dimethylformamide ) were spread over the surface of the LB-plate and allowed to absorb for 30 minutes at 37°C prior to use.

## **2 Antibodies**

### **2.1 Primary Antibodies**

For the immunochemical studies the following antibodies were used:

- 1 GST antibody for detection of GST fused SNAREs (rabbit) (Sigma).
- 2 p23 tail peptide antibody (rabbit).
- 3 Human ARF1 antibody (rabbit).
- 4  $\beta'$ -cop antibody (rabbit).
- 5  $\gamma$ -cop antibody (rabbit).

### **2.2 Secondary Antibodies**

HRP-conjugated goat anti-rabbit IgG(H+L) and HRP-conjugated goat anti-mouse IgG(H+L) were obtained from BioRad. HRP-conjugated Protein G Sepharose Beads was purchased from BioRad.

### 3 Plasmids

The following plasmids were used during this work various purposes as indicated below:

- pbb131** (Duronio et al., 1990). Expression of N-myristoyl transferase in *E. Coli* to that transfers the myristic acid to ARF1.
- pGEX** used for cloning of SNAREs as GST fusions (Amersham biosciences).  
Full length SNAREs (FL) were cloned as well as their cytoplasmic domains (CD) to which a cystein was added at the C-terminus:  
pGEX-Sec22p-FL, pGEX-Sec22p-CD  
pGEX-Gos1p-FL, pGEX-Gos1-CD  
pGEX-Bet1p-FL, pGEX-Bet1-CD  
pGEX-Vti1p-FL, pGEX-Vti1p-CD  
pGEX-Bos1p-FL, pGEX-Bos1-CD  
pGEX-Ykt6p-CD (Ykt6 does not have a transmembrane domain and therefore was made available with an additional cystein)
- pET11d** (Novagen). Was used that contains human ARF1, pET11d-hARF1
- pET-24 a (+)** (Novagen). Was used to clone native yeast ARF1p: pET-24 a-ARF1p
- pET-32 Xa/LIC** (Novagen). was used to clone the human p23 protein tagged to thioredoxin, 6XHis and S protein tag: pET-32 Xa/LIC-p23
- pACYCDuet-1** (Novagen). Bicistronic vector used to clone NMT1 alone: pACYDuet-1-NMT1 and both NMT1 and ARF1p: pACYDuet-1-NMT1-ARF1p
- pET-15 a (+)** (Novagen). Was used to clone Glo3p fused to a 6XHistidine Tag: pET15 a-Glo3p

### 4 Oligonucleotides

The oligonucleotides used in this thesis were synthesized by Thermohybrid (formally Interactiva) (HPLC grade). All oligonucleotides were solubilized in sterilized water to a final concentration of 100µM. All sequences are presented in

table 3.

<b>Designation</b>	<b>Sequence ( 5'-3')</b>
GST-Sec22-FL-Nter	gcgcgatccatgataaagtcaacactaatctacag
GST-Sec22-FL-Cter	cccggaattcttatttgaggaagatccaccagaag
GST-Sec22-CD-Cter	cccggaattcttagcaatcgaagtgatctttgcgcg
GST-Gos1-FL-Nter	gcgcgatccatgagctcacaaccgtcttcgtcacc
GST-Gos1-FL-Cter	cccggaattcttattaccatgtgaaaaacaaaaacag
GST-Gos1-CD-Cter	cccggaattcttagcagttttcttctctcgtg
GST-Bet1-FL-Nter	gcgcgatccatgagttcaagattgcaggg
GST-Bet1-FL-Cter	cccggaattcttattatgtaatccataccc
GST-Bet1-CD-Cter	cccggaattcttagcattttatactgatcccagatcttc
GST-Vti1p-FL-Nter	gcgcgatccatgagttccctattaatatcatcag
GST-Vti1p-FL-Cter	cccggaattcttattattaaactttgagaacaaaac
GST-Vti1p-CD-Cter	cccggaattcttagcatttattagcaactagccttctag
GST-Bos1-CD-Nter	gcgcgatccatgaacgctctttacaacctgctgtg
GST-Bos1p-CD-Cter	ctccccgggtagcatttattcttgaacaccgg
GST-Ykt6p-Nter	gcgcgatccatgagaatctactacatcgggtatttcg
GST-Ykt6p-Cter	cccggaattcttagcactacatgatgatgcaacacg
pET24a-ARF1p-Nter	gggttcatatgggttggttgccc
pET24a-ARF1-Cter	gggttggatcctaagttgagttttc
pET-32 Xa/LIC-p23-Nter	ggtattgagggtcgatgatctccttccatctgcc
pET-32 Xa/LIC-p23-Cter	agaggagagttagagccttattcaatcaacttctgg
pACYDuet-1-NMT1-Nter	gggttccatggggtcagaagaggataaagcg
pACYDuet-1-NMT1-Cter	gggaaaggatccctacaacataacaacacc
pACYDuet-1-ARF1p-Nter	gggttcatatgggttggttgccc
pACYDuet-1-ARF1p-Cter	gggttggatcctaagttgagttttc

pET15 a-Glo3p-Nter	gggttccatgatgagtaacgatgaaggagaaac
pET15 a-Glo3p-Cter	gggttggatccttattttcttaagtagtcc

**Table 3.** Oligonucleotides used to prepare constructs for cloning GST-fused yeast SNAREs, ARF1p, NMT1 and Glo3p

## 5 Equipments

PCR thermocycler was from ThermoHybaid, ultra-centrifuges were from either Beckman or Kontron Instruments (Watford, UK). Other centrifuges were from either Eppendorf or Heraeus. Rotors are from Beckman (JA-10.500, JA-20, JA-25.50 and SW55 Ti) or Kontron (TFT 50-38 and 55-38). Electrophoresis systems, including plates, spacers and combs, and blot systems, including semi-dry trans-blot and wet blot were from Bio-Rad (Munich, Germany) or Invitrogen (Karlsruhe). Cell incubators were from Heraeus.

## Methods

## 6 Biochemical Methods

### 6.1 Synthesis of p23 and p24 lipopeptides

The p23 and p24 proteins tail peptides were synthesized at ZMBH, Heidelberg University, and lyophilized. The sequences of peptides are:

p23: CLRRFFKAKKLIE

p24: CLKRFFEVRVV

A commercially available phosphatidylethanolamine (PE) derivative 1,2-dioleoyl-sn-glycero-3-phosphoethanolamine-n-[4-(maleimidophenyl)butyramide] (MPB-PE) was purchased from Avanti polar lipids. The maleimido group reacts with the free thiol group of the peptides cysteine to form a stable thioether.

Prior to use, the cystein containing peptides were analyzed for their potential

oxidation of the cysteine thiol group that reacts to the MBP-PE lipid. According to the manufacturer recommendations (Pierce), Ellman reagent was used for that purpose and typically 70% of the peptides were found to have a functional reduced thiol group.

Stock solutions:

MPB-PE in chloroform:	25 mg/ml (24.75 mM)
p23 and p24 peptides solubilized in dimethylformamide (DMF)	4mg/ml (2.2 mM)

MPB-PE (500 nmol) is added to a glass vial and solvent was removed under a gentle stream of Argon. Depending on the degree of oxidation of p23 peptide (typically 30%), suitable amount of p23 peptide dissolved in dimethylformamide (DMF) was added to the lipid film (10% excess of peptide over MPB-PE) and this mixture was kept at least 4 hours on a rotating wheel. Free maleimido groups were quenched by addition of 1  $\mu$ mol of  $\beta$ -mercaptoethanol. The mixture was dried under argon and the sample was resuspended in 1ml 30% Acetonitrile (AN) / 0.1% trifluoroacetic acid (TFA).

Sep-Pak C18 cartridges were used to purify the lipopeptides. Cartridge was washed with 1 bed volume (1ml) of 100% AN / 0.1% trifluoroacetic acid (TFA) and equilibrated with 30 ml of 30% AN/ 0.1% TFA before loading the sample. The cartridge is then submitted to a step gradient that consists of 2 ml of 30% AN / 0.1% TFA, 2 ml of 40% AN / 0.1% TFA, 2 ml of 60% AN / 0.1% TFA, 2 ml of 80% AN / 0.1% TFA, 4 ml of 90% AN / 0.1% TFA and 2 ml of 100% AN / 0.1% TFA. p23 lipopeptide elutes at 80% and 90% AN / 0.1% TFA while p24 lipopeptide elutes at 90% and 100% AN / 0.1% TFA (Fig. 16)

Each fraction is lyophilized and dissolved in 200  $\mu$ l 30% AN / 0.1% TFA and 10 $\mu$ l were analyzed by thin layer chromatography (standard silica gel 60 plates (20x20 cm) (Merck). The solvent used is a mixture of butanol, pyridine, acetic acid (glacial) and water (9.7:7.5:1.5:6;v:v:v:v). Silica plates are developed for 3 hours, then dried and placed in a chamber containing solide iodine that stains lipids and

lipopeptides. Peptides were also stained due to their hydrophobic amino acids (two phenylalanine residues).

After quantification of the phosphate content (see 6.5), aliquots of 15 nmol lipopeptide were dried and stored under argon at -80°C.

## 6.2 Preparation of p23 lipopeptide containing liposomes

To prepare liposomes, lipids were used that resemble the Golgi lipid composition:

PC (phosphatidyl choline)	42%
PE (phosphatidylethanolamine)	19%
PS (phosphatidylserine)	5mol%
PI (phosphatidylinositol)	10mol%
SM (sphingomyeline)	7 mol%
Cholesterol	16 mol%
Rhodamine-PE (fluorescent lipid tracer)	1mol%

Liposomes were prepared in glass tubes previously rinsed with chloroform. 100µl of a stock lipid solution (300 nmol in total) were added to 15 nmol lipopeptide and transferred to a glass tube. The solvent was removed under an argon stream. Liposomes form after addition of 300 µl of an aqueous buffer (25 mM HEPES-KOH (PH=7.4), 150 mM KCl, 2.5% Sucrose (w/v)) and kept at 37°C for 2 hours. The sample was then subjected to 10 cycles of freezing (liquid nitrogen, -180°C) and thawing (50°C in a water bath).

The suspension was extruded through polycarbonate membrane of a defined size (800nm) (Avestin extruder) by 21 passages through 2 membranes.

## 6.3 Electron microscopy

Negative staining was used for electron microscopy (Valentine et al., 1968).

Liposomes are allowed to adsorb onto the surface of a carbon support film previously deposited onto a piece of cleaved mica. A 3x3 mm piece of carbon



coated mica was cut and inserted in an angle into the liposomes suspension. The carbon film floats off the mica but by holding the mica with fine tweezers it still remain attached at one corner. When the mica is removed from the liposomes suspension the carbon film is brought with it, sandwiching the particles between mica and carbon. Since liposomes remain attached to the carbon film, fixation with a solution of 1% (w/v) uranyl acetate was carried out, followed by washing with water. Careful drying with filter paper ensures that sufficient stain will remain to prevent a deformation of the two films.

#### **6.4 Selection for large liposomes by size exclusion chromatography**

In addition to large liposomes (over 400nm), the liposomes obtained above contain also numerous small structures (below 100nm) as shown by electron microscopy and Dynamic Light Scattering (DLS). Gel filtration experiments were used to select only for the large ones.

Sephacryl-1000 medium (Amersham biosciences) was used to pack a 55 ml column. Column was equilibrated with 3 bed volumes of the liposomes buffer (25 mM Hepes-KOH (PH=7.4), 150 mM KCl) supplemented with 20 mg/ml BSA. Liposomes were loaded and eluted at 30% of the bed volume. As they contain Rhodamine-PE they were monitored by measuring the fluorescence of this component ( $\lambda_{\text{ex}}=558$  nm, at  $\lambda_{\text{em}}=592$  nm)

#### **6.5 Quantification of lipids**

phospholipids can be quantified by measuring their phosphate content (Rouser et al., 1970) or by measuring the fluorescence of Rhodamine-PE.

##### **Phosphate determination:**

Lipid samples are taken to dryness in the oven in capped glass tubes. 300 $\mu$ l of 70% perchloric acid are added and the tubes are moved to a heating block at

180°C for 40 minutes. 1ml H<sub>2</sub>O, 0.4 ml Ammonium Molybdate (1.25 % (w/v)) and 0.4 ml Ascorbic acid (5% (w/v)) are subsequently added and mixed after each addition.

Samples are heated again 5minutes at 100°C. Absorbance at 797 nm is measured. Standard amounts of KH<sub>2</sub>PO<sub>4</sub> (0, 4, 10, 20, 40, 60, 80 nmols) are subjected to the same procedure allow deduction of the phosphate amounts contained in the lipids tested (either liposomes or lipopeptides). The amount of cholesterol (16%) was subtracted since it is not a phospholipid.

### Fluorescence measurements:

To check the recovery of liposomes after gel filtration, 100µl of each fraction (volume 750 µl) was loaded in a 96 microplate spectrofluorometer (Spectra Max GeminiXS (Molecular devices)) and the fluorescence of Rhodamine-PE was measured by collecting the emitted fluorescence at  $\lambda_{em}$ =592 nm after excitation at  $\lambda_{ex}$ =558 nm. Rhodamine-PE containing liposomes of known amounts of phospholipids were used for standardisation.

## 6.6 *in vitro* budding assay using p23 containing liposomes and purified proteins

Incubation mixture:

Component	Liposomes (10 nmol)	H <sub>2</sub> O	10 fold buffer*	GTP- $\gamma$ -S (2mM)	ARF1 (2µg)	MgCl <sub>2</sub> (5mM)	Coatomer (22 µg)
p23 liposomes at 37°C	2.5	30.3	5	1	6.3	0.5	4.4
p23 liposomes at 0°C	2.5	30.3	5	1	6.3	0.5	4.4

\*: 250 mM Hepes-HOH (PH 7.4), 1.5 M KCl, 25 mM MgCl<sub>2</sub>.

After addition of ARF1, the sample is incubated for 40 minutes and then MgCl<sub>2</sub>

and coatomer are added and the incubation continues for an additional 40 minutes. The reaction is then stopped by incubation at 0°C. As a control, the same reaction mixture is kept at 0°C.

The sample is then adjusted to 55% sucrose (w/w) in a final volume of 325  $\mu$ l and placed in a SW55 rotor centrifugation tube. Sucrose solutions (w/w) were added as follows: 500 $\mu$ l of 50%, 500 $\mu$ l of 45%, 500 $\mu$ l of 40%, 500 $\mu$ l of 30%, 500 $\mu$ l of 20%. Membranes are floated by ultracentrifugation at 150,000g for 4 hours at 4°C and the gradient is fractionated from the top (light fractions) to the bottom (heavy fractions) in 11 fractions of 256 $\mu$ l.

Biochemical analysis of these fractions was carried out by western blotting using antibodies against ARF1 and  $\beta$ '-cop.

## 6.7 Tryptophan fluorescence assay

The tryptophan fluorescence experiments were done using a fluoremeter from JASCO (FR-6500) and the temperature was set to 37°C. In a fluorescence cuvette, 530  $\mu$ l of Hepes buffer (Hepes-KOH, pH 7.4, KCl 150 mM, MgCl<sub>2</sub> 2mM) were added, followed by addition of 60 $\mu$ l of liposomes (Golgi like). Once the base line was stable (1 minute), ARF1 was added (amounts for each experiment are indicated in "Results"), 5 $\mu$ l of a solution of 10 mM GTP, then 6 $\mu$ l of a stock solution of 400mM EDTA. Either MgCl<sub>2</sub> (6 $\mu$ l of a stock solution of 400mM) or Glo3 (1 $\mu$ g) were added (see results). Tryptophan was excited at  $\lambda_{ex}$ =297.5 nm and emitted at  $\lambda_{em}$ =340 nm.

Data were collected using software from JASCO and fitted to exponential curves using a Prism4 (GraphPad).

## 6.8 Liposomes size determination by dynamic Light Scattering (DLS)

Experiments were performed using DLS equipment from MALVERN INSTRUMENTS (ZetaSizer S1000 HAS, 10 mW max, output He Ne; 633 nm). This technique measures the particle diffusion due to Brownian motion (random movement of particles due to the bombardment by the solvent molecules that surround them) and relates this to the size of the particle. The parameter calculated is defined as the translational diffusion coefficient (D). The particle size is then calculated from D using the Stoke-Einstein equation;  $d(H) = (kT) / (3\pi\eta D)$ , where d(H) is the hydrodynamic diameter, k is the Boltzmann's constant, D the translational diffusion coefficient, T the absolute temperature and  $\eta$  the viscosity. The DLS equipment produces a correlation of the particle position decay based on its movement. Since a large particle diffuses slower than a smaller one, the decays are different and a mathematical model correlates this decay to the size of the particle.

Measurements were performed at a constant temperature (25°C) because the viscosity of a liquid is related to its temperature. Samples were diluted and loaded in fluorescence cuvette. 12 measurements of 10 seconds each were performed. The mode chosen was continuous and the detection angle is at 90°C. Three detection modes are available (Intensity, Volume and number). Only the number mean was taken into account since it was in perfect accordance with the size given by electron microscopy experiments.

## 7 Methods in Molecular Biology

### 7.1 Preparation of yeast genomic DNA

Yeast *Saccharomyces cerevisiae* was grown in 5ml YPD medium until an OD between 1 and 3. The culture was spun down 5 minutes at 2000g and washed with 10 ml water. After washing, the cells pellet was resuspended in 500µl water followed by addition of 200 µl a detergent mix (100mM NaCl, 10mM Tris-HCl pH

8.0, 1mM EDTA, 2% Triton X-100, 1% SDS, sterile filtered). Glass beads (0.1 to 0.2 ml) as well as 300µl of a 1 to1 mixture of Phenol and chloroform were added. After vortexing, the lysate was pelleted and soluble material was transferred to a 2ml cup. A 2.5-fold volume of 100% ethanol was added, thoroughly mixed and DNA was precipitated at -20°C for 10 minutes. After centrifugation at 10,000g, the pellet was dried and resuspended in 400µl of Tris-HCl buffer (10mM Tris-HCl, pH 8.3). After addition of 200µg of RNase A, sample was incubated at 37°C for 40 minutes. Genomic DNA was finally precipitated by addition of NaCl (3M) and cold ethanol (100%). Yeast genomic DNA was pelleted at 10,000g for 10 minutes. The pellet was then dried and resuspended in 30µl of a Tris-HCl buffer (pH 8.3).

## 7.2 Polymerase chain reaction (PCR)

All reactions were carried out according to the manufacturer's guidelines. The reaction volumes were 50 µl, using the *PfuTurbo* polymerase (Stratagene). The reaction mix contains the following components: 5 µl of 10 X reaction buffer (Stratagene), 2 µl (0.1 µg) of yeast genomic DNA, 1.25 µl of each oligonucleotide (100 ng/µl), 1 µl of dNTPs (0.2mM), 1 µl of *PfuTurbo* (2.5 U/µl), and MilliQ water to adjust the total volume to 50 µl. All PCR reactions were initiated with 1 cycle at 95°C for 30 sec, followed by 20 to 30 cycles starting at 95°C for 30 sec, 55°C for 1 min, and 68°C for 2 min.

The annealing reaction was performed at appropriate temperatures (based on different primer pairs (Table 3)). in principle 5°C lower than the T<sub>m</sub> of the primers for 30 - 60 sec. Elongation was performed at 68°C for 2 min (*PfuTurbo* amplified at 2 min/kb. In all cases, the reactions were performed for 30 cycles in the conditions indicated above. 5µl of PCR products were analyzed by agarose gel electrophoresis to ensure efficient amplification. Then, the PCR amplified fragments were purified from agarose gel slices with the use of Nucleobond extract kit (QIAGEN). Doubly digested plasmid vectors were also purified with this kit. Purified PCR products were directly used for cloning into the indicated vectors after digestion with restriction enzymes (double enzyme digestion). If the

two used enzymes could not work in the same buffer, the digestion mixtures were purified from gel, and the digestion repeated for the second enzyme.

### 7.3 Ligations and subcloning

All ligation reactions were carried out in a maximal volume of 20  $\mu$ l with the use of the DNA ligation kit version2 (TAKARA biomedical). This kit uses one solution that contains T4 DNA ligase and an optimized buffer system. A mixture containing the digested and purified PCR product and the plasmid of interest is added 1 to 1 to the kit solution and incubated at 16°C for 30 minutes. Typically, such incubation resulted in efficient transformation and numerous colonies grew. A volume of 5  $\mu$ l of ligation mixtures was used to transform competent DH5- $\alpha$  (Invitrogen) for subcloning. Transformation was carried out by heat-shock. Briefly, 50  $\mu$ l of competent cells were mixed gently with 5  $\mu$ l of ligation mixture and incubated on ice for 30 min. The cells were heat-shocked at 37°C for 20 seconds, followed by incubation on ice again for 2 min. A volume of 1ml of pre-warmed LB medium was added to the transformation mixture followed by incubation at 37°C for 1 hr with shaking. Cells were plated on LB agar plate containing appropriate antibiotics and incubated at 37°C overnight.

Several colonies were randomly picked and inoculated into 4 ml of LB media supplemented with appropriate antibiotics. The cultures were incubated at 37°C for 16-18 hrs. Plasmid DNA extraction was done using QIAgen miniprep kit or Machery-Nigel nucleospin kit. The protocol of these two kits is basically the same (modified alkaline lysis). Briefly, cells were pelleted by centrifugation at 4000 rpm 4°C for 10 min, and resuspended in 0.2 ml of solution I containing RNase. Cells were lysed by adding 250  $\mu$ l of solution II, followed by mixing carefully the solution (upside-down movement for several times). The lysates were neutralized by the addition of 300  $\mu$ l of solution III. The solution was cleared by centrifugation, and supernatants were loaded onto the binding column and spun down. The flow-through was discarded, and the columns washed with buffer PB and PE as indicated by the manufacturer. In the last wash, centrifugation was performed for 2 min to remove traces of ethanol. The plasmids were eluted with

50 µl MilliQ water sterile. All recombinant plasmids were identified by digestion with appropriated enzymes and confirmed by commercial DNA sequencing (SeqLab GmbH).

## **8 Protein expression and purification**

### **8.1 Endogenous rabbit coatomer**

Rabbit liver (30 to 40g) is cut into pieves by a scalpel. All subsequent steps are carried out at 4°C. It is then homogenized using a waring blender (3x20 seconds) in the following buffer (buffer A):

25 mM Tris-HCl (pH 7.4), 500 mM KCl, 250 mM sucrose, 2 mM EGTA, 1mM DTT, protease inhibitor tablets (Roche).

The homogenate was centrifuged at 10,000g for 1 hour and filtrated through cheese cloth. After two additional centrifugations at 100,000g, the supernatant is filtrated again through cheese cloth.

The sample is fractionated by Ammonium sulfate precipitation at 35% saturation. After stirring for 60 minutes, the precipitate is recovered by centrifugation at 8,000g for 30 minutes and resuspended in 100 ml of the following buffer (buffer B):

25 mM Tris-HCl (pH 7.4), 200 mM KCl, 1 mM DTT, 10% (w/v) Glycerol, protease inhibitors cocktail.

The sample is then dialyzed against 5 liters of the same buffer using a dialysis tubing (12 to 14 KD cutoff). The buffer was changed twice.

After dialysis, the sample is centrifugated at 100,000g for one hour. The supernatant is loaded onto a 500 ml DEAE Sepharose column Fast flow column (Amersham biosciences) pre equilibrated with buffer B.

After binding of proteins and equilibration of the column (flat base lane), bound proteins were eluted with a salt gradient (buffer C: 25 mM Tris-HCl (pH 7.4), 500 mM KCl, 1mM DTT, 10% (w/v) Glycerol). Fractions containing coatomer were diluted to lower the salt concentration to 200 mM. Column was operated at 10

ml/min.

The sample was then loaded onto a 6 ml Resource Q column (Amersham biosciences) equilibrated in the buffer B. After exchange of proteins on the resin and reaching base lane, a salt gradient allows elution of coatomer at 350 to 400 mM KCl with purity up to 60%.

Coatomer containing fractions were pooled and diluted to lower the salt concentration to 200 mM. Therefore, an additional Resource Q column (5 ml) was used to concentrate coatomer. Fractions were analyzed by SDS-PAGE and stained with Coomassie and coatomer is typically 50 to 60% pure.

## 8.2 Endogenous yeast TAP-tagged coatomer

A yeast strain TAP-tagged on the  $\gamma$ -cop coatomer subunit was purchased from Cellzome.

Yeast was grown in 2 liters YPD in 5 l flask with “breakers” to OD 3.5 - 4.0. They were then harvested and the pellet was washed with water. In addition, pellet was washed with LB Buffer.

Subsequent to the wash, pellet was resuspended in 25ml LB in presence of 0.5mM PMSF and 1 mM DTT and lysed with 25 ml glass beads (0.45 - 0.5 mm) into cold lysis container. The sample was recovered with a 50 ml syringe (LUERLOCK) over a 50 ml Falcon tube with a funnel and the lysate was pressed into the Falcon tube while beads stay in the syringe. The beads were washed with 10 ml LB (adding it to the beads in the syringe and pressing it through). Lysate was then spun at 4,000 rpm for 10 min at 4°C. The supernatant was transferred to ultracentrifuge tube and spun in a TI70 rotor for 1h at 100,000 g. The fatty top phase was removed with a water pump and the lysate transferred with 10 ml pipette to a Falcon tube. Glycerol was added to final concentration of 5%(w/v).

### First affinity purification with IgG beads



IgG beads (0.5 ml slurry) were washed with cold LB 3x times in a Falcon tube and added to the lysate. An additional Incubation for 1h at 4°C was carried out on a turning wheel. The sample was spun at 1,800 rpm for 3min at 4°C and the supernatant was removed.

The beads were then transferred to mobicol (purchased from Mobitec) and a syringe was screwd to the Mobicol. Beads were washed with 10 ml LB + 0.5 mM DTT.

### **TEV cleavage**

A volume of 150 µl LB (+ 0.5 mM DTT) was added to the beads as well as 4 µl TEV (1 mg/ml). Digestion is complete after 2 hours at 16°C on a turning wheel. After cleavage, the eluate is recovered in 150 µl.

### **Second affinity purification with calmodulin Beads**

Calmodulin beads were prepared as follows,

A volume of 600 µl slurry was washed with LB supplemented with 2 mM CaCl<sub>2</sub> and 1 mM DTT. Washed beads were transfered to mobicol and 150 µl LB + 4 mM CaCl<sub>2</sub> + 1 mM DTT and incubated with the TEV eluate (150 µl) for 1hour at 4°C on a turning wheel. Mobicol was connected to a 10 ml syringe and beads were washed by adding 5 ml LB + 2 mM CaCl<sub>2</sub> to the syringe.

### **Elution of affinity purified coatomer**

A volume of 600 µl elution buffer (10 mM TrisHCl, pH 8.0, 5 mM EGTA) was added to the beads and after 10 minutes incubation at 37°C, protein was eluted using a 3 ml syringe.

### **Gel filtration of purified coatomer**

The TAP-Tagged coatomer complex was polished further by size exclusion chromatography on a Superose6 (Amersham biosciences) following the manufacturer reommendations. The column was calibrated by runing Thyroglobulin, 660 KD; Alcohol dehydrogenase 150 KD; Ovalbumin, 45 KD; and Lysosyme, 14.5 KD as standard proteins.

### 8.3 Recombinant yeast ARF1p

BI21 (DE3) STAR cells were cotransformed with 1  $\mu$ l pET24a-ARF1p and 1  $\mu$ l pACYC-Duet1-NMT1 plasmids and plated. A single colony was grown in 5 ml LB in presence of Kanamycine (50  $\mu$ g/ $\mu$ l) and chloramphenicol (34  $\mu$ g/ $\mu$ l) and served as a preculture for 1 liter culture. Cells were grown until OD= 0.2-0.4 before addition of myristic acid. They were further grown until OD= 0.6 and then induced with 1 mM IPTG at 27°C. When the bicistronic construct containing ARF1p and NMT1 genes was used, the same conditions were used and only chloramphenicol was added (34  $\mu$ g/ $\mu$ l).

Cells were centrifuged and the bacterial pellet was resuspended in MES buffer (25 mM MES, 1mM DTT, 5 $\mu$ M GDP, 1mM MgCl<sub>2</sub>, pH=5.7) (buffer A). Cells were lysed and centrifuged at 30,000g for 15 minutes and 100,000g for 1 hour. The supernatant containing soluble proteins was precipitated with Ammonium sulfate at 35% saturation. Myristoylated ARF1p precipitates while its non-myristoylated counterpart remains soluble.

The precipitate is pelleted, resuspended in buffer A and desalted over a gel filtration column (PD10 Amersham biosciences). Two passages through this column allow removal of 99.75 % of the ammonium sulfate.

ARF1p has a PI of 7.46 and at the pH of buffer A (pH = 5.7), the protein is positively charged and can be purified by cation exchange chromatography (Source-S (Amersham biosciences)). After equilibration in buffer A and loading the column with its counter ion (Na<sup>+</sup>) in buffer B, the protein sample is loaded and the flow through is collected for control. Most of the proteins do not bind to the column at that pH. The column was equilibrated with buffer A until reaching the baseline and subjected to a NaCl linear gradient.

### 8.4 Recombinant human ARF1

The same purification procedure described above for yeast ARF1p was applied except that the plasmids used were pbb131 (that contains NMT1 gene and has a resistance for Kanamycin) and pET11d-hARF1 (has resistance for Ampicilin).

## 8.5 Recombinant Glo3p

BL21(DE3) star bacteria were transformed with pET15a-Glo3p plasmid and plated on an LB-agar plate containing 100 µl/ml Ampicilin. A single colony was grown in LB medium in presence of Ampicilin (100µg/ml). One liter culture was inoculated and grown. When cells density reached OD= 0.6, expression was induced with 1 mM IPTG.

The post-lysate pellet was resuspended in 8 M urea and pelleted again and Glo3p-His was purified from the soluble fraction by affinity chromatography over Nickel-Agarose beads (Novagen) and eluted with 250 mM Imidazole in presence of 8 M urea (Fig. 9, panel A). The protein concentration was adjusted to 0.1mg/ml and the buffer was exchanged to Hepes buffer (25 mM Hepes, 150 mM KOAc, 1mMDTT, 100 µM ZnCl<sub>2</sub>, 20% glycerol, pH 7.2) by the usage of PD10 column (Amersham biosciences).

## 8.6 Recombinant human p23

Origami (DE3) cells (that have mutations in both the thioredoxin reductase (*trxB*) and glutathione reductase (*gor*) genes, which greatly enhances disulfide bond formation in the cytoplasm) pET-32 Xa/LIC-p23 purified over Nickel beads (Novagen). Origami bacteria were transformed with 1 µl pET-32 Xa/LIC-p23 plasmid and plated on an LB-agar plate containing 100µl/ml Ampicilin. A single colony was grown in LB medium in presence of Ampicilin (100µg/ml) at 37°C. One liter culture was inoculated and grown. When cells density reached OD= 0.6, expression was induced with 1 mM IPTG, cells were transferred to 16°C and protein expression was induced with 1 mM IPTG over night. Cells were harvested and resuspended in lysis buffer (50 mM Na<sub>2</sub>HPO<sub>4</sub> pH 8, 400mM NaCl, 10 mM Imidazole, 4% (w/v) Triton X-100)). Cells were then broken after 3 passages

through a cell disrupter (Avestin EmulsiFlex-C5) at a pressure of 10,000 to 15,000 psi. The lysate was centrifuged once at 30,000g for 15 minutes followed by a centrifugation at 100,000g for 1 hour. The soluble material was incubated with 0.5 ml Nickel beads previously washed with the lysis buffer. After 1 hour incubation, beads were pelleted (5 minutes at 500g) and the supernatant removed. Beads were washed with 50 mM Na<sub>2</sub>HPO<sub>4</sub> pH 8, 400mM NaCl, 10 mM Imidazole, 1% (w/v) OG (20 ml). Two additional washes with the same buffer containing 20 mM and 50 mM Imidazole respectively, were performed. The bound protein was eluted with 50 mM Na<sub>2</sub>HPO<sub>4</sub> pH 8, 400mM NaCl, 250 mM Imidazole, 1% (w/v) OG. Samples could be stored for 4 days at 4°C without apparent precipitation.

## 8.7 Recombinant yeast SNAREs

SNAREs were cloned into pGEX vector (Amersham Biosciences) as GST fusion proteins and purified using Glutathione Sepharose 4 Fast flow beads (Amersham Biosciences) under the manufacturer recommendations.

BI21 (DE3) STAR cells were transformed with 1 µl pGEX2T-SNAREs, plated in LB-Agar Petri dishes containing 100µg/ml Ampicilin and incubated at 37°C over night. One single clone was picked to start a pre culture in 5 ml LB. 1 liter LB was inoculated with this pre culture and grown at 37 °C until OD= 0.5-0.6. Protein expression was then induced by addition of 0.1 mM IPTG for 3 hours.

Bacterial cells were pelleted and resuspended in PBS buffer supplemented with 4% (v/v) Triton X-100 and protease inhibitor tablets (1 tablet for 50 ml). Cells were then broken after 3 passages through a cell disrupter (Avestin EmulsiFlex-C5) at a pressure of 10,000 to 15,000 psi. The lysate was centrifuged once at 30,000g for 15 minutes followed by a centrifugation at 100,000g for 1 hour. The supernatant was incubated with 500µl Glutathione Sepharose beads, previously washed in PBS + 4% Triton X-100, at 4 °C for 1 hour. GST fusion SNAREs bind to the Glutathione Sepharose beads under these conditions. Beads were sedimented. (500g for 5 minutes) and washed with PBS supplemented with 1 % (w/v) OG (5 ml to each 1 ml slurry). After 5 minutes agitation on a rotating wheel,

the beads were pelleted again and the supernatant removed. This procedure was repeated three times. Bound GST-SNAREs were eluted from the beads by adding 0.5 ml 50 mM Tris-HCl, 20 mM reduced Glutathione, 1% (w/v) OG, pH 8. Four elutions of 0.5 ml each were collected.

## **8.8 Thrombin cleavage of GST fusion proteins**

Thrombin (Amersham Biosciences) was dissolved in cold PBS (500 Units in 500  $\mu$ l) and aliquots of 80 Units were frozen and kept at  $-80^{\circ}\text{C}$  until usage. Ten Units of thrombin were added to each mg of fusion protein. The reaction took place at room temperature for 2 to 16 hours.

## **9 SDS-PAGE and Western Blot analysis**

### **9.1 SDS-PAGE for separation of proteins**

Gels for SDS-PAGE were prepared according to the guidelines of Molecular cloning (3rd ed.). 12% and 14% separation gels were used in this experimental work or 12% and 4-12% pre-cast separation gels commercially available from Invitrogen. After electrophoresis, the gels were stained in coomassie blue solution and destained. For radioactive gels, after staining, the gels were dried and exposed to a film. Other gels were used for western blot analysis of the proteins of interest.

### **9.2 Transfer proteins from SDS-PAGE to a PVDF membrane or Nitrocellulose**

After performing SDS-PAGE, the proteins were electro-transferred to PVDF membranes (Immobilon-P® Milipore). The PVDF-membrane was submerged in methanol prior to soaking in the Anode buffer II. In semi-dry blotting discontinuous buffer system is used, composed of two anode buffers and one cathode buffer. The SDS-PAGE gel and PVDF membrane were arranged as follows: 2 sheets of Whatman 3MM filter paper pre-soaked in Anode buffer I were placed on the platinum anode, followed by 2 sheets of Whatman paper pre-soaked in Anode buffer II, the PVDF-membrane, the gel, and firmly 3 sheets of

Whatman paper pre-soaked in Cathode buffer on top. The air was removed carefully by rolling out the air bubbles either by using a pipette or a 50ml tube. The cathode was placed on the stack and the blotting was executed at 24V for 1.5 hrs.

### 9.3 Incubation of PVDF membranes with antibodies

Once the transfer was completed, the PDVF membrane was rinsed in water and stained with a Ponceau S solution. Excess of Ponceau S dye was washed away with water until protein marker bands appeared on the membrane and their positions could be marked on the membrane. The markers used throughout most of the thesis were broad range protein marker from Bio-Rad. The size of the protein markers is outlined in Table 3.

Protein	Molecular mass (kD)
Myosin	200
$\beta$ -galactosidase	116
Phosphorylase-b	97
Serum albumin	66
Ovalbumin	45
Carbonic anhydrase	31
Trypsin inhibitor	21
Lysozyme	14
Aprotinin	6.5

**Table 3: Protein standards (Broad Range)**

The PVDF membrane was blocked with 50 ml of 5% BSA in PBS for 1 hr at room temperature or overnight at 4°C. The blot was rinsed for 1min in PBS to remove BSA and incubated with the diluted primary antibodies (in 1% BSA PBS-T) for 1 hr at room temperature, followed by washing 3 times with PBST for 15 min. The blot was incubated with the HRP-conjugated secondary antibodies (1/5000 dilution) or HRP-conjugated Protein-G (1/1000 dilution) in 50 ml 1% BSA in PBST for 1 hr at room temperature. The blot was washed 3 times with PBST for 15 min

and developed using ECL® western blotting detection system (Amersham-Biotech).

## 10 Protein Determination

### 10.1 Protein Determination by BCA

For soluble protein determination the BCA protein assay was employed (Pierce). All samples, including a set of standards (BSA: 2.5 µg, 5.0 µg, 10 µg, 15 µg, 20 µg, 25 µg, 30 µg and 35 µg), were prepared in aqueous solution. For 10 µl of each sample 200 µl of working reagent was added. The solution was prepared by mixing 50 parts of Reagent A with 1 part of Reagent B. The samples, including standards and blanks, were incubated at 37°C for 30 min, followed by measurement of absorbance at 562nm on a plate reader.

### 10.2 Protein Determination by Lowry

Lowry Solution A:	2 g Na <sub>2</sub> -tartrate 100 g Na <sub>2</sub> CO <sub>3</sub>	Dissolved in 500 ml 1N NaOH, adjusted to 1 L with MiliQ water
Lowry Solution B:	2 g Na <sub>2</sub> -tartrate 1 g CuSO <sub>4</sub> ·5H <sub>2</sub> O	Dissolved in 90 ml H <sub>2</sub> O, 10ml NaOH adjusted to 500 ml with MiliQ water
Lowry Solution C:	Folin-Cicalteus.	Reagent prepared prior to use by diluting 1/10 with MiliQ water

Protein determination for membrane protein was performed according to Lowry. The protein standards were prepared with BSA (2.5 µg, 5.0 µg, 10 µg, 15 µg, 20 µg, 25 µg, 30 µg and 35 µg) dissolved in water. The samples and standards were prepared by adding 10 µl of deoxycholate stock solution (Stock solution: Sodium deoxycholate 2 mg/ml) to 50 µl of sample. 150 µl of TCA (10%) (TriChloroacetic acid) were added to the sample, vortexed and centrifuged for 10 min at 14000 rpm. The supernatant was removed, and 10 µl of SDS were added, followed by 50 µl of Lowry solution A. The sample was incubated at 50°C for 10min, and cooled down for 3min to room temperature. 10 µl of Lowry solution B was added,

and the sample incubated for 15min at room temperature. 150  $\mu$ l of Lowry solution C were added, and the sample was placed at 50°C for 10 min. Once the sample was at room temperature again, the absorbance was measured at 620nm on a plate reader.

## 11 Protein Precipitation

### 11.1 Chloroform-Methanol Precipitation

Chloroform-Methanol Solution 1:2      20 ml  $\text{CHCl}_3$ : 40 ml  $\text{CH}_3\text{OH}$

One volume of sample was mixed with 3 volumes of Chloroform-Methanol solution. The mix was vortexed until the solution was clear (1 or 2 drops of methanol were added when the solution did not become clear). The sample was centrifuged 14000 rpm for 15min at 15°C. The supernatant was discarded and the pellet was dried for 1hr at 37°C or overnight at room temperature. The pellet was dissolved by adding Sample cocktail. Once dissolved, the sample was suitable for protein determination and/or protein electrophoresis.

### 11.2 TCA precipitation

TCA solution 72% (w/v)

Sodium deoxycholate 2%

Acetone                                      kept at -20°C

The protein sample was diluted to a final volume of 1ml with MilliQ water, followed by addition of 16.7  $\mu$ l of 2% sodium deoxycholate. The sample was vortexed and incubated for 15min at room temperature. 100  $\mu$ l of TCA solution 72% was added to the sample and vortexed, and then centrifuged for 7 min at 10,000g. The supernatant was aspirated and 1ml of acetone at -20 added to wash the pellet. The sample was centrifuged as described above, and the pellet was allowed to dry.



## REFERENCES

**Antonny, B., Beraud-Dufour, S., Chardin, P. and Chabre, M.** (1997). N-terminal hydrophobic residues of the G-protein ADP-ribosylation factor-1 insert into membrane phospholipids upon GDP to GTP exchange. *Biochemistry* **36**, 4675-84.

**Aoe, T., Huber, I., Vasudevan, C., Watkins, S. C., Romero, G., Cassel, D. and Hsu, V. W.** (1999). The KDEL receptor regulates a GTPase-activating protein for ADP-ribosylation factor 1 by interacting with its non-catalytic domain. *J Biol Chem* **274**, 20545-9.

**Ballensiefen, W., Ossipov, D. and Schmitt, H. D.** (1998). Recycling of the yeast v-SNARE Sec22p involves COPI-proteins and the ER transmembrane proteins Ufe1p and Sec20p. *J Cell Sci* **111 ( Pt 11)**, 1507-20.

**Barlowe, C.** (2000). Traffic COPs of the early secretory pathway. *Traffic* **1**, 371-7.

**Barlowe, C., Orci, L., Yeung, T., Hosobuchi, M., Hamamoto, S., Salama, N., Rexach, M. F., Ravazzola, M., Amherdt, M. and Schekman, R.** (1994). COPII: a membrane coat formed by Sec proteins that drive vesicle budding from the endoplasmic reticulum. *Cell* **77**, 895-907.

**Barlowe, C. and Schekman, R.** (1993). SEC12 encodes a guanine-nucleotide-exchange factor essential for transport vesicle budding from the ER. *Nature* **365**, 347-9.

**Beraud-Dufour, S., Paris, S., Chabre, M. and Antonny, B.** (1999). Dual interaction of ADP ribosylation factor 1 with Sec7 domain and with lipid membranes during catalysis of guanine nucleotide exchange. *J Biol Chem* **274**, 37629-36.

**Bremser, M., Nickel, W., Schweikert, M., Ravazzola, M., Amherdt, M., Hughes, C. A., Sollner, T. H., Rothman, J. E. and Wieland, F. T.** (1999). Coupling of coat assembly and vesicle budding to packaging of putative cargo receptors. *Cell* **96**, 495-506.

**Brugger, B., Erben, G., Sandhoff, R., Wieland, F. T. and Lehmann, W. D.** (1997). Quantitative analysis of biological membrane lipids at the low picomole level by nano-electrospray ionization tandem mass spectrometry. *Proc Natl Acad Sci U S A* **94**, 2339-44.

**Brugger, B., Sandhoff, R., Wegehingel, S., Gorgas, K., Malsam, J., Helms, J. B., Lehmann, W. D., Nickel, W. and Wieland, F. T.** (2000). Evidence for segregation of sphingomyelin and cholesterol during formation of COPI-coated vesicles. *J Cell Biol* **151**, 507-18.

**Chardin, P., Paris, S., Antonny, B., Robineau, S., Beraud-Dufour, S., Jackson, C. L. and Chabre, M.** (1996). A human exchange factor for ARF contains Sec7- and pleckstrin-homology domains. *Nature* **384**, 481-4.

**Cukierman, E., Huber, I., Rotman, M. and Cassel, D.** (1995). The ARF1 GTPase-activating protein: zinc finger motif and Golgi complex localization. *Science* **270**, 1999-2002.

**De Camilli, P., Emr, S. D., McPherson, P. S. and Novick, P.** (1996). Phosphoinositides as regulators in membrane traffic. *Science* **271**, 1533-9.

**Denzel, A., Otto, F., Girod, A., Pepperkok, R., Watson, R., Rosewell, I., Bergeron, J. J., Solari, R. C. and Owen, M. J.** (2000). The p24 family member p23 is required for early embryonic development. *Curr Biol* **10**, 55-8.

**Dominguez, M., Dejgaard, K., Fullekrug, J., Dahan, S., Fazel, A., Paccaud, J. P., Thomas, D. Y., Bergeron, J. J. and Nilsson, T.** (1998). gp25L/emp24/p24 protein family members of the cis-Golgi network bind both COP I and II coatomer. *J Cell Biol* **140**, 751-65.

**Donaldson, J. G. and Klausner, R. D.** (1994). ARF: a key regulatory switch in membrane traffic and organelle structure. *Curr Opin Cell Biol* **6**, 527-32.

**Duronio, R. J., Jackson-Machelski, E., Heuckeroth, R. O., Olins, P. O., Devine, C. S., Yonemoto, W., Slice, L. W., Taylor, S. S. and Gordon, J. I.** (1990). Protein N-myristoylation in Escherichia coli: reconstitution of a eukaryotic protein modification in bacteria. *Proc Natl Acad Sci U S A* **87**, 1506-10.

**Emery, G., Rojo, M. and Gruenberg, J.** (2000). Coupled transport of p24 family members. *J Cell Sci* **113 ( Pt 13)**, 2507-16.

**Faurobert, E., Otto-Bruc, A., Chardin, P. and Chabre, M.** (1993). Tryptophan W207 in transducin T alpha is the fluorescence sensor of the G protein activation switch and is involved in the effector binding. *Embo J* **12**, 4191-8.

**Fiedler, K., Veit, M., Stamnes, M. A. and Rothman, J. E.** (1996). Bimodal interaction of coatomer with the p24 family of putative cargo receptors. *Science* **273**, 1396-9.

**Fleischer, B., Zambrano, F. and Fleischer, S.** (1974). Biochemical characterization of the golgi complex of mammalian cells. *J Supramol Struct* **2**, 737-50.

**Franco, M., Boretto, J., Robineau, S., Monier, S., Goud, B., Chardin, P. and Chavrier, P.** (1998). ARNO3, a Sec7-domain guanine nucleotide exchange factor for ADP ribosylation factor 1, is involved in the control of Golgi structure and function. *Proc Natl Acad Sci U S A* **95**, 9926-31.

**Franco, M., Chardin, P., Chabre, M. and Paris, S.** (1996). Myristoylation-facilitated binding of the G protein ARF1GDP to membrane phospholipids is required for its activation by a soluble nucleotide exchange factor. *J Biol Chem* **271**, 1573-8.

**Franco, M., Paris, S. and Chabre, M.** (1995). The small G-protein ARF1GDP binds to the Gt beta gamma subunit of transducin, but not to Gt alpha GDP-Gt beta gamma. *FEBS Lett* **362**, 286-90.

**Frank, S., Upender, S., Hansen, S. H. and Casanova, J. E.** (1998). ARNO is a guanine nucleotide exchange factor for ADP-ribosylation factor 6. *J Biol Chem* **273**, 23-7.

**Fullekrug, J., Scheiffele, P. and Simons, K.** (1999). VIP36 localisation to the early secretory pathway. *J Cell Sci* **112 ( Pt 17)**, 2813-21.

**Futatsumori, M., Kasai, K., Takatsu, H., Shin, H. W. and Nakayama, K.** (2000). Identification and characterization of novel isoforms of COP I subunits. *J Biochem (Tokyo)* **128**, 793-801.

**Goldberg, J.** (1998). Structural basis for activation of ARF GTPase: mechanisms of guanine nucleotide exchange and GTP-myristoyl switching. *Cell* **95**, 237-48.

**Goldberg, J.** (1999). Structural and functional analysis of the ARF1-ARFGAP complex reveals a role for coatamer in GTP hydrolysis. *Cell* **96**, 893-902.

**Goldberg, J.** (2000). Decoding of sorting signals by coatamer through a GTPase switch in the COPI coat complex. *Cell* **100**, 671-9.

**Gommel, D., Orci, L., Emig, E. M., Hannah, M. J., Ravazzola, M., Nickel, W., Helms, J. B., Wieland, F. T. and Sohn, K.** (1999). p24 and p23, the major transmembrane proteins of COPI-coated transport vesicles, form hetero-oligomeric complexes and cycle between the organelles of the early secretory pathway. *FEBS Lett* **447**, 179-85.

**Gommel, D. U., Memon, A. R., Heiss, A., Lottspeich, F., Pfannstiel, J., Lechner, J., Reinhard, C., Helms, J. B., Nickel, W. and Wieland, F. T.** (2001). Recruitment to Golgi membranes of ADP-ribosylation factor 1 is mediated by the cytoplasmic domain of p23. *Embo J* **20**, 6751-60.

**Harter, C. and Wieland, F. T.** (1998). A single binding site for dilysine retrieval motifs and p23 within the gamma subunit of coatamer. *Proc Natl Acad Sci U S A* **95**, 11649-54.

**Hay, J. C., Klumperman, J., Oorschot, V., Steegmaier, M., Kuo, C. S. and Scheller, R. H.** (1998). Localization, dynamics, and protein interactions reveal distinct roles for ER and Golgi SNAREs. *J Cell Biol* **141**, 1489-502.

**Helms, J. B., Palmer, D. J. and Rothman, J. E.** (1993). Two distinct populations of ARF bound to Golgi membranes. *J Cell Biol* **121**, 751-60.

**Helms, J. B. and Rothman, J. E.** (1992). Inhibition by brefeldin A of a Golgi membrane enzyme that catalyses exchange of guanine nucleotide bound to ARF. *Nature* **360**, 352-4.

**Howell, K. E. and Palade, G. E.** (1982). Hepatic Golgi fractions resolved into membrane and content subfractions. *J Cell Biol* **92**, 822-32.

**Jackson, C. L. and Casanova, J. E.** (2000). Turning on ARF: the Sec7 family of guanine-nucleotide-exchange factors. *Trends Cell Biol* **10**, 60-7.

**Jackson, M. R., Nilsson, T. and Peterson, P. A.** (1990). Identification of a consensus motif for retention of transmembrane proteins in the endoplasmic reticulum. *Embo J* **9**, 3153-62.

**Jackson, M. R., Nilsson, T. and Peterson, P. A.** (1993). Retrieval of transmembrane proteins to the endoplasmic reticulum. *J Cell Biol* **121**, 317-33.

**Jenne, N., Frey, K., Brugger, B. and Wieland, F. T.** (2002). Oligomeric state and stoichiometry of p24 proteins in the early secretory pathway. *J Biol Chem* **277**, 46504-11.

**Kahn, R. A. and Gilman, A. G.** (1986). The protein cofactor necessary for ADP-ribosylation of Gs by cholera toxin is itself a GTP binding protein. *J Biol Chem* **261**, 7906-11.

**Kinuta, M. and Takei, K.** (2002). Utilization of liposomes in vesicular transport studies. *Cell Struct Funct* **27**, 63-9.

**Kinuta, M., Yamada, H., Abe, T., Watanabe, M., Li, S. A., Kamitani, A., Yasuda, T., Matsukawa, T., Kumon, H. and Takei, K.** (2002). Phosphatidylinositol 4,5-bisphosphate stimulates vesicle formation from liposomes by brain cytosol. *Proc Natl Acad Sci U S A* **99**, 2842-7.

**Kirchhausen, T.** (2000). Clathrin. *Annu Rev Biochem* **69**, 699-727.

**Lanoix, J., Ouwendijk, J., Stark, A., Szafer, E., Cassel, D., Dejgaard, K., Weiss, M. and Nilsson, T.** (2001). Sorting of Golgi resident proteins into different subpopulations of COPI vesicles: a role for ArfGAP1. *J Cell Biol* **155**, 1199-212.

**Lippincott-Schwartz, J., Cole, N. B. and Donaldson, J. G.** (1998). Building a secretory apparatus: role of ARF1/COPI in Golgi biogenesis and maintenance. *Histochem Cell Biol* **109**, 449-62.

**Lupashin, V. V., Pokrovskaya, I. D., McNew, J. A. and Waters, M. G.** (1997). Characterization of a novel yeast SNARE protein implicated in Golgi retrograde traffic. *Mol Biol Cell* **8**, 2659-76.

**Majoul, I., Straub, M., Hell, S. W., Duden, R. and Soling, H. D.** (2001). KDEL-cargo regulates interactions between proteins involved in COPI vesicle traffic: measurements in living cells using FRET. *Dev Cell* **1**, 139-53.

**Makler, V., Cukierman, E., Rotman, M., Admon, A. and Cassel, D.** (1995). ADP-ribosylation factor-directed GTPase-activating protein. Purification and partial characterization. *J Biol Chem* **270**, 5232-7.

**Malhotra, V., Serafini, T., Orci, L., Shepherd, J. C. and Rothman, J. E.** (1989). Purification of a novel class of coated vesicles mediating biosynthetic protein transport through the Golgi stack. *Cell* **58**, 329-36.

**Malsam, J., Gommel, D., Wieland, F. T. and Nickel, W.** (1999). A role for ADP ribosylation factor in the control of cargo uptake during COPI-coated vesicle biogenesis. *FEBS Lett* **462**, 267-72.

**Marsh, B. J., Mastronarde, D. N., Buttle, K. F., Howell, K. E. and McIntosh, J. R.** (2001a). Organellar relationships in the Golgi region of the pancreatic beta cell line, HIT-T15, visualized by high resolution electron tomography. *Proc Natl Acad Sci U S A* **98**, 2399-406.

**Marsh, B. J., Mastronarde, D. N., McIntosh, J. R. and Howell, K. E.** (2001b). Structural evidence for multiple transport mechanisms through the Golgi in the pancreatic beta-cell line, HIT-T15. *Biochem Soc Trans* **29**, 461-7.

**Marzioch, M., Henthorn, D. C., Herrmann, J. M., Wilson, R., Thomas, D. Y., Bergeron, J. J., Solari, R. C. and Rowley, A.** (1999). Erp1p and Erp2p, partners for Emp24p and Erv25p in a yeast p24 complex. *Mol Biol Cell* **10**, 1923-38.

**Matsuoka, K., Morimitsu, Y., Uchida, K. and Schekman, R.** (1998a). Coat assembly directs v-SNARE concentration into synthetic COPII vesicles. *Mol Cell* **2**, 703-8.

**Matsuoka, K., Orci, L., Amherdt, M., Bednarek, S. Y., Hamamoto, S., Schekman, R. and Yeung, T.** (1998b). COPII-coated vesicle formation reconstituted with purified coat proteins and chemically defined liposomes. *Cell* **93**, 263-75.

**McNew, J. A., Coe, J. G., Sogaard, M., Zemelman, B. V., Wimmer, C., Hong, W. and Sollner, T. H.** (1998). Gos1p, a *Saccharomyces cerevisiae* SNARE protein involved in Golgi transport. *FEBS Lett* **435**, 89-95.

**McNew, J. A., Parlati, F., Fukuda, R., Johnston, R. J., Paz, K., Paumet, F., Sollner, T. H. and Rothman, J. E.** (2000a). Compartmental specificity of cellular membrane fusion encoded in SNARE proteins. *Nature* **407**, 153-9.

**McNew, J. A., Sogaard, M., Lampen, N. M., Machida, S., Ye, R. R., Lacomis, L., Tempst, P., Rothman, J. E. and Sollner, T. H.** (1997). Ykt6p, a prenylated SNARE essential for endoplasmic reticulum-Golgi transport. *J Biol Chem* **272**, 17776-83.

**McNew, J. A., Weber, T., Parlati, F., Johnston, R. J., Melia, T. J., Sollner, T. H. and Rothman, J. E.** (2000b). Close is not enough: SNARE-dependent membrane fusion requires an active mechanism that transduces force to membrane anchors. *J Cell Biol* **150**, 105-17.

**Mossessova, E., Gulbis, J. M. and Goldberg, J.** (1998). Structure of the guanine nucleotide exchange factor Sec7 domain of human arno and analysis of the interaction with ARF GTPase. *Cell* **92**, 415-23.

**Mueller, P., Chien, T. F. and Rudy, B.** (1983). Formation and properties of cell-size lipid bilayer vesicles. *Biophys J* **44**, 375-81.

**Nichols, B. J.** (2002). A distinct class of endosome mediates clathrin-independent endocytosis to the Golgi complex. *Nat Cell Biol* **4**, 374-8.

**Nickel, W., Sohn, K., Bunning, C. and Wieland, F. T.** (1997). p23, a major COPI-vesicle membrane protein, constitutively cycles through the early secretory pathway. *Proc Natl Acad Sci U S A* **94**, 11393-8.

**Nickel, W., Weber, T., McNew, J. A., Parlati, F., Sollner, T. H. and Rothman, J. E.** (1999). Content mixing and membrane integrity during membrane fusion driven by pairing of isolated v-SNAREs and t-SNAREs. *Proc Natl Acad Sci U S A* **96**, 12571-6.

**Nickel, W. and Wieland, F. T.** (2001). Receptor-dependent formation of COPI-coated vesicles from chemically defined donor liposomes. *Methods Enzymol* **329**, 388-404.

**Olson, E. N. and Spizz, G.** (1986). Fatty acylation of cellular proteins. Temporal and subcellular differences between palmitate and myristate acylation. *J Biol Chem* **261**, 2458-66.

**Olson, E. N., Towler, D. A. and Glaser, L.** (1985). Specificity of fatty acid acylation of cellular proteins. *J Biol Chem* **260**, 3784-90.

**Orci, L., Glick, B. S. and Rothman, J. E.** (1986). A new type of coated vesicular carrier that appears not to contain clathrin: its possible role in protein transport within the Golgi stack. *Cell* **46**, 171-84.

**Orci, L., Palmer, D. J., Ravazzola, M., Perrelet, A., Amherdt, M. and Rothman, J. E.** (1993). Budding from Golgi membranes requires the coatamer complex of non-clathrin coat proteins. *Nature* **362**, 648-52.

**Orci, L., Stamnes, M., Ravazzola, M., Amherdt, M., Perrelet, A., Sollner, T. H. and Rothman, J. E.** (1997). Bidirectional transport by distinct populations of COPI-coated vesicles. *Cell* **90**, 335-49.

**Ossipov, D., Schroder-Kohne, S. and Schmitt, H. D.** (1999). Yeast ER-Golgi v-SNAREs Bos1p and Bet1p differ in steady-state localization and targeting. *J Cell Sci* **112 ( Pt 22)**, 4135-42.



**Pavel, J., Harter, C. and Wieland, F. T.** (1998). Reversible dissociation of coatomer: functional characterization of a beta/delta-coat protein subcomplex. *Proc Natl Acad Sci U S A* **95**, 2140-5.

**Pearse, B. M.** (1975). Coated vesicles from pig brain: purification and biochemical characterization. *J Mol Biol* **97**, 93-8.

**Pelkmans, L., Kartenbeck, J. and Helenius, A.** (2001). Caveolar endocytosis of simian virus 40 reveals a new two-step vesicular-transport pathway to the ER. *Nat Cell Biol* **3**, 473-83.

**Peng, R., De Antoni, A. and Gallwitz, D.** (2000). Evidence for overlapping and distinct functions in protein transport of coat protein Sec24p family members. *J Biol Chem* **275**, 11521-8.

**Peyroche, A., Paris, S. and Jackson, C. L.** (1996). Nucleotide exchange on ARF mediated by yeast Gea1 protein. *Nature* **384**, 479-81.

**Pisam, M., Boeuf, G., Prunet, P. and Rambourg, A.** (1990). Ultrastructural features of mitochondria-rich cells in stenohaline freshwater and seawater fishes. *Am J Anat* **187**, 21-31.

**Poon, P. P., Wang, X., Rotman, M., Huber, I., Cukierman, E., Cassel, D., Singer, R. A. and Johnston, G. C.** (1996). *Saccharomyces cerevisiae* Gcs1 is an ADP-ribosylation factor GTPase-activating protein. *Proc Natl Acad Sci U S A* **93**, 10074-7.

**Rambourg, A. and Clermont, Y.** (1990). Three-dimensional electron microscopy: structure of the Golgi apparatus. *Eur J Cell Biol* **51**, 189-200.

**Rein, U., Andag, U., Duden, R., Schmitt, H. D. and Spang, A.** (2002). ARF-GAP-mediated interaction between the ER-Golgi v-SNAREs and the COPI coat. *J Cell Biol* **157**, 395-404.

**Reinhard, C., Harter, C., Bremser, M., Brugger, B., Sohn, K., Helms, J. B. and Wieland, F.** (1999). Receptor-induced polymerization of coatomer. *Proc Natl Acad Sci U S A* **96**, 1224-8.

**Reinhard, C., Schweikert, M., Wieland, F. T. and Nickel, W.** (2003). Functional reconstitution of COPI coat assembly and disassembly using chemically defined components. *Proc Natl Acad Sci U S A* **100**, 8253-7.

**Rigaut, G., Shevchenko, A., Rutz, B., Wilm, M., Mann, M. and Seraphin, B.** (1999). A generic protein purification method for protein complex characterization and proteome exploration. *Nat Biotechnol* **17**, 1030-2.

**Robineau, S., Chabre, M. and Antonny, B.** (2000). Binding site of brefeldin A at the interface between the small G protein ADP-ribosylation factor 1 (ARF1) and the nucleotide-exchange factor Sec7 domain. *Proc Natl Acad Sci U S A* **97**, 9913-8.

**Roth, M. G. and Sternweis, P. C.** (1997). The role of lipid signaling in constitutive membrane traffic. *Curr Opin Cell Biol* **9**, 519-26.

**Rothman, J. E.** (1994). Intracellular membrane fusion. *Adv Second Messenger Phosphoprotein Res* **29**, 81-96.

**Rouser, G., Fkeischer, S. and Yamamoto, A.** (1970). Two dimensional thin layer chromatographic separation of polar lipids and determination of phospholipids by phosphorus analysis of spots. *Lipids* **5**, 494-6.

**Schekman, R. and Orci, L.** (1996). Coat proteins and vesicle budding. *Science* **271**, 1526-33.

**Schimmoller, F., Singer-Kruger, B., Schroder, S., Kruger, U., Barlowe, C. and Riezman, H.** (1995). The absence of Emp24p, a component of ER-derived COPII-coated vesicles, causes a defect in transport of selected proteins to the Golgi. *Embo J* **14**, 1329-39.

**Serafini, T., Orci, L., Amherdt, M., Brunner, M., Kahn, R. A. and Rothman, J. E.** (1991). ADP-ribosylation factor is a subunit of the coat of Golgi-derived COP-coated vesicles: a novel role for a GTP-binding protein. *Cell* **67**, 239-53.

**Sohn, K., Orci, L., Ravazzola, M., Amherdt, M., Bremser, M., Lottspeich, F., Fiedler, K., Helms, J. B. and Wieland, F. T.** (1996). A major transmembrane protein of Golgi-derived COPI-coated vesicles involved in coatamer binding. *J Cell Biol* **135**, 1239-48.

**Sollner, T., Whiteheart, S. W., Brunner, M., Erdjument-Bromage, H., Geromanos, S., Tempst, P. and Rothman, J. E.** (1993). SNAP receptors implicated in vesicle targeting and fusion. *Nature* **362**, 318-24.

**Spang, A., Matsuoka, K., Hamamoto, S., Schekman, R. and Orci, L.** (1998). Coatamer, Arf1p, and nucleotide are required to bud coat protein complex I-coated vesicles from large synthetic liposomes. *Proc Natl Acad Sci U S A* **95**, 11199-204.

**Spang, A. and Schekman, R.** (1998). Reconstitution of retrograde transport from the Golgi to the ER in vitro. *J Cell Biol* **143**, 589-99.

**Springer, S., Chen, E., Duden, R., Marzioch, M., Rowley, A., Hamamoto, S., Merchant, S. and Schekman, R.** (2000). The p24 proteins are not essential for vesicular transport in *Saccharomyces cerevisiae*. *Proc Natl Acad Sci U S A* **97**, 4034-9.

**Springer, S., Spang, A. and Schekman, R.** (1999). A primer on vesicle budding. *Cell* **97**, 145-8.

**Stamnes, M. A., Craighead, M. W., Hoe, M. H., Lampen, N., Geromanos, S., Tempst, P. and Rothman, J. E.** (1995). An integral membrane component of coatamer-coated transport vesicles defines a family of proteins involved in budding. *Proc Natl Acad Sci U S A* **92**, 8011-5.

**Stenbeck, G., Harter, C., Brecht, A., Herrmann, D., Lottspeich, F., Orci, L. and Wieland, F. T.** (1993). beta'-COP, a novel subunit of coatamer. *Embo J* **12**, 2841-5.

**Szoka, F., Jr. and Papahadjopoulos, D.** (1978). Procedure for preparation of liposomes with large internal aqueous space and high capture by reverse-phase evaporation. *Proc Natl Acad Sci U S A* **75**, 4194-8.

**Takei, K., McPherson, P. S., Schmid, S. L. and De Camilli, P.** (1995). Tubular membrane invaginations coated by dynamin rings are induced by GTP-gamma S in nerve terminals. *Nature* **374**, 186-90.

**Takei, K., Slepnev, V. I. and De Camilli, P.** (2001). Interactions of dynamin and amphiphysin with liposomes. *Methods Enzymol* **329**, 478-86.

**Tanigawa, G., Orci, L., Amherdt, M., Ravazzola, M., Helms, J. B. and Rothman, J. E.** (1993). Hydrolysis of bound GTP by ARF protein triggers uncoating of Golgi-derived COP-coated vesicles. *J Cell Biol* **123**, 1365-71.

**Timofeev, B. A., Bolotin, I. M., Stepanova, L. P., Bogdanov, A. A., Jr., Georgiu, K., Malyshev, S. N., Petrovsky, V. V., Klibanov, A. L. and Torchilin, V. P.** (1994). Liposomal diamidine (imidocarb): preparation and animal studies. *J Microencapsul* **11**, 627-32.

**Togawa, A., Morinaga, N., Ogasawara, M., Moss, J. and Vaughan, M.** (1999). Purification and cloning of a brefeldin A-inhibited guanine nucleotide-exchange protein for ADP-ribosylation factors. *J Biol Chem* **274**, 12308-15.

**Towler, D. A., Adams, S. P., Eubanks, S. R., Towery, D. S., Jackson-Machelski, E., Glaser, L. and Gordon, J. I.** (1987). Purification and characterization of yeast myristoyl CoA:protein N-myristoyltransferase. *Proc Natl Acad Sci U S A* **84**, 2708-12.

**van Meer, G.** (1998). Lipids of the Golgi membrane. *Trends Cell Biol* **8**, 29-33.

**Van Valkenburgh, H. A. and Kahn, R. A.** (2002). Coexpression of proteins with methionine aminopeptidase and/or N-myristoyltransferase in *Escherichia coli* to increase acylation and homogeneity of protein preparations. *Methods Enzymol* **344**, 186-93.

**Wada, I., Rindress, D., Cameron, P. H., Ou, W. J., Doherty, J. J., 2nd, Louvard, D., Bell, A. W., Dignard, D., Thomas, D. Y. and Bergeron, J. J.** (1991). SSR alpha and associated calnexin are major calcium binding proteins of the endoplasmic reticulum membrane. *J Biol Chem* **266**, 19599-610.

**Wagner, S. and Paltauf, F.** (1994). Generation of glycerophospholipid molecular species in the yeast *Saccharomyces cerevisiae*. Fatty acid pattern of phospholipid classes and selective acyl turnover at sn-1 and sn-2 positions. *Yeast* **10**, 1429-37.

**Weber, T., Zemelman, B. V., McNew, J. A., Westermann, B., Gmachl, M., Parlati, F., Sollner, T. H. and Rothman, J. E.** (1998). SNAREpins: minimal machinery for membrane fusion. *Cell* **92**, 759-72.

**Wegmann, D., Hess, P., Baier, C., Wieland, F. T., Reinhard, C.** (2003). Novel isotopic  $\gamma/\zeta$ -subunits reveal three coatomer complexes in mammals. Submitted

**Wilcox, C., Hu, J. S. and Olson, E. N.** (1987). Acylation of proteins with myristic acid occurs cotranslationally. *Science* **238**, 1275-8.

**Xu, Y., Martin, S., James, D. E. and Hong, W.** (2002). GS15 forms a SNARE complex with syntaxin 5, GS28, and Ykt6 and is implicated in traffic in the early cisternae of the Golgi apparatus. *Mol Biol Cell* **13**, 3493-507.

**Yang, J. S., Lee, S. Y., Gao, M., Bourgoin, S., Randazzo, P. A., Premont, R. T. and Hsu, V. W.** (2002). ARFGAP1 promotes the formation of COPI vesicles, suggesting function as a component of the coat. *J Cell Biol* **159**, 69-78.

**Zhang, T., Wong, S. H., Tang, B. L., Xu, Y. and Hong, W.** (1999). Morphological and functional association of Sec22b/ERS-24 with the pre-Golgi intermediate compartment. *Mol Biol Cell* **10**, 435-53.

**Zhao, L., Helms, J. B., Brugger, B., Harter, C., Martoglio, B., Graf, R., Brunner, J. and Wieland, F. T.** (1997). Direct and GTP-dependent interaction of ADP ribosylation factor 1 with coatamer subunit beta. *Proc Natl Acad Sci U S A* **94**, 4418-23.

**Zhao, L., Helms, J. B., Brunner, J. and Wieland, F. T.** (1999). GTP-dependent binding of ADP-ribosylation factor to coatamer in close proximity to the binding site for dilysine retrieval motifs and p23. *J Biol Chem* **274**, 14198-203.

**Zinser, E. and Daum, G.** (1995). Isolation and biochemical characterization of organelles from the yeast, *Saccharomyces cerevisiae*. *Yeast* **11**, 493-536.

## ACKNOWLEDGMENTS

After three years of hard work, this thesis is eventually coming to the end. Here I wish to express my gratefulness to the people who have contributed to its completion.

First, I would like to sincerely thank Prof. Dr. Wieland for giving me the opportunity to work on such an interesting field in his lab. I am deeply grateful to him for his supervision, helpful discussions and support.

I am beholden to Prof. Dr. Brunner for being my second adviser.

During my work, I have appreciated working with the members of the lab. Here I would like to thank them for the good moments we spent together. My thoughts go to Armin, Jörg, Zhe, Li yun, Sandra, Dominik, Connie, Britta, Karolin, Nicole, Per, Oliver, Anke, Raphael, Andre and Walter.

I am grateful to Julien Béthune and Leonardo Serrano who became close friends during my training in Heidelberg. Their valuable help has contributed to motivate me during difficult moments. Here I sent them my faithful gratitude.

Une pensée particulière va à mes parents qui m'ont soutenu moralement durant mes années de thèse.

Enfin, je voudrais rendre hommage à Julia qui a été auprès de moi à chaque instant depuis le début de ma thèse. Son aide dans les moments de doute et de frustration m'a toujours permis de remonter la pente et de continuer. Ce travail lui doit énormément et je le lui dédie entièrement.